Interconnecting Solar Home Systems in Developing Nations

Bryan Oscareino Malik

Technische Universiteit Delft

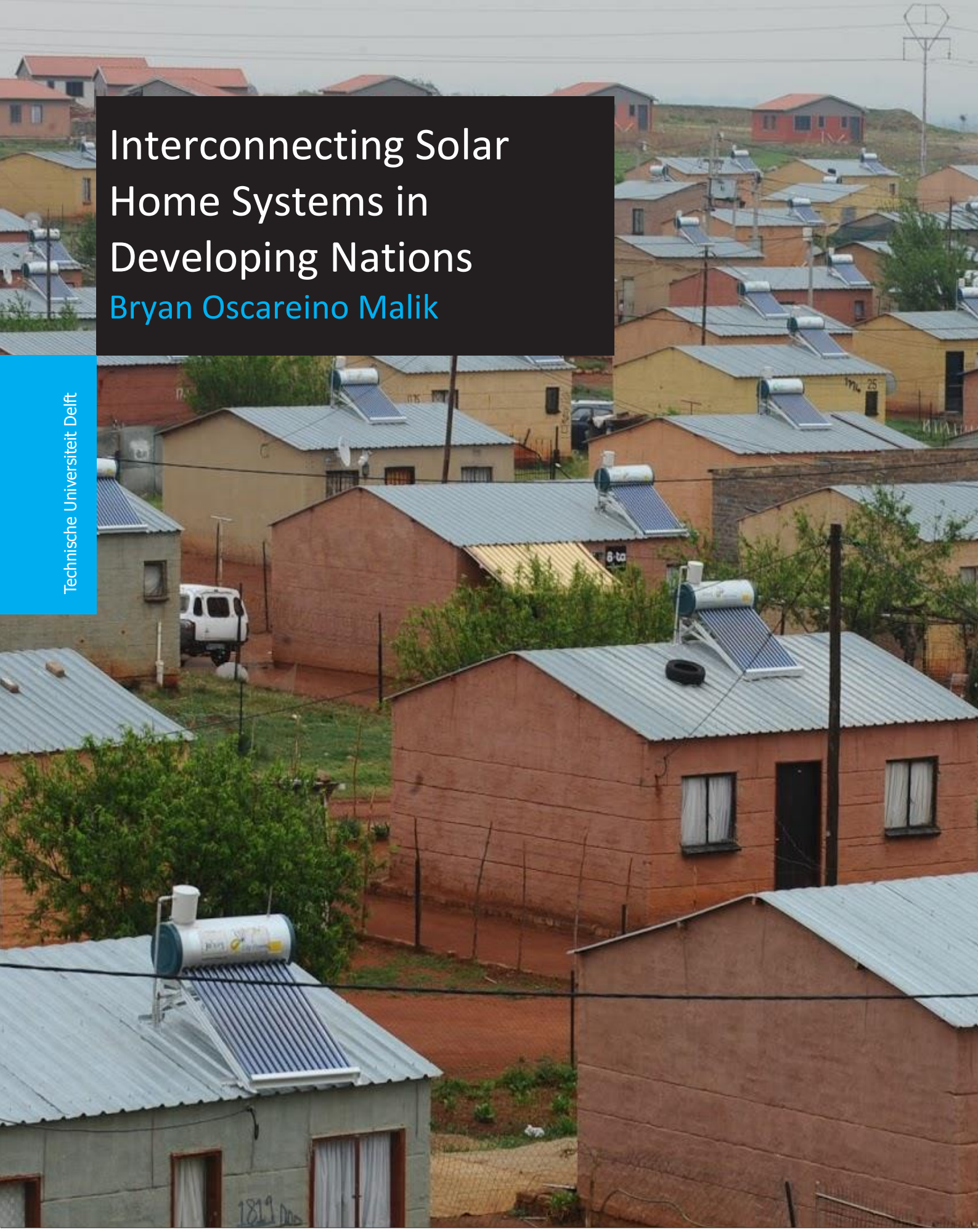

TU Delft Delft University of Technology

Challenge the future

Interconnecting Solar Home Systems in Developing Nations

By

Bryan Oscareino Malik

In partial fulfillment of the requirements for the degree of

Master of Science
in Electrical Sustainable Energy

at the Delft University of Technology,
to be defended publicly on Wednesday, August 30, 2017 at 10:00 AM.

Supervisor:	Prof.dr. eng. P. Bauer	
	Dr. ir. L.M. Ramirez Elizondo	
Advisor:	MSc Nishant Narayan	
	MSc Laurens Mackay	
Thesis Committee:	Prof.dr. eng. P. Bauer,	TU Delft
	PhD. Zian Qin,	TU Delft
	Dr. ir. Milos Cvetkovic,	TU Delft

This thesis is confidential and cannot be made public until August 31, 2018.

An electronic version of this thesis is available at http://repository.tudelft.nl/

TU Delft Delft University of Technology

Abstract

Rural area electrification is one of the challenging issues to be solved by the engineer as it is often constrained by several issues such as geographical condition and underdeveloped infrastructures. As a result, off-grid DC system is expected to answer the need of electricity in these areas.

Solar Home System (SHS) as one of the practical implementation of off-grid DC system has been used widely due to the low operating cost of PV panel which requires no fuel to operate. Besides that, this system offers more modularity rather than conventional power generator due to the absence of frequency and reactive power parameter in the static component. Decentralized control for energy management between component is preferred rather than centralized, so it does not require additional communication lines. Moreover, it allows each component to work independently when there is a failure or disturbance in the distribution lines. Equal power balance for multiple batteries is maintained by the additional controller in each local battery converter. Thus, the batteries rate of charge and discharge will be adjusted on their capacity.

Optimization of the individual SHS is conducted by interconnecting them as an attempt to form a low voltage DC off-grid network. It enables power-sharing mechanism to happen within connected houses. Additional power converters are required to provide bi-directional power flow within coupled houses, and decentralized secondary control needs to be introduced to give an equal independence level between these houses. Direct interconnection on the same voltage level allows the system to be simply coupled through cables, yet the current in the interconnection cable could increase sharply according to the sum of total connected SHS. On the other hand, interconnection in higher voltage level requires additional bi-directional converter between SHS and interconnection cables. However, the current is much lower and, thus provides a better location for high power-consuming loads to be installed.

Acknowledgment

This master thesis represents the result of my study in Electrical Sustainable Energy at TU Delft. Knowledge and experience that I got during my study here is a valuable opportunity for me to grow and begin to give impact to the society. I come from Indonesia to study here with the aim to contribute to renewable electrical energy development back in my country. I am very grateful that the topic for my thesis is corresponding to my motivation for studying here. The journey itself is not smooth, and a lot of obstacles had me fell several times. It taught me that the road to success is only not giving up and keep up the work. I hope that I could not only contribute for Indonesia but also for the development of future research related to this field of knowledge.

First of all, I would like to express my gratitude to Prof.dr.eng. P. Bauer for his guidance and discussion in the finalization process of this research. I would thank him for encouraging me to be more critical and thorough in my work. I would also like to thank Dr. ir. L.M. Ramirez Elizondo for being very helpful and kind during my early stage of this thesis. She is the first one who connects me with this thesis project which I am looking for.

Also, all of the work in this thesis could not be done without help from Nishant Narayan and Laurens Mackay as my Ph.D. Supervisor. They have guided me step by step in this past nine months, and have been very patient and supportive during the process. They always spare their time for me to have a discussion and a lot of constructive suggestion along the way.

Besides them, this thesis would also never be finished without the support from my family. To my parents, brother and sister, thank you for all the prayers, motivations and trust you have given me. Thank you also for the new family I found here, my friends. I am thankful for all the moments that we shared during our stay in Delft. It is truly memorable and makes life much more fun with you here. To Indriana Adani, thanks for all the patience, and great support through all the ups and downs this past two years.

Lastly, I would like to express my gratitude to the Ministry of Finance of Indonesia that has given me the opportunity to pursue my master degree. Thanks to Lembaga Pengelola Dana Pendidikan (LPDP) which has granted me this lifetime experience to study here in TU Delft.

Bryan Oscareino Malik
Delft, August 2017

“The world is 3 days: As for yesterday, it has vanished along with all that was in it. As for tomorrow, you may never see it. As for today, it is yours, so work on it.”
– **al-Hasan al-Basri**

“Never stop learning, because life never stops teaching. “
- Ki Hajar Dewantara

Contents

ABSTRACT ---- **IV**

ACKNOWLEDGMENT ---- **VI**

CONTENTS ---- **VIII**

LIST OF FIGURES ---- **IX**

LIST OF TABLES ---- **X**

1 INTRODUCTION ---- **1**

1.1. BACKGROUNDS ---- 1
1.1.1. Load Profile in Rural Areas ---- 2
1.1.2. Breakeven of Grid Expansion ---- 2
1.1.3. Modularity of Off-Grid Power System ---- 3
1.2. RESEARCH MOTIVATIONS ---- 4
1.3. RESEARCH OBJECTIVE ---- 5
1.4. RESEARCH QUESTIONS ---- 5
1.5. METHODOLOGY ---- 6

2 LITERATURE REVIEW ---- **7**

2.1. SOLAR HOME SYSTEM ---- 7
2.2. NANO-GRID FORMING ---- 8
2.3. DC DISTRIBUTION NETWORK ---- 10
2.4. COORDINATED CONTROL ---- 13

3 MODELLING SOLAR HOME SYSTEM ---- **19**

3.1. LOAD PROFILES ---- 21
3.2. COMPONENTS MODELLING AND SIZING ---- 23
3.2.1. Unidirectional Components ---- 23
3.2.2. Bidirectional Components ---- 25
3.2.3. Components Sizing ---- 27
3.3. ENERGY MANAGEMENT OF SOLAR HOME SYSTEM ---- 29
3.3.1. Primary Decentralized Controller ---- 33
3.3.2. Additional Adaptive Controller ---- 38
3.4. SOLAR HOME SYSTEM OPERATION ---- 45
3.5. BALANCING MULTIPLE BATTERIES ---- 50

4 INTERCONNECTION OF SOLAR HOME SYSTEM ---- **53**

4.1. INTERCONNECTION TOPOLOGY IN 48 V GRID ---- 56
4.2. INTERCONNECTION TOPOLOGY IN 350 V GRID ---- 62

5 CONCLUSIONS AND RECOMMENDATIONS ---- **73**

5.1. CONCLUSIONS ---- 73
5.2. RECOMMENDATIONS ---- 75

BIBLIOGRAPHY ---- **76**

A. SHS SIMULATION ---- **79**

B. MULTIPLE BATTERIES SIMULATION ---- **80**

C. 48 V INTERCONNECTION SIMULATION ---- **81**

D. 350 V INTERCONNECTION SIMULATION ---- **82**

List of Figures

FIGURE 1-1 GLOBAL SOLAR RADIATION LEVEL 4
FIGURE 1-2 RESEARCH METHODOLOGY 6
FIGURE 2-1 SOLAR HOME SYSTEM 7
FIGURE 2-2 BUILDING BLOCKS OF NANO-GRID 8
FIGURE 2-3 (A) POINT TO POINT (B) COMMON POINT SHARING 9
FIGURE 2-4 LOW VOLTAGE DIRECT CURRENT DISTRIBUTION NETWORK [21] 11
FIGURE 2-5 BOTTOM-UP APPROACH FOR LVDC FORMING 11
FIGURE 2-6 MULTILEVEL CONTROL SCHEME 12
FIGURE 2-7 (A) DECENTRALIZED CONTROL, (B) CENTRALIZED CONTROL, (C) DISTRIBUTED CONTROL [23] 13
FIGURE 2-8 SMALL DROOP AND HIGH DROOP CONTROL [26] 15
FIGURE 2-9 MODIFIED DROOP CONTROL BASED ON SOC [25] 15
FIGURE 2-10 MODIFIED DROOP CONTROL THROUGH NEIGHBOUR TO NEIGHBOUR COMMUNICATION [27] 16
FIGURE 2-11 EFFECT OF LINE RESISTANCES ON DROOP GAIN [29] 17
FIGURE 2-12 (A) UTILITY MODE (B) STORAGE MODE (C) GENERATION MODE (D) MODE SELECTION 18
FIGURE 3-1 SOLAR HOME SYSTEM MODELLING WORKFLOW 19
FIGURE 3-2 MODULAR SHS 20
FIGURE 3-3 LOAD PROFILES FOR 2017 21
FIGURE 3-4 LOAD PEAK FOR EACH LOAD PROFILE 22
FIGURE 3-5 DAILY LOAD CONSUMPTION 22
FIGURE 3-6 PV POTENTIAL POWER GENERATOR 23
FIGURE 3-7 PV GENERATOR BLOCK MODEL 24
FIGURE 3-8 EQUIVALENT SUN HOURS BASED ON AVERAGE GLOBAL HORIZONTAL IRRADIANCE [30] 25
FIGURE 3-9 DEPTH OF DISCHARGE CHARACTERISTIC OF BATTERY [32] 25
FIGURE 3-10 BATTERY MODEL 26
FIGURE 3-11 SOLAR PANEL MEASURED POWER 29
FIGURE 3-12 POWER FLOW IN SHS 31
FIGURE 3-13 MODEL OF IDEAL SHS UNIT 32
FIGURE 3-14 PRIMARY DECENTRALIZED CONTROLLER 33
FIGURE 3-15 VOLTAGE SET POINTS FOR DIFFERENT OPERATION MODES [38] 34
FIGURE 3-16 CONVERTER OPERATION MODES 36
FIGURE 3-17 CURRENT DETERMINATION 36
FIGURE 3-18 CONSTANT POWER CONTROLLED MODELS 37
FIGURE 3-19 DROOP CONTROLLED MODELS 37
FIGURE 3-20 ADAPTIVE CONTROLLER 39
FIGURE 3-21 (A) CURRENT ABSORBING LIMITER (B) CURRENT INJECTION LIMITER 40
FIGURE 3-22 SOC DEPENDANT DROOP CONTROL 41
FIGURE 3-23 LINEAR CHARGING DROOP MULTIPLICATION FACTOR 43
FIGURE 3-24 LINEAR DISCHARGING DROOP MULTIPLICATION FACTOR 43
FIGURE 3-25 BATTERY DROOP VARIATION 44
FIGURE 3-26 SHS OPERATION MODEL 46
FIGURE 3-27 CONVERTER OPERATION MODE 48
FIGURE 3-28 CONVERTER OUTPUT VOLTAGE 48
FIGURE 3-29 CONVERTER OUTPUT CURRENT 49
FIGURE 3-30 BATTERY SOC LEVEL 49
FIGURE 3-31 MULTIPLE BATTERIES MODEL 50
FIGURE 3-32 MULTIPLE BATTERIES OPERATING MODE 51
FIGURE 3-33 CURRENT CHARACTERISTIC OF MULTIPLE BATTERIES 51
FIGURE 3-34 SOC LEVEL OF BATTERIES 52
FIGURE 4-1 (A) LOW (B) MEDIUM (C) HIGH POWER DIFFERENCE WITH PV PRODUCTION 54
FIGURE 4-2 INTERCONNECTION TOPOLOGY IN 48V 56
FIGURE 4-3 ADDITIONAL LOW LOAD PROFILE 58
FIGURE 4-4 ADDITIONAL MEDIUM LOAD PROFILE 58
FIGURE 4-5 HOUSE 1 CURRENT CHARACTERISTIC 58

FIGURE 4-6 HOUSE 2 CURRENT CHARACTERISTIC 59
FIGURE 4-7 HOUSE 3 CURRENT CHARACTERISTIC 59
FIGURE 4-8 HOUSE 4 CURRENT CHARACTERISTIC 59
FIGURE 4-9 HOUSE 5 CURRENT CHARACTERISTIC 60
FIGURE 4-10 SOC OF BATTERIES IN THE INTERCONNECTED HOUSES 60
FIGURE 4-11 INTERCONNECTION TOPOLOGY IN 350V 62
FIGURE 4-12 LOAD POWER CONSUMPTION IN 350V GRID 63
FIGURE 4-13 CURRENT MULTILEVEL CONTROLLER 64
FIGURE 4-14 CURRENT OUTPUT LIMIT CHECK 66
FIGURE 4-15 CURRENT FLOW IN HOUSE 1 70
FIGURE 4-16 CURRENT FLOW IN HOUSE 2 70
FIGURE 4-17 CURRENT FLOW IN HOUSE 3 70
FIGURE 4-18 CURRENT FLOW IN HOUSE 4 71
FIGURE 4-19 CURRENT FLOW IN HOUSE 5 71
FIGURE 4-20 SOC LEVEL OF INTERCONNECTED BATTERIES 71
FIGURE 4-21 CURRENT FLOW IN 350 V LINE 72

List of Tables

TABLE 1-1 2016 WORLD ELECTRIFICATION RATE [1] 1
TABLE 3-1 PV MODULE AND BATTERY SIZING 28
TABLE 3-2 CURRENT CALCULATION FOR DIFFERENT OPERATION MODE 38
TABLE 3-3 DROOP SHIFTING VALUE 43
TABLE 3-4 SHS PARAMETERS 45
TABLE 3-5 CURRENT LIMIT 46
TABLE 3-6 VOLTAGE SET POINTS 47
TABLE 4-1 BATTERY SYSTEM SIZING ACCORDING TO PV PANEL CAPACITY 55
TABLE 4-2 48 V INTERCONNECTION SYSTEM CHARACTERISTIC 57
TABLE 4-3 350 V INTERCONNECTION SYSTEM PARAMETER 68

1

Introduction

1.1. Backgrounds

According to the research conducted by the International Energy Agency [1] in 2016, nearly 15% of world population is still living in the "dark" due to the unavailability of electricity power as presented in Table 1-1. More than 90% of them come from the developing countries, with 85% of this population is living in the rural areas [1]. Therefore, hybrid off-grid power system has been introduced as one of the viable solutions for increasing the rate of electricity penetration in rural areas along with the conventional method of primary grid connection [2]. Even though the electrification ratio has already increased from 80% in 2010 [2] to 85% in 2016, the rate of population growth in rural areas might outnumber the growth of electricity ratio [3]. The lack of power grid infrastructures, the challenging geographical condition, and the low purchasing power of the consumers are several reasons that can be related to this problem. Further explanations regarding the background issues of this problem will be accounted separately on each subsection of this part.

Table 1-1 2016 World Electrification Rate [1]

Region	Population without electricity millions	Electrification rate %	Urban electrification rate %	Rural electrification rate %
Developing countries	**1,185**	**79%**	**92%**	**67%**
Africa	634	45%	71%	28%
North Africa	*1*	*99%*	*100%*	*99%*
Sub-Saharan Africa	*632*	*35%*	*63%*	*19%*
Developing Asia	512	86%	96%	79%
China	*0*	*100%*	*100%*	*100%*
India	*244*	*81%*	*96%*	*74%*
Latin America	22	95%	98%	85%
Middle East	18	92%	98%	78%
Transition economies & OECD	**1**	**100%**	**100%**	**100%**
WORLD	**1,186**	**84%**	**95%**	**71%**

1.1.1. Load Profile in Rural Areas

The load profile is an important parameter in off-grid power system design, as it characterizes the power demand that should be met by the available renewable sources and storage system. Research conducted in Cambodia on September - October 2016 [4] has generated recent load profiles for optimization of Solar Home System (SHS). The load profiles are classified as low, medium and high consumption with a sample of efficient and inefficient usage. Also, future load profiles have been predicted based on field survey through a sample of the population. The result is a huge difference in load demand as the consumers tend to use static load appliances with enormous power consumption. The appliances are preferable to be used in the future for supporting their daily needs such as rice cooker, water kettle, and iron. All of those instruments are labelled only require a few Watts of power to be operated. However, the duration of the usage for the appliances to optimally work takes an hour and may be longer. Therefore, the demand for the power will increase sharply at the time it is operated, not to mention the common usage time for each consumer is similar. As a result, it is predicted that in upcoming years the designed SHS could not fulfill the load requirement from consumers anymore. Consequently, grid expansion and off-grid power system modularity has been proposed to be the solution for anticipating the varying load demands in the future.

1.1.2. Breakeven of Grid Expansion

The distribution network in the rural area is classified in poor state mainly due to reasons such as low quality of power supply, electricity thefts, and a different pattern of electricity consumption. On the other hand, the power distribution in this type of area also has two main challenging issues [5]. The first one is the expenses for dispatching dispersed needs in such a wide area will be incredibly high. The geographical condition has affected the initial cost for distribution network infrastructure. Secondly, the main power plants normally have to export the generated power to the distribution companies which will sell the electricity at increased price as the exchange of their services. This second condition makes the less-fortunate families unable to purchase the electric power for their needs. This qualitative assessment of grid expansion gives us an explanation about why the investment in a big power system for long distribution system will not providing the best solution for solving the electricity issues in rural areas. Furthermore, the Breakeven Grid Extension Distance (BGED) can be drawn by comparing the Levelized Cost of Energy (LCOE) of grid connection with off-grid hybrid system [6]. The BGED occurs at the time the LCOE of grid connection equals to the LCOE of the hybrid system under the same interest rate and power demands [7]. The study has shown that the area with a distance of > 17 km from the main grid is considered to be not attractive anymore for grid expansion [8].

1.1.3. Modularity of Off-Grid Power System

There are two limitations that should be anticipated in designing the off grid power system. The PV array peak power is related to the maximum amount of power that can be obtained at any instant or the anticipated peak load power demand. The second one is storage system capacity which is designed for supplying power at the time the power generating source is unavailable through charging and discharging process. The storage system should be charged on a regular basis without exceeding the Depth of Discharge (DOD) level to maintain the battery condition. Consecutive usage of battery system below determined State of Charge (SOC) level with the addition of failure in fully charging the battery will degrade the quality of battery condition. This degradation may lead to the need of storage system replacement with considerable cost. Accordingly, system scaling should consider the optimum number of PV panel and storage system size based on reliability criteria [9]. One of the methods to determine the trade-off between system size and reliability in power system is by using Loss of Load Probability (LLP). It shows the probability of the system load exceeds the available power generation capacity. When the LLP equals to 1, it means the load will be surely be not satisfied completely, and the value of 0 shows that the load will be fully satisfied even the power generating sources are unavailable due to an environmental condition. Therefore, the optimum amount of PV panel and storage capacity will be vary based on the load profiles.

In [10], it is concluded that the LLP curves for each load profiles have their asymptotic limit. The research states that there will be a breakeven point where the increase in some PV modules with specific storage capacity will not lower the value of LLP anymore. When this limit is reached, the only way to decrease the value of LLP is by adding more storage capacity which is more expensive than the expenses of adding PV panel. By assuming that the load demand will keep increasing, there will be some point where the cost of a storage system is considerably high just for supplying the load peak demand. This issue is considered to be not economically wise for providing such an unpromising area even for grid integration.

1.2. Research Motivations

Most of the rural areas have limited access to the main power grids due to their geographical condition and unfavorable investment for grid expansion as an effect of low electricity demands. Therefore, off-grid power system with Distributed Renewables Energy (DRE) has been designed and built to fulfill electrical demands for daily loads. DRE is suitable for rural areas regarding lower maintainability and operational price rather than kerosene cost for using a local generator. Moreover, the location of rural areas which are situated majority in solar belt region [11] as depicted in Figure 1-1 and the decreasing price of PV panels have introduced Solar Home System (SHS) as the suitable method for electrifying those areas.

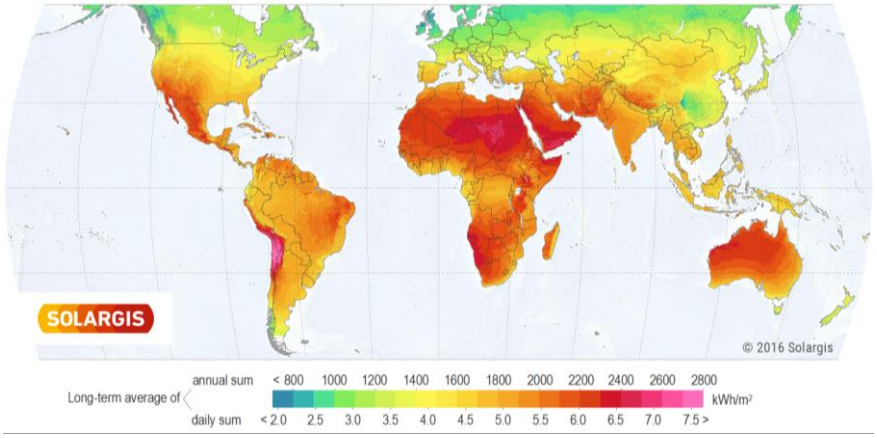

Figure 1-1 Global Solar Radiation Level [11]

In the past, the requirement of electricity is low, and the designed SHS still able to satisfy the load demands. As the time goes by, the penetration of electricity in this area also has triggered the urge of the population for using power consuming loads such as iron, rice cooker, and water kettle. As a result, the existing SHS is not sufficient anymore for providing the power needed due to these additional load characteristic. While waiting for the electricity demand characteristic to be attractive for grid expansion, some actions need to be taken for bridging the condition of current state and prospect of grid integration. The additional storage system may be considered as one of the solutions for this condition. However, the amount of energy that could be stored is also limited by the maximum generated power from existing power sources. Moreover, the investment on additional storage is considered to be profitable only under the condition of high cost for cable and with the assumption that the storage system certainly operates for a long lifetime [12]. The proposed method is by interconnecting each SHS to form off-grid Low Voltage Distribution (LVDC) network.

1.3. Research Objective

Developing rural area electrification through interconnection between Solar Home Systems with decentralized power sharing mechanism.

1.4. Research Questions

1. What control method can we use to maintain power balance in Solar Home System without communication link?

2. How to preserve SOC balance between batteries in the Solar Home System?

3. How can Solar Home Systems be connected into off-grid LVDC network?

4. How to control the interconnected Solar Home Systems with the two voltage levels DC-DC converter?

1.5. Methodology

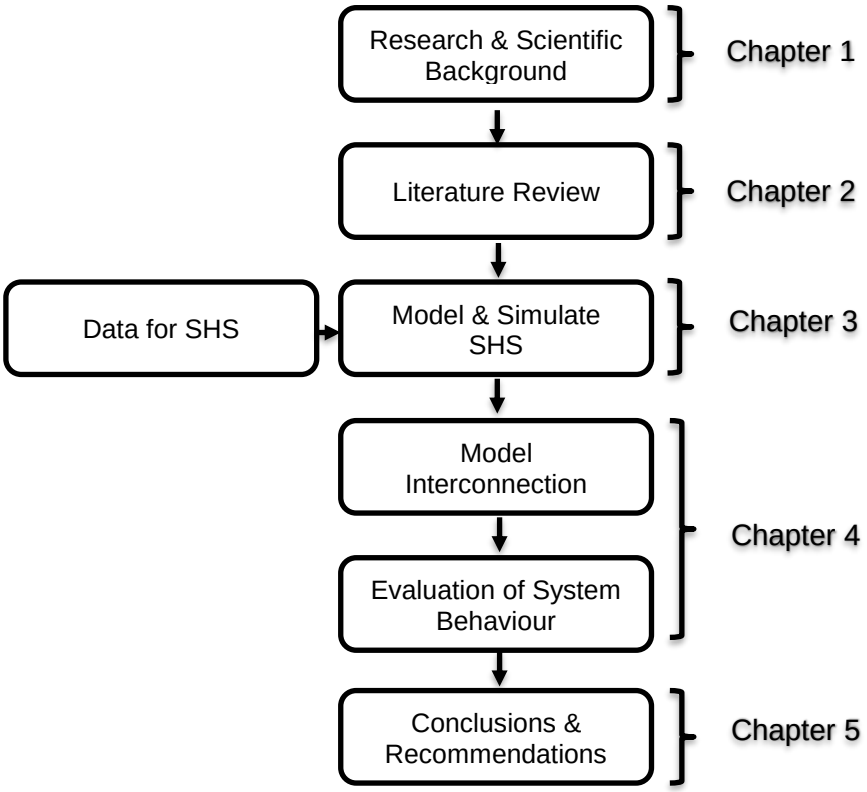

Figure 1-2 Research Methodology

This thesis work is documented in this report into 5 Chapters as illustrated in Figure 1-2. Chapter 1 mainly informs about the reason of the conducted research and what questions are expected to be answered at the end of the work. Chapter 2 delivers the information about previous works related to the questions in Chapter 1, it also gives an illustration of what are the missing things that could be improved for this thesis. The measurement data used in this thesis is presented in Chapter 3, as the feasibility of this research is expected to be applied in real system. Besides that, it also explains how the components in individual SHS are modeled. This Chapter also describes how the proposed local controller able to maintain power flow under single SHS. The interconnection behavior between SHS and power-sharing mechanism are presented in Chapter 4. In this thesis, the interconnection model is divided into 48 V and 350 V level. In the end, the simulation and limitation findings which bring several recommendations for future works are summed up in Chapter 5.

2

Literature Review

2.1. Solar Home System

The desire of increasing electrification ratio in each country is always an interesting topic as each of them has unique and different challenges. One of the challenges is the issue about electrification of rural areas through the grid expansion. The problem appears as the load requirements in this area are considerably low and seem unpromising for the grid company to invest on the grid expansion. This issue has given the opportunity of renewables energy as the main power source not only to electrifying the area but also to satisfy the international carbon emission target in 2020 [13], [14].

The common locations of this rural area are suitable for using solar energy as their power generation sources due to the high intensity of available sunlight hour. Also, DC system is considered to be the most efficient method of supplying loads in rural areas because the majority electrical equipment in this region is DC loads. Therefore, the simplest way to allow electricity penetration for this individual consumer is through the independent PV system which is further known as Solar Home System (SHS). PV module generates power through the photovoltaic effect of the semiconductor when it is exposed to light, resulting in the emitted electrons. Another component is the battery system for storing generated power at the time the power generated is more than the power demanded. This stored energy can be used later when there is an increase in the load demand and the available power from generating source is inadequate. The energy flow between PV modules, battery, and loads are regulated by the charge controller which also determines the charging and discharging process of the battery system according to the load demand and power generation. The general SHS topology is illustrated in Figure 2-1.

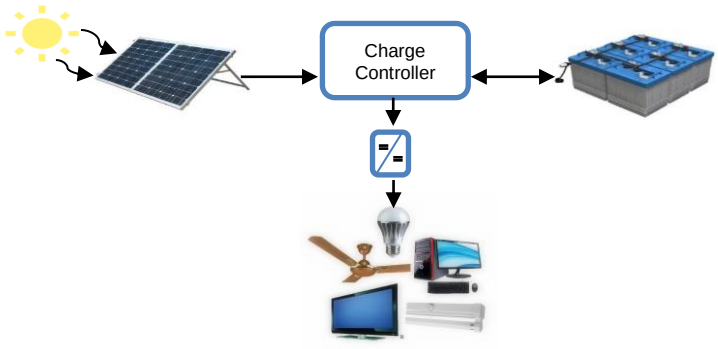

Figure 2-1 Solar Home System

2.2. Nano-grid Forming

The concept of nano-grid comes from the idea of sharing power between consumers with regards to the waste excess energy in the designed power system. Stand-alone PV system is commonly designed according to the lowest average peak sun hours per day, so it anticipates the worst condition of sunlight intensity while still supplying the loads. Based on that status, it is assured that there will be excess energy which could not be stored anymore in the designed system when the sun intensity is more than the lowest average value. Rather than just let this excess power gone nowhere, it is subtle to share this power for those who do not have access to electricity at all. Another consideration of nano-grid is for allowing power exchange mechanism in the certain neighborhood under a limited amount of power sources and storage. This limitation occurs at the moment when the condition of whether scaling up the storage or power sources capacity is not economically beneficial anymore according to the increase in load demands [10].

Even the electricity purchasing power of rural area is considered to be low, it is assumed there will be disproportionality in the capability of purchasing PV system component. Some of them have the complete PV system which consists of PV panel, DC converter, and battery system. On the contrary, some other may only have the PV panel or battery only or even does not have any access to the PV system [15]. Therefore, interconnecting independent SHS to form low voltage DC nano-grid as illustrated in Figure 2-2, will increase the availability of power in the system through the power exchange mechanism. As a result, not only primary electricity user demand is satisfied, but also public load requirements such as irrigation and street lighting could be fulfilled with minimum losses due to the short distribution lines between consumers [13].

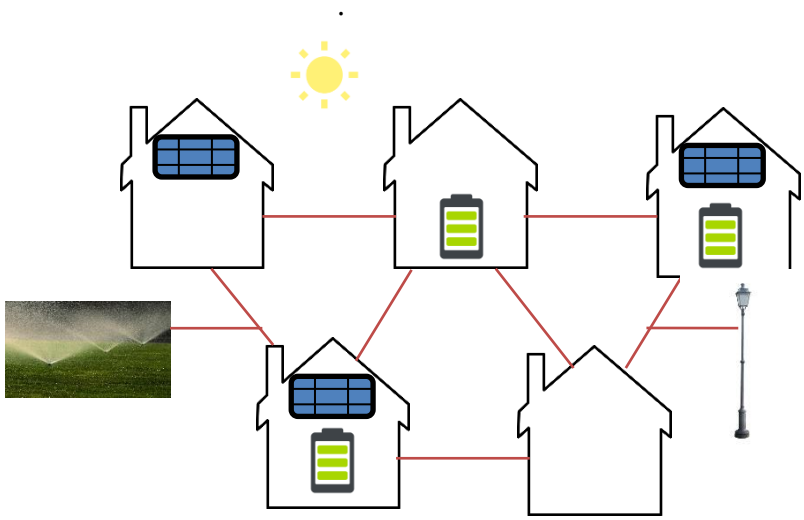

Figure 2-2 Building Blocks of Nano-grid

Based on the research conducted in [16], the independent SHS is only capable of supplying present load characteristics while the load demand is predicted to increase shortly. Hence, nano-grid interconnection is one of the appropriate solutions while waiting for the load characteristic to be attractive enough for grid expansion. Accordingly, some appropriate topologies for connecting the SHS in rural areas are a point to point and common point sharing as illustrated in Figure 2-3 [15]. The point to point interconnection mode has the advantage of higher resilience over disturbance due to the more robust topology, while the amounts of converters are likely to be higher than in common point sharing mode. Each connection may need different converter specification due to the variance of the voltage level in load which leads to the increase in initial cost. On the contrary, common point sharing needs fewer converters, and line connection which leads to the lower initial cost as the flow of the energy is directed to a common bus in the area. However, an additional communication link is needed for monitoring the power flow correspondingly to the purchased electricity amount. In the case of prepaid electricity, it is needed for preventing individuals to consume more than what they have paid.

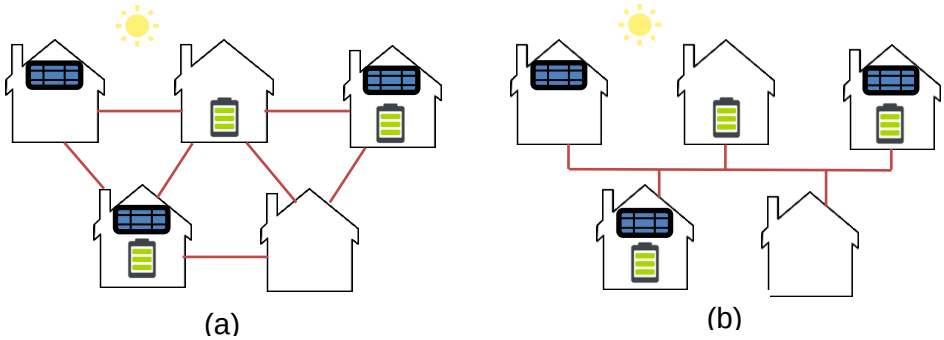

Figure 2-3 (a) Point to Point (b) Common Point Sharing

Meshing grid is one of the important aspects that need to be studied further as the DC system assumed to have more resilience over the disturbance rather than AC networks. Existing AC distribution grid is designed radial to keep the protection and synchronization less complex [17], while the redundancy is sacrificed. The absence of synchronization requirement in DC results in the flexibility of DC distribution system to be designed either in radial or mesh.

2.3. DC Distribution Network

100 years ago, AC power system seemed to be promising as the power level transformation could be done easily by using a power transformer. This allows the delivery of electrical power through the high voltage AC cables through the transmission network. However, the main problems occurred from this method is some energy losses in the network due to the reactive power and the conversion losses due to the required conversion steps from AC into DC in consumer's load. The flexibility of taking into account the distributed renewable energy is also limited in AC system, as frequency synchronization is needed to maintain the system stability.

The advancement in a semiconductor device has triggered the development of power electronic devices such as power converters for transforming electricity power either in AC or DC. Therefore, the stigma about impracticable DC network from the previous years could be handled and even makes DC network may rise again. One of the advantages of DC system compared to the AC is the higher level of reliability and efficiency due to the fewer conversion steps. Secondly, it has higher energy flow capability in the network due to the higher voltage threshold [18]. It also has lower power losses compared to the AC system in the same voltage level, due to the absence of reactive power component [19]. The drawback is DC network protection may be a challenging issue because of the absence of zero voltage crossing component which is normally occurred in AC system. However, DC voltage is considered to be more stable and resulted in higher RMS voltage that can be used for the same level of insulation in AC [17].

Shifting the whole existing AC system into DC may not be the best option as the life cycle estimation cost for DC system is still under research due to the lack of system maturity. Hence, the transition could be made in several steps [20] while allowing the DC components to grow for future integration. The initial step could be done by shifting the low voltage distribution network into DC due to the increase in distributed renewable energy penetration such as solar panels, wind turbines and consumer's load characteristic which are mostly DC. According to that, the renewable generating sources and DC loads are most suitable to be interfaced with DC distribution system instead of AC as illustrated in Figure 2-4 [21].

Low Voltage Direct Current Distribution Network (LVDC) has also presented a lot of opportunities for shifting into the microgrid system. One of them is by supporting microgrid's key actors to apply the market model. The concept of prosumer as a load consumer with the capability of generating its electricity through Distributed Renewables Energy (DRE) will increase due to the simplicity of integrating Distributed Generation (DG) into the distribution grid in LVDC distribution network. This leads to the realization of power exchange mechanism between grid and user which can contribute to the higher level of electrification ratio in rural areas. As a result, the DC nano-grid concept of interconnected Solar

Home System for supporting local area consumption can be explained further as an attempt to form LVDC distribution network.

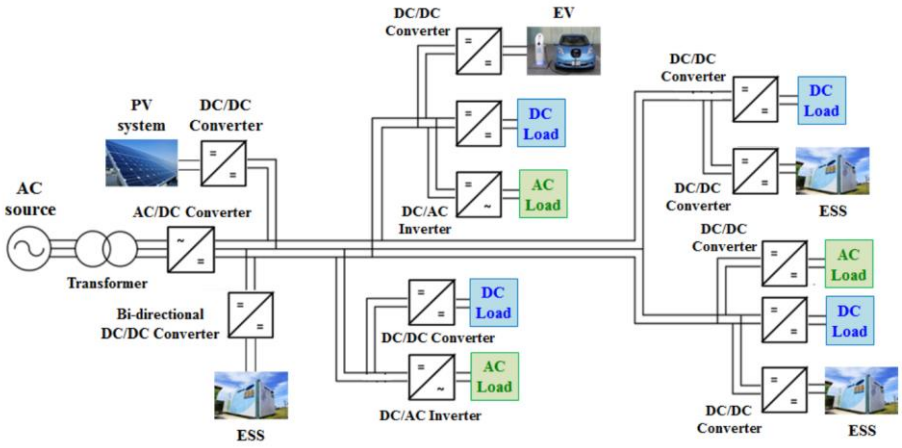

Figure 2-4 Low Voltage Direct Current Distribution Network [21]

The intermittency level of renewable energy is considerably high due to its dependency on the environment condition, therefore interconnecting SHS to form low voltage DC distribution grid is considered to be a better solution for solving this problem rather than increasing the storage and generation system [10]. Under normal circumstances, the SHS should have at least basic controller for managing the power flow operation within its system. Thus, integrating several SHS into one system requires additional control for coordinating unit to unit operation mode and serves as a communication link between them. The formation of a whole LVDC distribution network from individual SHS is formed through 3 layered structure as depicted in Figure 2-5.

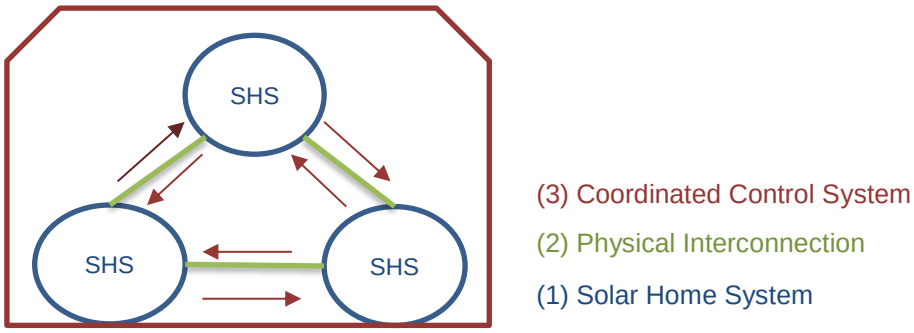

Figure 2-5 Bottom-up Approach for LVDC Forming

The first layer is determined as each independent SHS which already have their local power control. The second one is the physical realization of interconnection between SHS through DC power bus and communication lines. The last layer is the control system of a whole interconnection system, in which the power exchange mechanism is executed according to individual SHS requests and responses. As a result, this bottom-up method will replace the conventional top-down electrification approach which requires an existing power grid and mature power transmission at a first place. It is also allowing the mechanism of Open Energy System (OES) to be practically realized in the DC network [22].

DC nano-grid can be seen as a multilayer power system that needs to be controlled on each level of the system for efficient and stable operation. In consequence, the overall control scheme is classified into local control and global coordinated control [23], [24]. Local control or known as primary control deals with local parameter such as current, voltage, and droop of each installed component. It is also responsible for executing specific component functions such as Maximum Power Point Tracking (MPPT) for PV panels, SOC calculation, and SOC level limitation for battery operation. On top of that, there is the coordinated control which consists of secondary and tertiary control of the system. It is responsible for executing energy management system on a global scale to enable intelligent coordination between each SHS independently. Some issues handled by them are DG coordination, power quality regulation, and power-sharing mechanism [24]. The overall multilevel control scheme of DC nano-grid is illustrated in Figure 2-6.

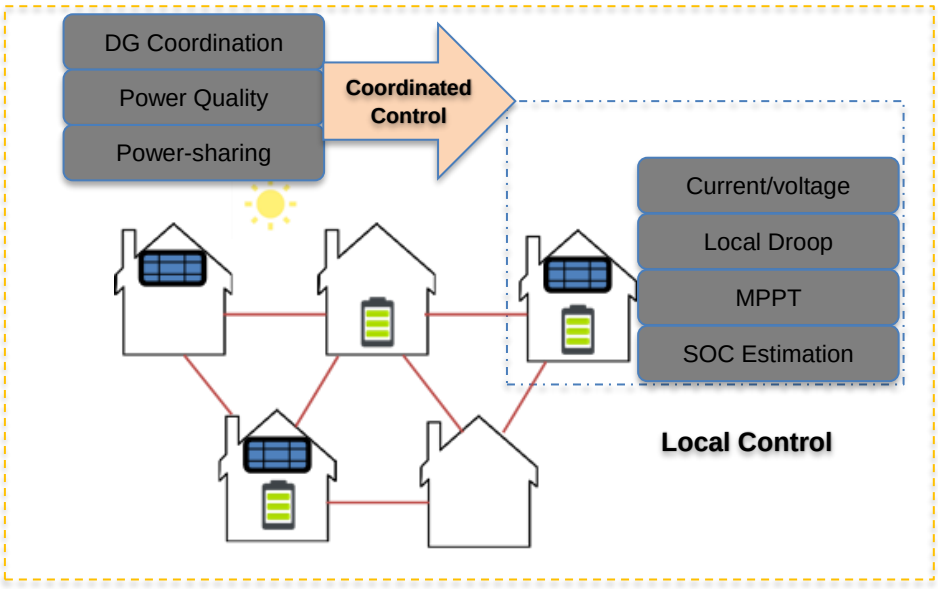

Figure 2-6 Multilevel Control Scheme

2.4. Coordinated Control

Global coordinated control can be executed in some ways according to the communication perspectives infrastructure in the system and classified as [23]:

1) *Decentralized controller*: communication channel is not needed, all the regulations are based only on local measurements

2) *Centralized controller*: communication channel is needed from each DG to the central control unit. The central unit will transmit the collected information to each local DG so that they can perform the regulations

3) *Distributed Controller*: the central control unit is not needed, but sparse communication is needed between neighbors. The regulations will be based both on local measurement and comparison to their neighbors.

The configuration of mentioned control types above is presented in Figure 2-7 below.

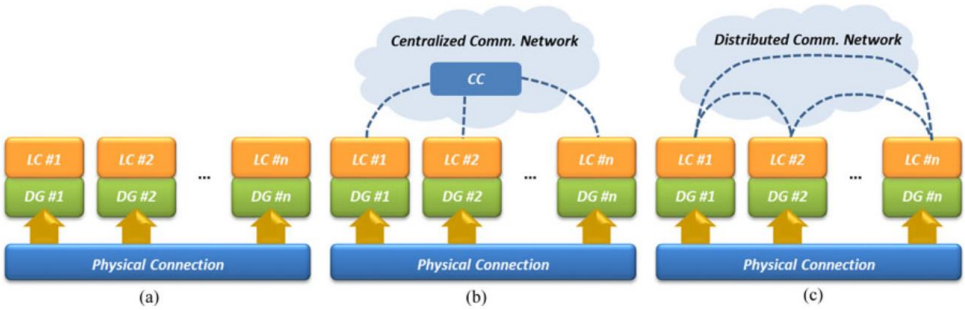

Figure 2-7 (a) Decentralized Control, (b) Centralized Control, (c) Distributed Control [23]

The power balance in DC interconnection bus can be maintained by shifting the voltage level through voltage droop control. This is allowing the load sharing between each distributed Energy Storage (ES) devices in DC nano-grid [25]. However, there is a trade-off between the voltage regulation and load sharing capability at the time DC nano-grid is interconnected through conventional droop control. It results due to the presence of cable resistance in the interconnection point [26]. In DC nano-grid, the voltage magnitude in each node whereas the SHS is integrated with Power Electronic Converter (PEC) varies along the interconnection cable. DC voltage in the cable will decrease due to the voltage drop that increases along the distance. Therefore, it is common for two different nodes at the interconnection line to have voltage deviation. As a result, DC power bus is designed to operate under the regulated amount of voltage deviation (± 10%) [27].

The droop method as illustrated in Figure 2-8 is constructed by decreasing the voltage as the delivered current from PEC increases. Therefore, the droop gain (R_d) is selected to be slight as possible for minimizing voltage deviation within the allowed voltage operation range. The slight slope indicates that the droop control is small which gives good voltage regulation, yet degrades load sharing equality. It can be explained by considering the nominal voltages of several PEC generally are not exactly equal, due to the small error in voltage sensing of closed loop calculation. Figure 2-8 shows that slight different in nominal voltage of two parallel connected converters generates large current deviation ($i_1 - i_2$). On the other hand, the current deviation ($i_1 - i_2$) is getting smaller as the droop gain is increased with the trade-off of huge voltage regulation which is not wanted in the system operation. Therefore, high droop value with huge slope generates better load sharing capability, yet worse voltage regulation [26].

The expression of droop control in DC networks is presented as

$$V_{dc} = V_{0dc} - R_d * Idc \quad (1)$$

Where V_{dc}, V_{0dc}, and I_{dc} are the converter reference output voltage, nominal voltage (voltage when the source current is zero), and converter current output. One method to satisfy good voltage regulation and equal load sharing is through centralized controller, such as master and slave control [2]. However, it needs a solid high-speed communication infrastructure and susceptible to single point of failure. Moreover, centralized controller is not expected to be applied in rural areas with low maintainability requirement. Hence, the decentralized control seems to be more suitable for answering the necessity of rural areas, along with its advantage in higher independency of local system to maintain its operability while there is a failure in the interconnection line [26], [27].

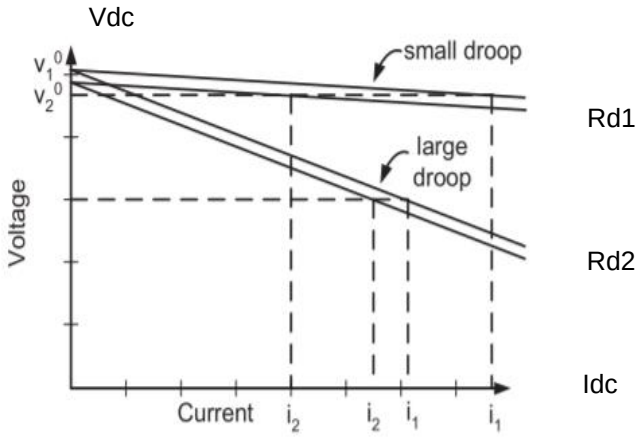

Figure 2-8 Small Droop and High Droop Control [26]

Due to the uncertain character of renewable energy and the difference of load profiles for each local SHS, the SoC level of the storage systems may differ even they started at the same level. It is also related to the output current set by each droop controller illustrated in Figure 2-8. The voltage drop across the interconnection line generates a different output current from each battery which may deplete some of them earlier. Thereupon, the amount of power-sharing should be proportional according to each SoC level of local SHS. It implies that the battery with higher SoC should give more power than the battery with lower SoC, so the power capacity of each battery is maintained [27]. The SoC of each battery is measured locally for shifting the droop control by controlling the duty cycle in the converter as illustrated in Figure 2-9 [25].

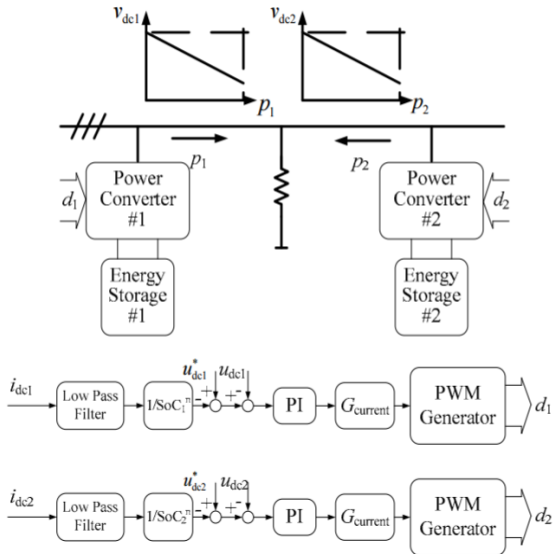

Figure 2-9 Modified Droop Control Based on SOC [25]

Another attempt to adjust the droop controller is by modifying the V - P droop control equation based on the cooperative control which takes into account power reference from a neighbor through a sparse communication network. The communication infrastructure needed in this method is not as complex as in the centralized control and offers more degree of modularity and robustness [27]. As depicted in Figure 2-10, the proposed V-P droop equation is:

$$v^* = V_{MG} - m(p - p^*) \quad (2)$$

v^*, V_{MG}, m, p, p^* are the reference voltage, nominal voltage, droop gain, output the power of the converter, and the output power of neighbour's converter. v^* is compared with the actual converter output voltage v_1 through PI controller to generate the duty cycle d for control the converter gate, so the desired output voltage is regulated.

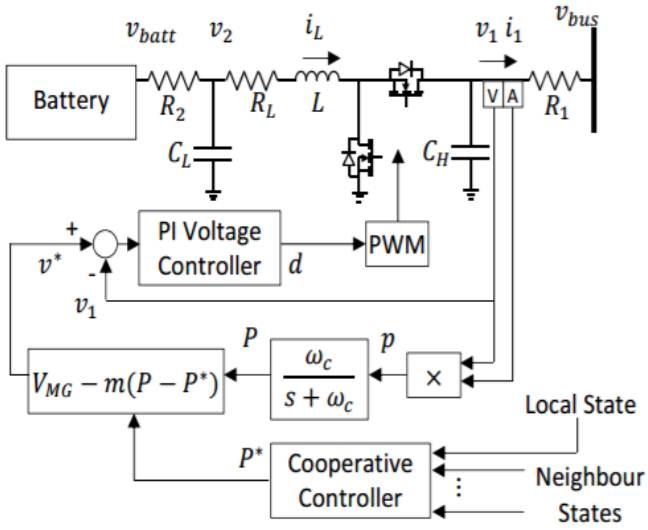

Figure 2-10 Modified Droop Control through Neighbour to Neighbour Communication [27]

Another method proposed in [28] is by compensating the load sharing due to the small droop and by compensating voltage deviation due to high droop selection. Accordingly, the control method is decentralized with additional of low bandwidth communication line that shares common load condition i_{avg} in each terminal of local controller. The common load condition can be described as average module current in per unit. The compensation for voltage deviation is stated in Equation (3) and, compensation for load sharing is in Equation (4).

$$\Delta V'_j = K_j i_{avg} \quad (3)$$

$$\Delta V''_j = \frac{K_{pj}S + K_{Ij}}{S} (i_{avg} - i_j) \quad (4)$$

Where K_j is the compensation coefficient for restoring microgrid voltage, should be smaller than droop resistance K_{pj} and the load sharing compensator for *j*-th the local controller K_{Ij}. Although the effective droop gain has been designed, the voltage droop caused by line resistance will shift the droop gain and degrade the voltage regulation as depicted in Figure 2-11. R_V is the designed droop gain, and R_{li} denotes for line resistance in corresponding node.

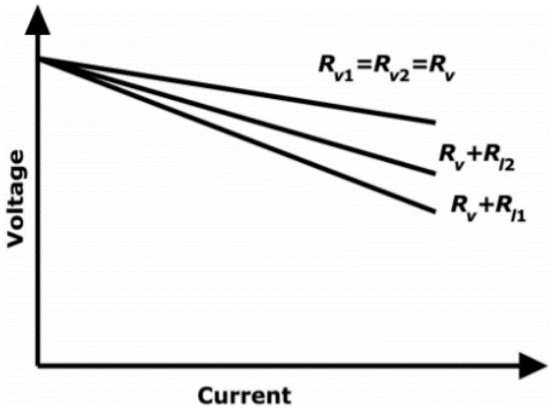

Figure 2-11 Effect of Line Resistances on Droop Gain [29]

Besides of the droop method, another notable method is by using DC Bus Signalling (DBS) for power management between multiple sources and loads. It is executed by measuring the local voltage at the coupling point. Initially, some voltage ranges have been defined, and then the measured voltage is coordinated in which voltage range it is corresponded. Considering that multiple sources are common in nano-grid, the operation voltage range is classified as; utility dominating mode, generation dominating mode, and storage dominating mode. It is related to which power source is dominating the operation at certain time. The dominant power source then set up the DC bus voltage. Different operation modes in DBS are presented in Figure 2-12 [24].

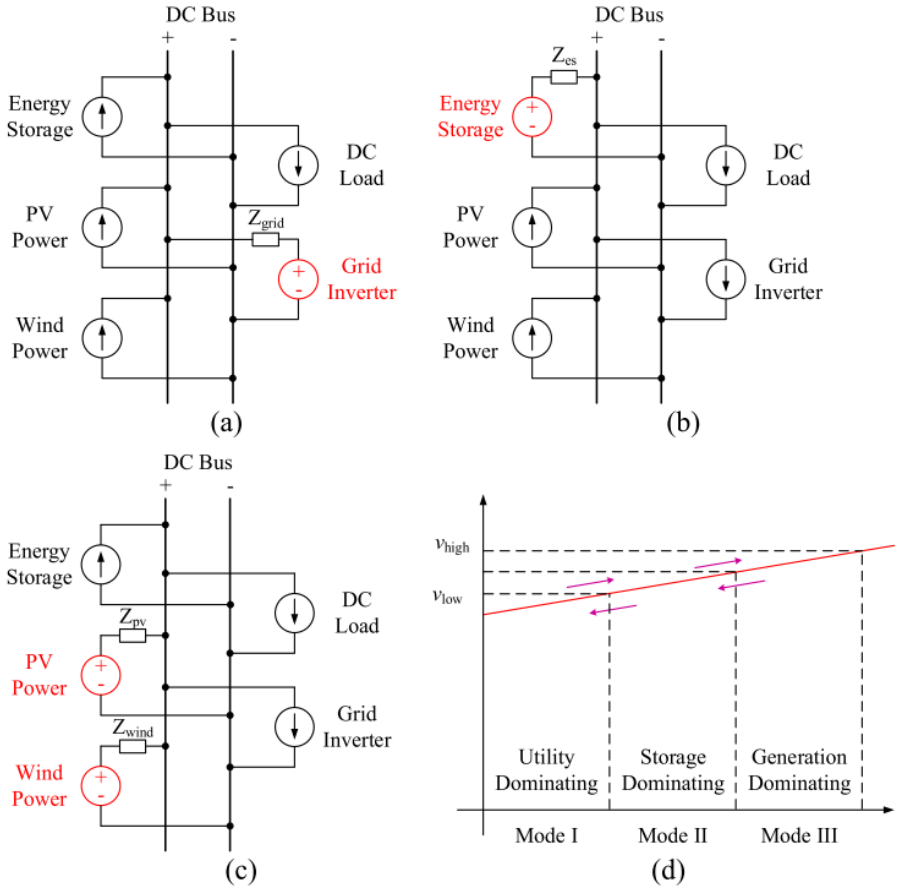

Figure 2-12 (a) Utility Dominating Mode (b) Storage Dominating Mode (c) Generation Dominating Mode (d) Operation Mode Selection [24]

To sum up all the methods above, it can be said that adaptive droop mode is preferred to be applied in distributed storage system for the rural area rather than conventional droop mode. The reason is that it gives better power-sharing performance for balancing load flow demands. On top of that, DBS can be applied for giving the instructions to the converter to operate on certain mode based only on local information.

3

Modelling Solar Home System

To generate the proper model of Solar Home System, some parameters have to be retrieved for design purpose, and the workflow of the modeling has to be executed in a proper sequence. Figure 3-1 illustrates the workflow of the conventional Solar Home System with the green lines as a representation of signal flow and black lines for power flow.

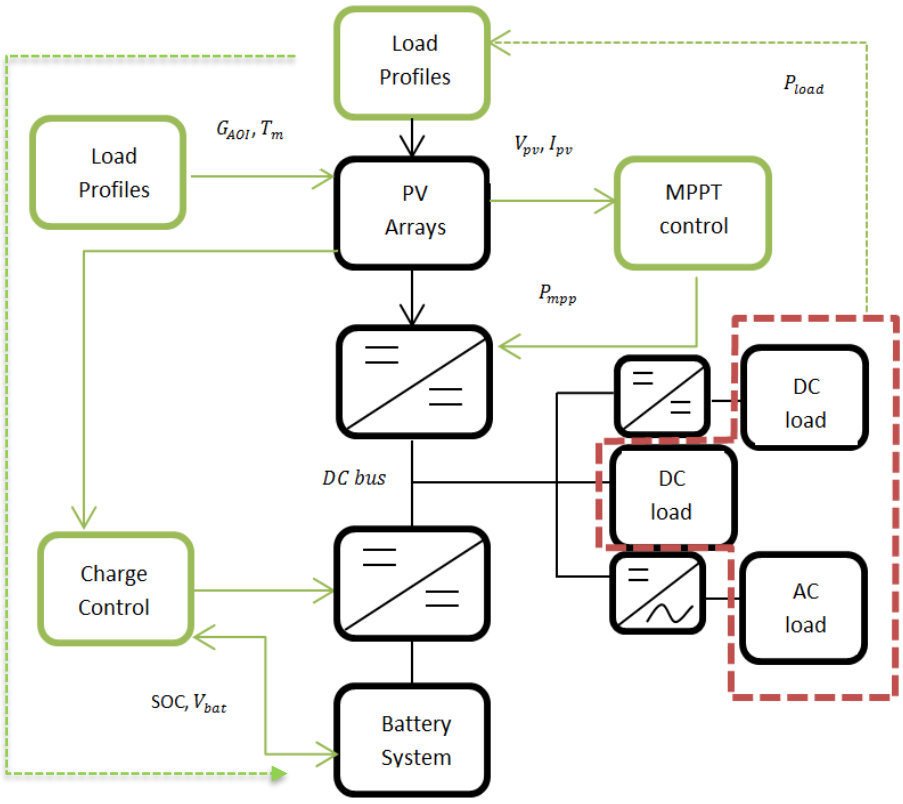

Figure 3-1 Solar Home System Modelling Workflow

The scope of the work in this research is limited to the usage of DC loads as it is assumed that the majority load in rural areas are generally in DC. However, it does not rule out the possibility of integrating AC loads for supporting community activities such as in irrigation and water pumping. Therefore, AC loads are also depicted in Figure 3-1 above. The main corresponded components in SHS design are load profiles, power converter, PV modules, storage system, and energy management which will be explained further separately.

The drawback of the conventional SHS illustrated above is the need for providing information signal on each converter through an additional communication network. It is seen that the charge control of the battery needs the information of PV power production and load profile at the corresponded time. This type of SHS is susceptible to the single failure in the system that might be occurred because of the future increased load demands. One failure in any component will lead to overall failure system operation because each of component needs the information from the other. Therefore, the proposed modular SHS should be able to independently operate without knowing the information on the common bus as depicted in Figure 3-2.

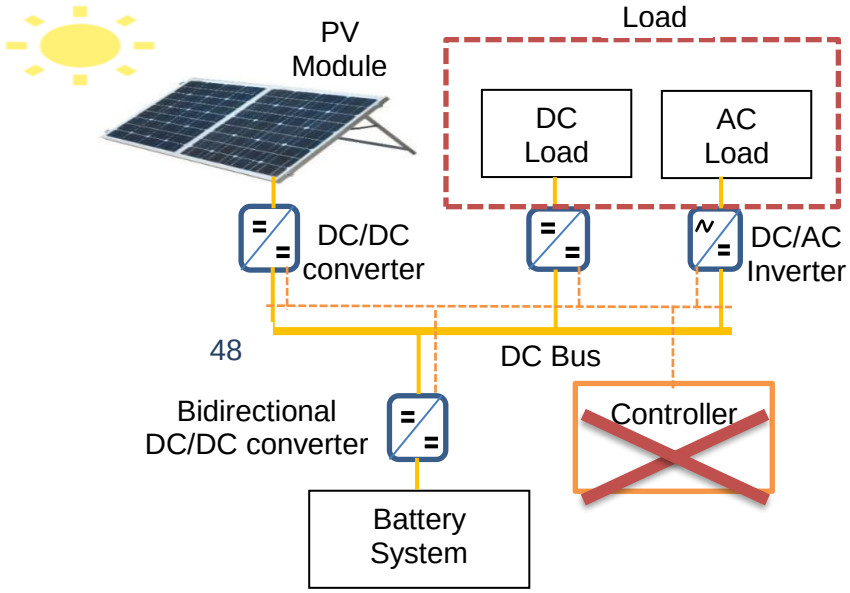

Figure 3-2 Modular SHS

3.1. Load Profiles

The initial step for developing the SHS model is by formulating the amount of energy consumption based on load profiles for each house. After that, the measured load data will be used for determining the number of solar panels, battery capacity and ratings of related components [1]. Load measurement is recorded every minute to generate sufficient amount of data for observing a sudden fluctuation in load demand. Based on recent load profile data, they are classified as low (±131 Wh), medium (±1242 Wh), and high power (±6255 Wh) consumption as presented in Figure 3-3 [4].

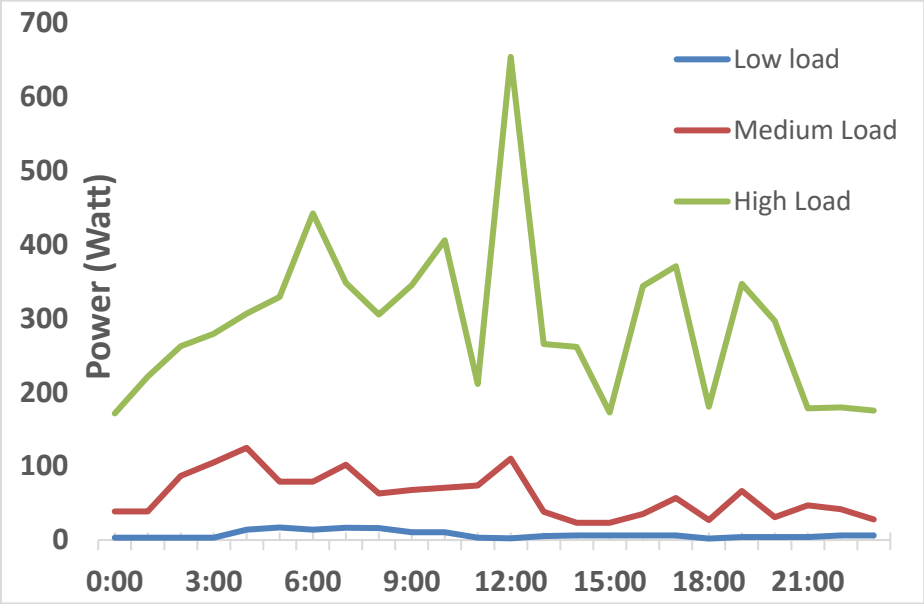

Figure 3-3 Load Profiles for 2017

From the generated load profile above, the load peak and daily energy consumption from each load consumption can be estimated. The first value is used for determining the required capacity of PV panel in the SHS, while the other one is for estimating the battery capacity. The load peak for each consumption level is presented in Figure 3-4 and the corresponding daily consumption is shown in Figure 3-5.

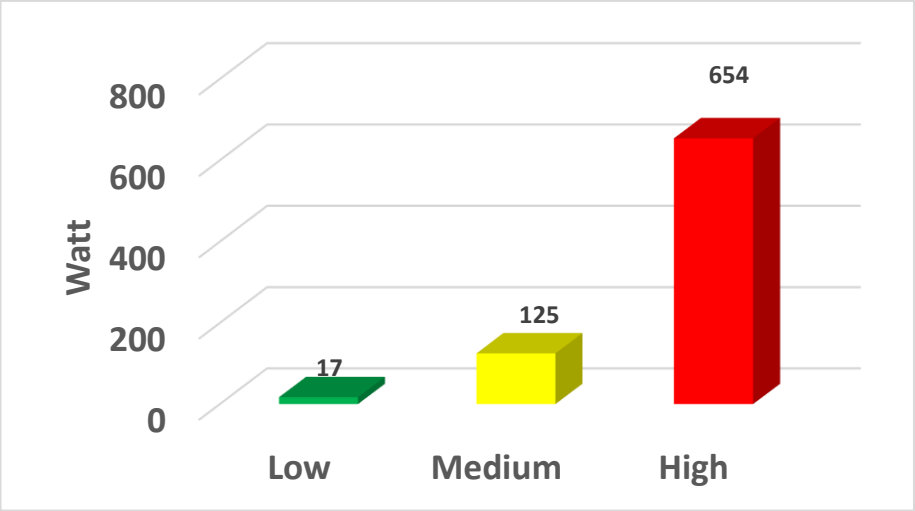

Figure 3-4 Load Peak for each Load Profile

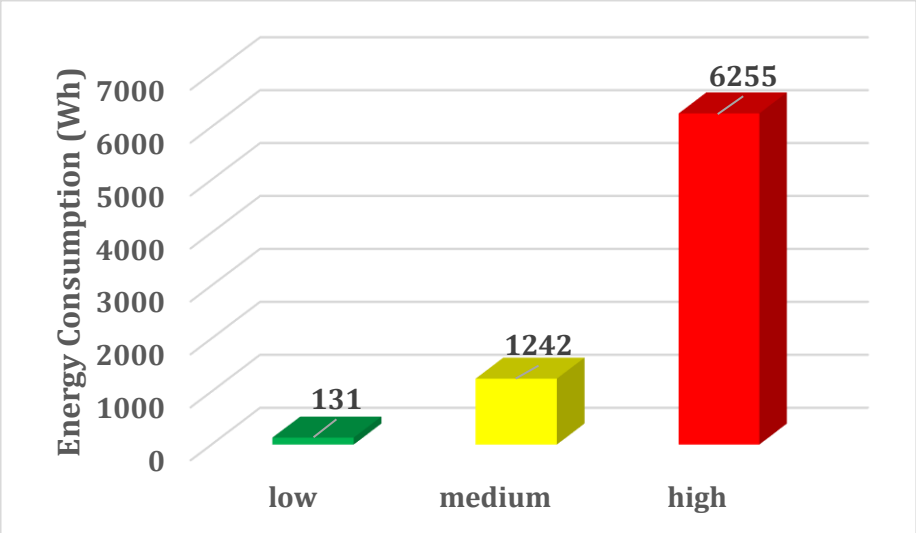

Figure 3-5 Daily Load Consumption

All the data presented above are taken from an average consumption of several houses with the same load consumption level. Hence, a slight variation in the load profile between two houses might occur. The additional load profile is not needed for single SHS operation that will be presented in this Chapter, yet it will be introduced in the later Chapter for interconnection model.

3.2. Components Modelling and Sizing

Solar Home System as an off-grid solution for electrification in rural area consists of independent components which are linked through the power lines. In general, they are classified into two different types based on their power flow behavior on the system itself. Unidirectional components are those who could only either generate or absorb power, in which including power sources and loads. Therefore, PV panels and electrical loads in this research are categorized as the unidirectional components. On the other hand, the components with both capability of generating and consuming power are labeled as bi-directional components. This component type represents storage system which can be charged or discharged, depends on the power condition of the system.

The method of components modeling in this thesis is done specifically to analyze autonomous power flow mechanism in DC grid. Therefore simplified model is performed rather than the physical model. Each component is coupled with its power converter block for maintaining the dc grid voltage stability because of the intermittent characteristic introduced by Distributed Renewable Energy (DRE). It is also efficiently reducing simulation time because the dynamics of switching phenomena is unregistered with the simplified block converter model. The same converter block model can be used both as the unidirectional or the bi-directional converter. When it works in power generating mode or as a power source, the current notation will be positive (+). Otherwise, negative (-) current is indicating the converter absorbs power from the grid.

3.2.1. Unidirectional Components

It is mentioned above that the unidirectional components modeled in this thesis are the loads and the PV panels. The modeling method for both components is not built up from the physical components. The potential power output from PV measurement and load demand are used as the input data for battery and PV block controller. The PV potential power is generated through some process illustrated in Figure 3-6 [29].

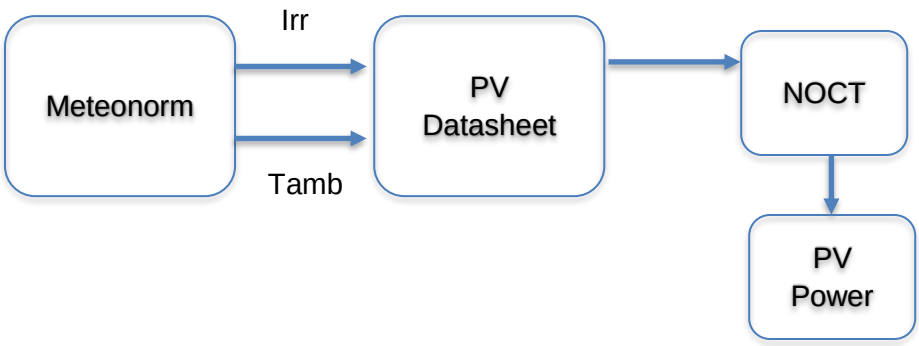

Figure 3-6 PV Potential Power Generator

The PV generator model above is developed to simulate the amount of power that can be produced by selected PV panel under specific irradiation level and ambient temperature. The ambient temperature will be an input for equation (5), while the irradiation level will be used for estimating the incident light current under Standard Test Condition (STC) based on manufacturer specification. However, the PV array in this research is modeled as a block of measured potential power from the fieldwork done in [4].

The input of PV model is the amount of power generated from one solar panel which multiplied by the total installed solar panel. Furthermore, the number of series and parallel composition can be adjusted to the voltage and current requirements. Although the output power from PV panel model is already generated, it cannot be directly used in in the system. The output power from the panel should be coupled with the DC/DC converter that regulates the output voltage of the PV array to meet the requirement of DC bus voltage. The block model of PV array with its converter is illustrated in Figure 3-7.

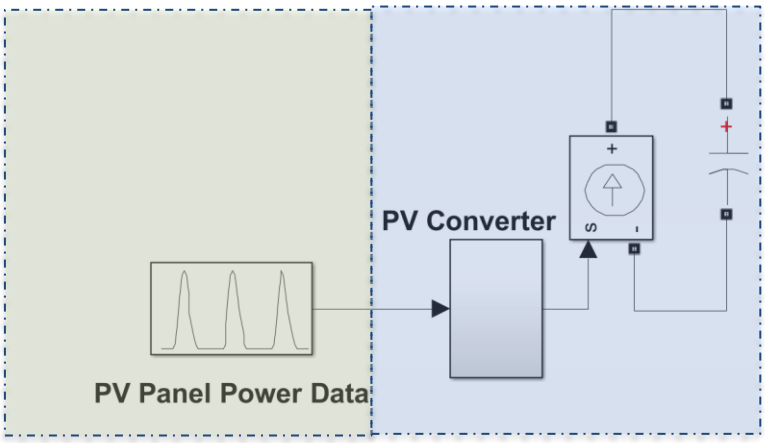

Figure 3-7 PV Generator Block Model

The location of PV system installation will affect the PV panel sizing and performance as it is determining the Equivalent Sun Hours of that area as depicted in Figure 3-8. The seasonal weather will also impact the performance of PV panel, as the PV power output may be above annual average in summer while it may be less than the yearly average in the winter.

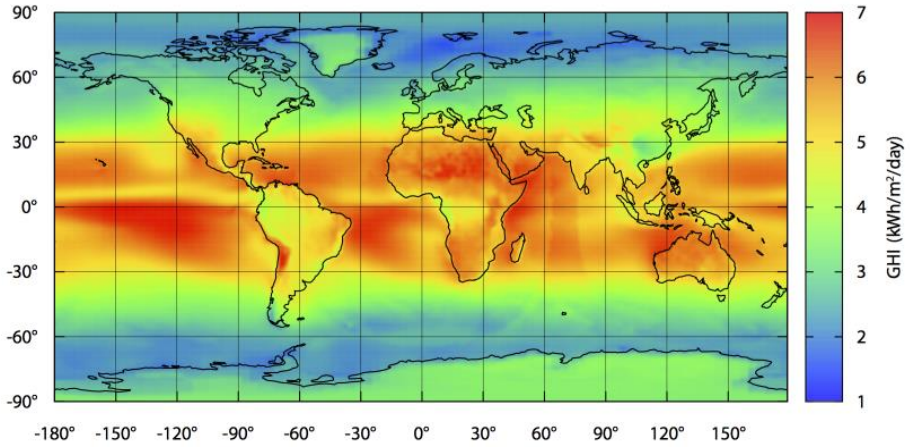

Figure 3-8 Equivalent Sun Hours of The World based on Average Global Horizontal Irradiance [30]

3.2.2. Bidirectional Components

The storage system is the substantial component in off grid power system for maintaining the power availability in the network due to its function either as a backup or as a load demand support. It serves as the main power provider for load at night or when the sunlight condition is limited due to an environmental condition. As the cost of the battery system took a huge part of initial expenses, the sizing of the storage system has to be done appropriately for avoiding oversizing or under sizing. The trade-off gap between cost and power availability can be minimized by taking into account the days of autonomy at the sizing process besides average sun hour and load profiles parameter. It tells the period where the PV system able to satisfy the load demand without primary generated power from PV array at that moment [30].

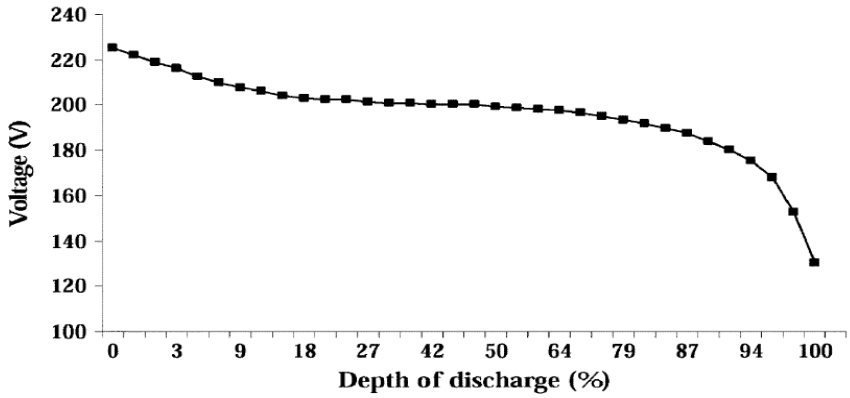

Figure 3-9 Depth of Discharge Characteristic of Battery [32]

The first step of sizing the minimum battery capacity is by summing up the total load demand whether AC or DC load expressed in Ampere-hour (Ah) with the PV system losses. The later parameter describes the amount of energy consumed by certain components such as charge controller and the battery itself to operate their tasks [30]. After that, the daily Ah requirement should be multiplied by some autonomy days which is variously based on the priority of the load. To maintain the battery lifetime, it should be noted that the battery should not be completely depleted and overcharged simultaneously. Hence by employing a nonlinear relation between battery depth of discharge level and battery voltage level as illustrated in Figure 3-9, it can be concluded that the battery State of Charge (SOC) should not surpass 80 % of battery capacity for the best battery life [31]. Therefore, the final step is by dividing the amount of load demand which has already taken autonomy days into account with the usable capacity of the battery. As a result, battery capacity in this model is selected to be 40 Ah.

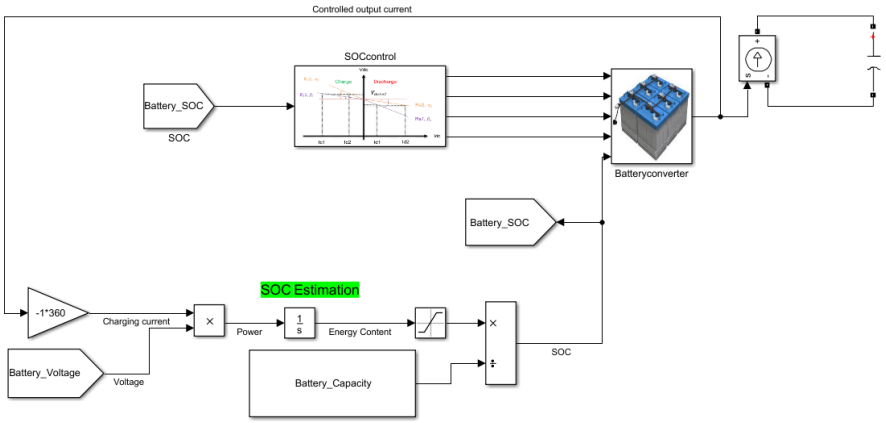

Figure 3-10 Battery Model

Storage unit with its related bi-directional converter is modeled as one subsystem block depicted in Figure 3-10. The input parameter of the block is not the same as PV block model, as it is expected that the communication link in the SHS does not exist. As a result, the power difference between power sources and loads that should be supported by batteries could not be informed. The current output of the battery is controlled according to the voltage level of converter terminal and their respected SOC, which will be explained further in Chapter 4. A mathematical model of the battery is selected for simplicity of calculation and rapidity of the simulation, rather than using the chemical model of the battery. Thereupon, the SOC estimation as in Figure 3-10 is calculated from [32]:

$$SOC_i(t) = SOC_i(0) - \int_0^t \eta_i \frac{I_{BAT,i}(\tau)}{C_{BAT,i}}(\tau)d\tau \quad (5)$$

$SOC_i(0)$ is the initial level of battery SOC, η_i is the discharging and charging efficiency, $I_{BAT,i}$ is the battery output current which is controlled by the converter, and $C_{BAT,i}$ is the capacity of the battery. In this model, the efficiency of charging and discharging process is assumed to be ideal.

3.2.3. Components Sizing

As the load profile has been generated and the components modeling method has been determined previously, the next step of building the SHS is determining the components capacity based on the demand. The highest load peak from high load demand is considered as the base for determining the PV module capacity. The reason is because by assuming that if the high load demand is fulfilled, the lower load demand will be covered as well. Thus, the expected PV module requirement is at least 654 Wp. However, the designed system should not only fulfill the consumer's demand but also conform the regulations. According to IEEE standards in [33], the suitable operating voltage for PV systems in a rural area is 48 V. Furthermore, it is also stated that the maximum power allowed in 48 V system should be less or equal than 400 Watt. As a result, the PV module power rating to be installed on the rooftop is 400 Wp.

Knowing that the installed PV capacity would not be able to fulfill the highest load demand, it can be predicted that a stand alone SHS is not suitable for those consumers level. Therefore, solutions for this issue will be presented in Chapter 4 of this thesis. Even the PV capacity has already failed to satisfy one of the load demand, the battery capacity still needs to be determined for the rest of the consumers. The steps of battery sizing calculation are conducted based on [30]. First of all, the daily energy consumption is divided with the nominal voltage operation. Here, the medium load demand is taken instead of the highest one due to the same reason as PV module selection above. After that, the autonomy days is decided depends on the amount of the day when the sun might not shine. The average autonomy days for region of Asia is about 3 days based on, however the amount of 2 days is considered to be more realistic by the author for worst-case scenario. Then, the result of multiplication between total energy requirements and autonomy days is divided with the allowed usable battery capacity. Although the battery usage is not limited from the perspective of the author as a system designer, the limit of 80% is taken as the common limit regulated by battery companies. The amount of PV module and battery capacity calculation are summarized in Table 3-1.

Table 3-1 PV Module and Battery Sizing

PV Panel Sizing		
load peak	654 W	
Low Power Limit	400 W	
Selected PV capacity		400W
Battery Sizing		
Nominal Voltage (V)	48	
Daily Energy Requirements (Wh)	1242	
Daily Energy Requirements (Ah)	25.875	
System Losses (10% * Daily Energy Requirements)	2.5875	
Total Energy Requirements (Ah)	28.4625	
Reserve time days	2	
Total Energy Requirements (Ah) * Reserve Time	56.925	
Usable battery capacity (80%)	71.15625	
Selected Battery Capacity	48	72Ah
		3500Wh

The amount of PV power yield over the one-day period is presented in Figure 3-11 with hourly data sampling interval. As we can see in the graph, there is an increase in PV power yield around 6 am in the morning as the sun is rising and reach its peak at around 11 am. After that, the power output is decreasing along the sunset and stop generating power at around 6 pm. The investigated area is located near the equator line and does not take into account the seasonal weather changes. The average weather is mainly sunny, and it can be assumed that the annual PV characteristic will be approximately equal to each day during the one-year period.

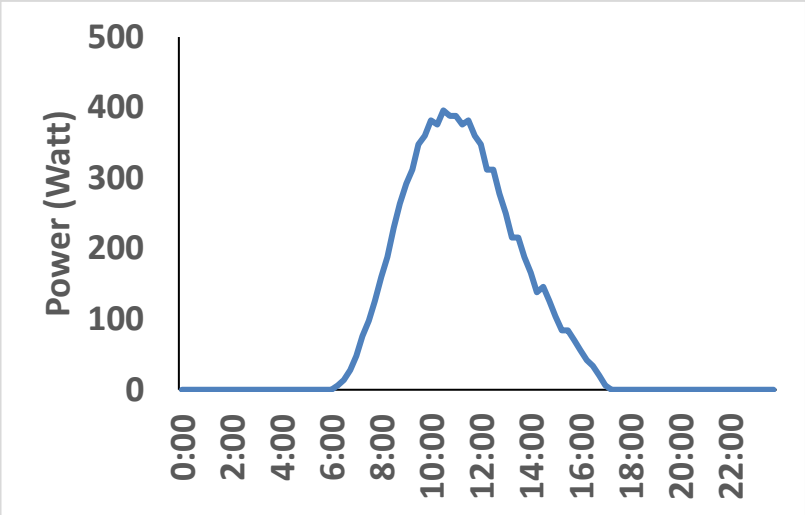

Figure 3-11 Solar Panel Measured Power

3.3. Energy Management of Solar Home System

The common electrical network should consist of generation, transmission and distribution system to be categorized as an electrical power system. Each of this system should be able to work simultaneously for producing a good power quality even they have their function differently. Thereupon, energy controller has a significant role in the coordination process of the electrical system, not to mention the importance of decentralized system control in nano-grid.

Energy management & control is crucial for maintaining power availability in the presence of intermittent power generation of renewables. It is appropriate for the PV system which has a dynamical character over environment conditions such as temperature, irradiance, and shading factor [2]. Moreover, the battery input and output current at charging and discharging process should operate at its designed limit for optimal function. It can be said that the energy management and control are the communicator and brain of the system that coordinates the power flow between energy sources, storage system and loads. For the decentralized control algorithm, the power flow is controlled based on the local measurement parameter in the converter terminal which will be explained further in the next sub-Chapter. Despite the absence in communication line for decentralized control method, the power flow in the local SHS can be categorized into several modes [34] as illustrated in Figure 3-12

a) *Power from PV array is far greater than load demand*. At this rate, the controller will send the excess power to the storage system. So, the available power from sources is not only used for supplying load, but also for charging

the storage system. This operation mode normally occurs at the daytime where the sun intensity is at its maximum.

b) *Power from PV array is equal to the load demand.* The controller will set the generated power only to satisfy the load demand. Hence the storage system is assumed to be fully charged in the previous operation mode. This pattern may happen in the afternoon when the sun is started to going down and resulted in a decrease in the output PV power while the load profile is not changing significantly.

c) *Power from PV array is less than the load demand due to the drop in PV*. When the PV output drops significantly, the DC-DC converter unable to maintain the output voltage under allowed operating conditions and resulted in PV array disconnection. Under this condition, the power deficiency will be backed up by the power from the battery system. Therefore, the discharging process is taken place and decreasing the SOC level of the battery.

d) *Power from PV array is less than the load demand due to sudden load increase*. On the contrary with the previous condition, under this form, the output of PV array is still in the operating conditions. The Power from PV is not sufficient due to the sudden increase in the load demand, which will be compensated with the additional power from the battery system. As a result, the PV and battery system will work together to comply the load demand.

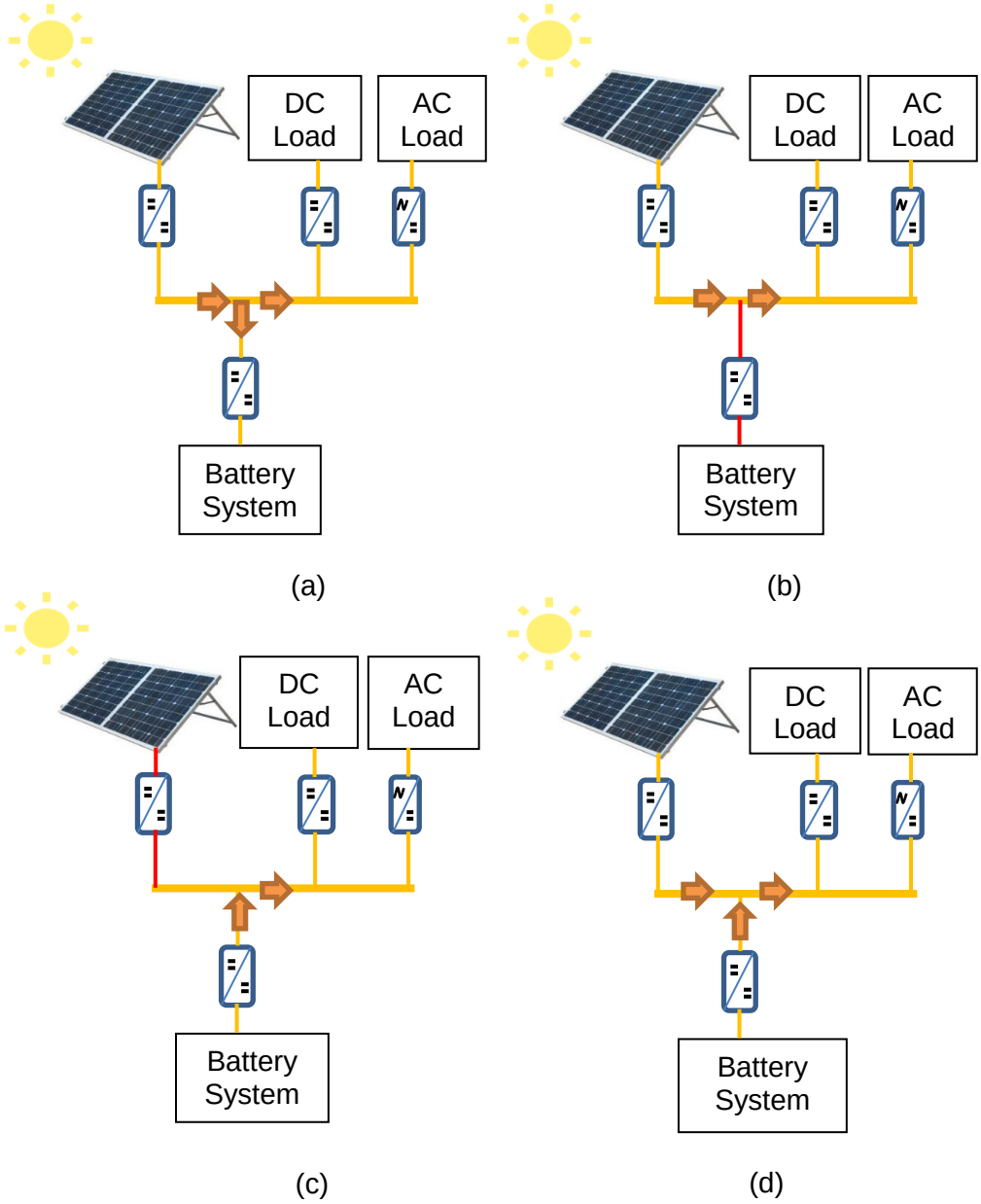

Figure 3-12 Power Flow in SHS

After each component of SHS has been correspondingly modeled with their converter, they are then put together as an example of one independent house. One can be categorized as an ideal SHS if it is fully equipped with its PV panel and storage system. The illustration of one ideal house is illustrated in Figure 3-13.

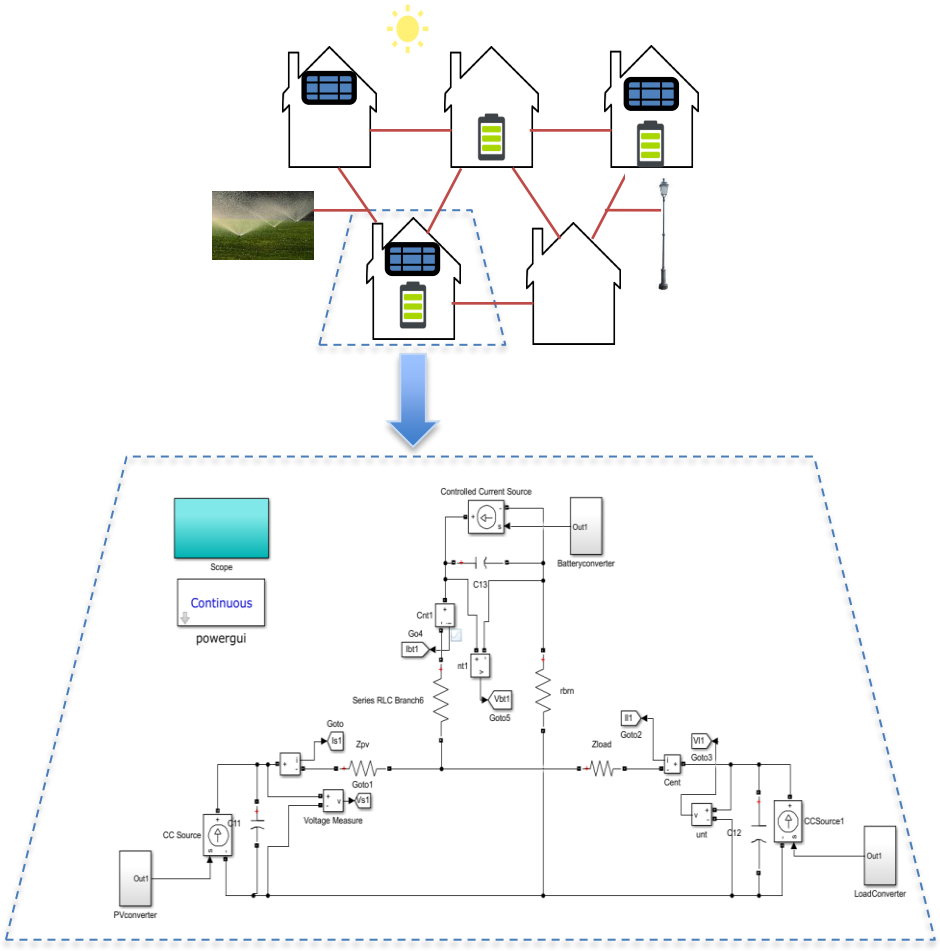

Figure 3-13 Model of Ideal SHS Unit

Each of the converter blocks is already equipped with the independent controller that will adjust its output current according to the terminal parameters condition. The combination of DBS and adaptive droop control can give a better performance of distributed power management in rural areas by providing equal power-sharing between multiple batteries only on local measurement. Thus, the power flow in the SHS will be determined according to the proposed controller. As a result, each converter can work seamlessly as a unit without the need to know the information of others. The proposed controller consists of two level control method which is primary controller and additional adaptive controller.

3.3.1. Primary Decentralized Controller

The concept of primary controller proposed in this research is designed for fulfilling the requirements of local interconnected houses, which are:

- Independent
- Low Maintenance
- Flexible for plug and play properties

These requirements had been identified to compromise some of the issues analyzed in research background of this work. The output current from each converter is determined with consideration from 3 basic control. These three basic controls are a current limiter, droop control, and constant power. They are regulated according to the local parameter such as voltage level at converter output. Thus each converter keeps the control independent yet provides flexible operation. The primary controller is modeled as a Matlab function block that changes its output value based on input parameter assigned. The block controller is illustrated in Figure 3-14

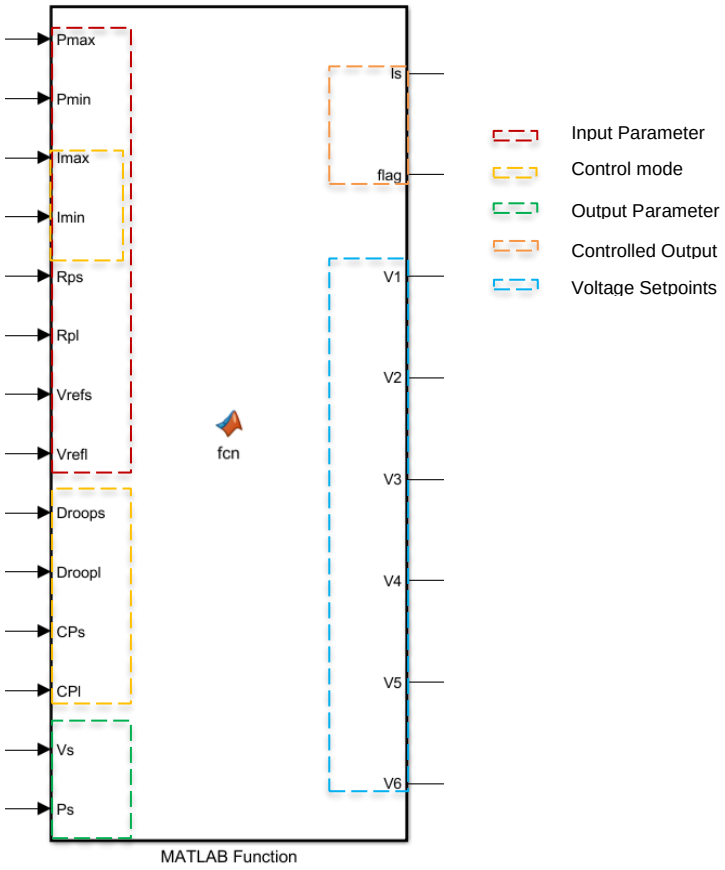

Figure 3-14 Primary Decentralized Controller

First of all, the process starts from the output parameter measurement. Then, current output calculation is determined according to a control mode in which

depends on the voltage terminal from the measurement. The voltage output level is then compared with the voltage set point to be categorized. Voltage set points are initialized based on [35] as depicted in Figure 3-15, thus classifying operation mode of the converter into 7 modes

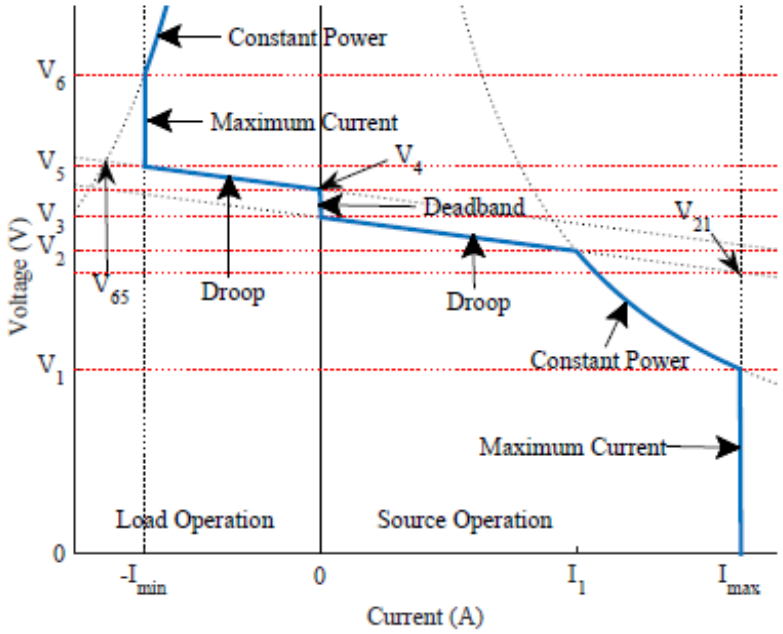

Figure 3-15 Voltage Set Points for Different Operation Modes [38]

first of all the *V*0 is the intersection point when the current output is set to be maximum:

$$V_0 = 0 \tag{6}$$

If the voltage keeps increasing until a certain point which is defined by *V1*, the converter goes into constant power mode:

$$V_1 = \frac{Pmax}{Imax} \tag{7}$$

Pmax is the maximum potential power from the source of energy, which is PV in our case. Thus, the value will keep changing as it depends on the light intensity at particular time. Imax is the maximum current that is set on the converter. As a result of varying *Pmax* value, the curve for constant power mode will also keep shifting. After that, converter goes into droop operation mode when the voltage reaches *V2*:

$$V_2 = \frac{Vref_s + \sqrt{Vref_s{}^2 - 4\,Pmax_s * Rps}}{2} \tag{8}$$

$Vref_s$ is the desired voltage reference for power source, *Rps* is the chosen droop gain for source operation mode. When the voltage is too high for power source converter to operate, it switches off the current flow for device protection and current goes to zero. The voltage level where the current goes into zero is defined as *V3*:

$$V_3 = Vnom - \frac{V_{deadband}}{2} \tag{9}$$

Where $Vnom$ is the nominal voltage when the grid current is zero, $V_{deadband}$ is the voltage range where the current stays zero. On the other hand, the deadband shows the range of allowed voltage deviation in the related system. Uni-directional converter is not affected by this deadband, however bi-directional converters need to have it for the transition between source and load operation mode. When the grid voltage reaches the upper limit of the deadband voltage, the converter starts to operate as a load converter with the droop mode marked by *V4*:

$$V_4 = Vnom + \frac{V_{deadband}}{2} \tag{10}$$

*V*5 is the point where the converter shifts to a maximum current mode for absorbing power:

$$V_5 = V_{refl} - I_{min} * Rpl \tag{11}$$

V_{refl} is the desired voltage reference for load operation mode, I_{min} is the maximum current allowed by converter when absorbing power, Rpl is the droop gain for load side. The highest voltage limit is the signal when the converter goes into Constant power load operation marked by *V6*:

$$V_6 = \frac{Pmin}{Imin} \tag{12}$$

According to the method of defining voltage set points as illustrated in Figure 3-15, operation points for each converter is determined. The PV converter should be set as the upper limit of DC nano-grid operation voltage, as it is assumed to be the only power generating source. On the other hand, the load converter sets the lower voltage that is allowed within the system. The reason is that load converter should only absorb power according to the load profiles. The battery converter operates in between of the PV and load converter voltage range, as it works in a bidirectional way. The defined operation points for each converter is illustrated in Figure 3-16.

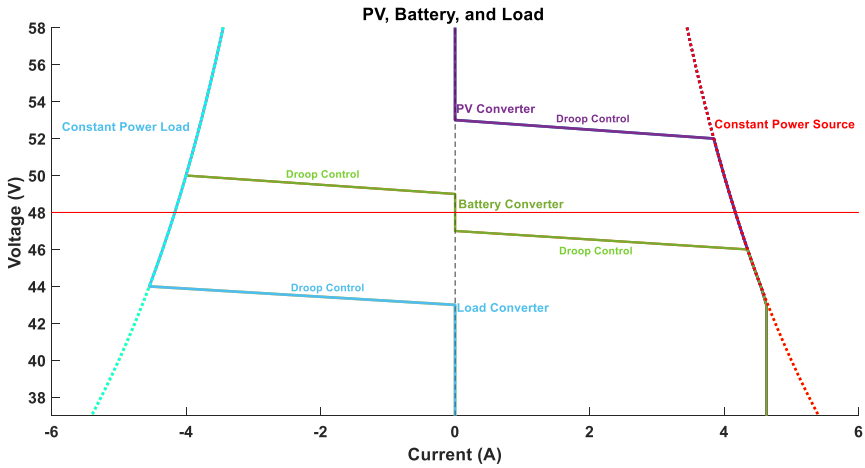

Figure 3-16 Converter Operation Modes

After voltage at the output terminal (V_s) of the converter is measured, the current output (I_s) for the next cycle is calculated according to the voltage level of Vs as depicted in Figure 3-17.

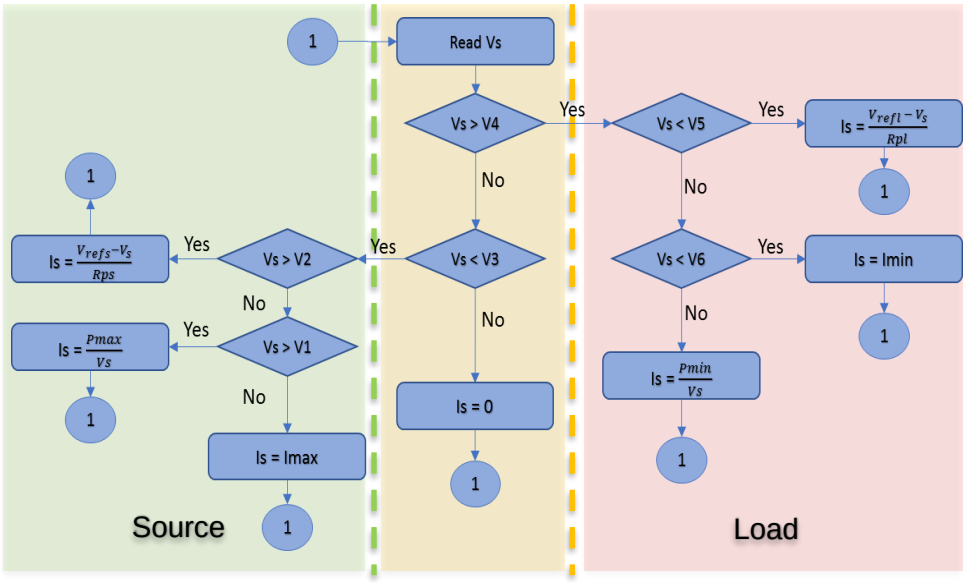

Figure 3-17 Current Determination

In general, the flowchart explains output current calculation according to the terminal voltage condition at that time. Every time the current output has been calculated, the controller will repeat the process from reading the terminal voltage. Thus, any voltage deviation in converter's terminal could affect the converter to shift their current output independently without any need of information exchange with their neighbor. Once the voltage has been categorized in which set point it belongs, the current output will be calculated according to its operation mode. The

converter calculation model for constant power mode is illustrated in Figure 3-18, and model for droop mode is presented in Figure 3-19. Diverse current calculation for source mode and load mode of the converter is summarized in Table 3-2.

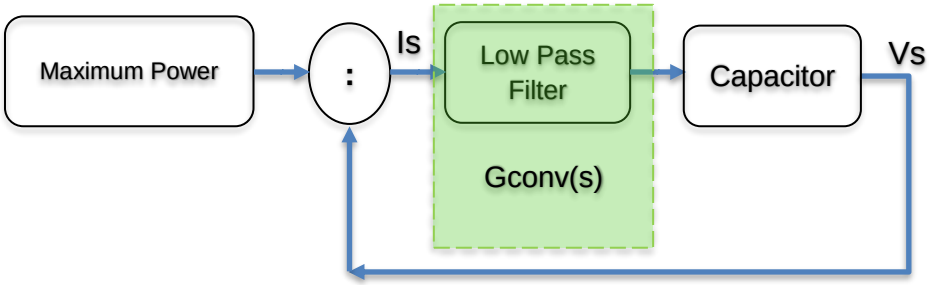

Figure 3-18 Constant Power Controlled Models

Maximum power is a value assigned in the converter for indicating the highest power capability of the component. While its value for the battery is fixed, the value for PV and load might vary due to the dynamic characteristic of their power. It means that even the highest value of the converter has been assigned, the taken maximum power value on the model above is related to the corresponding power at that time. PV operation is the example of changing maximum power, as it follows the curve of the MPPT tracker.

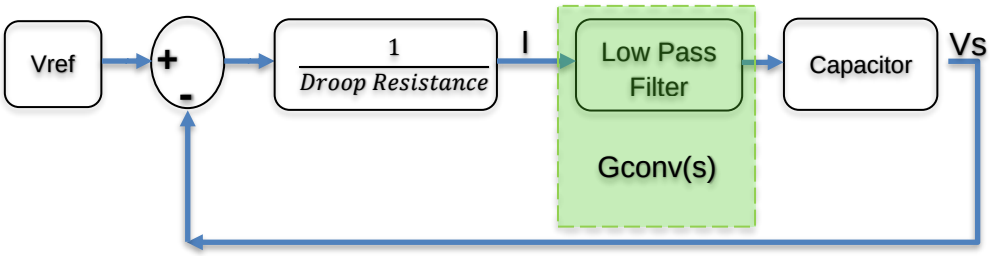

Figure 3-19 Droop Controlled Models

Vref is the desired voltage limit operation either for the source or load components as described in equation (8) and (11) previously. The droop resistance for source side operation is denoted by *Rps* as mentioned in equation (8) and depicted by *Rpl* when operating for load side. Gconv(s) denotes the converter's dynamics response of the current, which is modeled as a low-pass filter in the model.

Table 3-2 Current Calculation for Different Operation Mode

Converter mode	Current in Source side (Is)	Current in Load side (Is)	
Maximum Current	Imax	Imin	(13)
Constant Power	$\frac{Pmax}{Vs}$	$\frac{Pmin}{Vs}$	(14)
Droop	$\frac{Vref - Vs}{Dsource}$	$\frac{Vref - Vs}{Dload}$	(15)

3.3.2. Additional Adaptive Controller

Aside from the primary control, additional control should be given for bi-directional electrical power component such as for storage system. The idea behind this extra control is for adapting the power flow amount of the battery based on the local SOC level. Each of the battery converters can independently limit and controls the amount of power that can be absorbed or inject with regards to balance in power-sharing mechanism between batteries. To cover all the three converter operation modes, two additional controllers are applied in this research. The adaptive current limiter is applied for maximum current and constant power mode, while adaptive droop control is requested droop operation mode.

Seeing that the primary controller algorithm proposed in this research is using terminal parameters of the converter, the objective of the additional controller is for shifting those parameters according to the battery SOC. This can be done by multiplying those parameters with variable generated from the additional controller. Therefore, the term of adaptive is used because the additional controller is constantly changing its output value according to each battery capacity level. Just like the primary controller, MATLAB function block is also used for the adaptive controller as depicted in Figure 3-20.

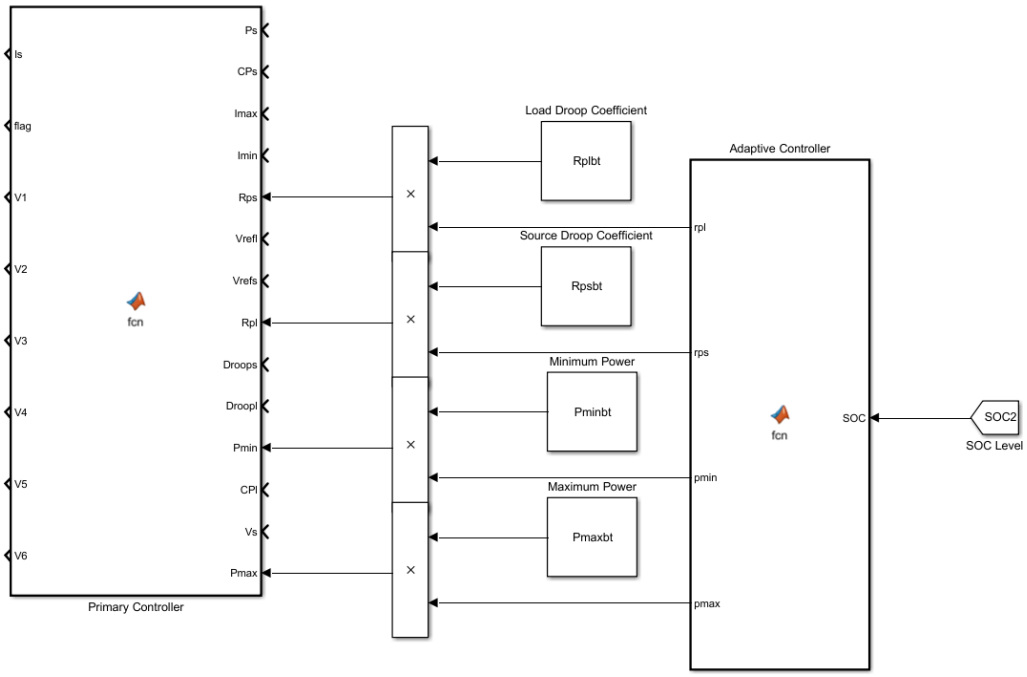

Figure 3-20 Adaptive Controller

3.3.2.1. Adaptive Current Limiter Based on SOC

In real life, people tended to use as much power as possible due to the increase in power demand and resulted in depleted battery capacity. Even more, the fully charged battery may be left while still plugged into the charging station for an extended period. Hence, the converter initially sets the limit of the battery power capacity that can be used to preserve the age of the battery itself according to the indicator stated by SOC and Depth of Discharge. The current limiter works for discharging and charging process of the battery as depicted in Figure 3-21.

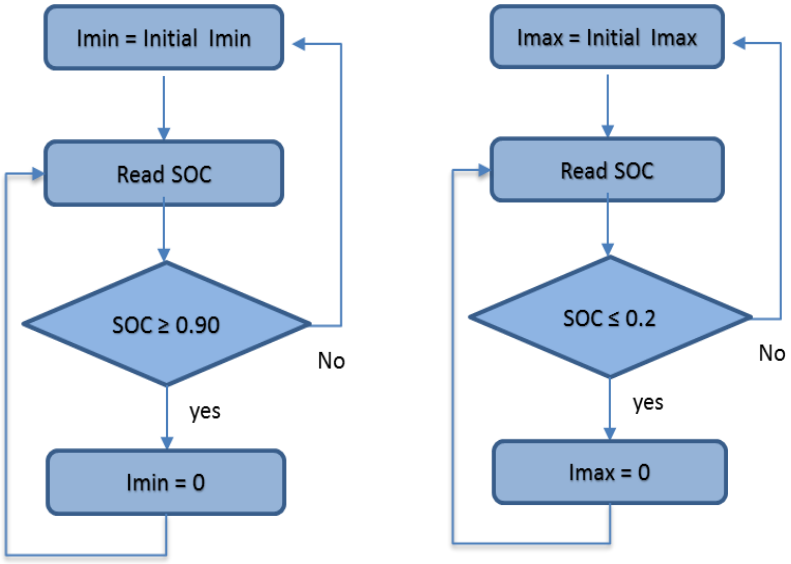

Figure 3-21 (a) Current Absorbing Limiter (b) Current Injection Limiter

At the moment when the SOC of the battery reaches the limit, the converter sets the amount of maximum current injection and maximum current absorption to zero under maximum current operation mode. Furthermore, the amount of generated or absorbed power in constant power operation mode also turn into zero as the current flow is blocked. Therefore, the converter will prevent the battery from overcharged or overused which results in maintained battery life expectation time.

3.3.2.2. Adaptive Droop Control Based on SOC

Flexible expansion of loads in SHS has been identified as one of the advantages due to the plug and play properties of the DC system. However, it will be better if also escorted by the increase of storage capacity for more stable operation. Furthermore, a healthy life cycle of the battery needs to be maintained by keeping the depth of discharge as small as possible [36]. Therefore, introducing new battery string into the existing storage system would bring new issue due to the different battery condition at the corresponding time. Battery for an isolated system such as in SHS will mostly operate in droop region which depends on the Virtual Resistance (VR) of droop controller [32]. Hence, It is not feasible to use the same VR for battery with different SOC level, even the slightest one. The lower one will be depleted sooner and resulted in bad lifecycle operation. The ideal mechanism for equivalent power operation is by allowing the battery with lower SOC to be charged more while discharged less. On the contrary, to be charged less and discharged more for the higher one. Since the droop resistance is applied in both operation mode of the battery, the droop resistance for charging is denoted as R_l and R_s for discharging mode. l is used under charging mode because the battery

acts as a load, while s is for discharging mode because it represents the power source. As a result, SOC dependent adaptive change of VRs is proposed for charging operation according to:

$$R_d(SOC) = R_d * SOC \tag{16}$$

While the discharging operation with:

$$R_d(SOC) = \frac{R_l}{SOC} \tag{17}$$

$R_d(SOC)$ and R_d are the new value of droop resistance and the initial value of droop resistance.

From equation (16), it is fulfilled that the new charging droop resistance is proportional to the SOC level of the battery. On the contrary, equation (17) shows that the new discharging droop resistance is inversely proportional to the SOC level. As also already illustrated in Figure 2-8, slight slope of droop value allows the current output to be increased significantly rather than the steeper droop value. Thus, it is suitable for applying smaller slope of battery with lower SOC under charging mode. Conversely, the slighter slope is better to be applied to a battery with higher SOC under discharging mode. Below, Figure 3-22 depicts the concept of droop shifting method between 2 batteries with $SOC_2 > SOC_1$.

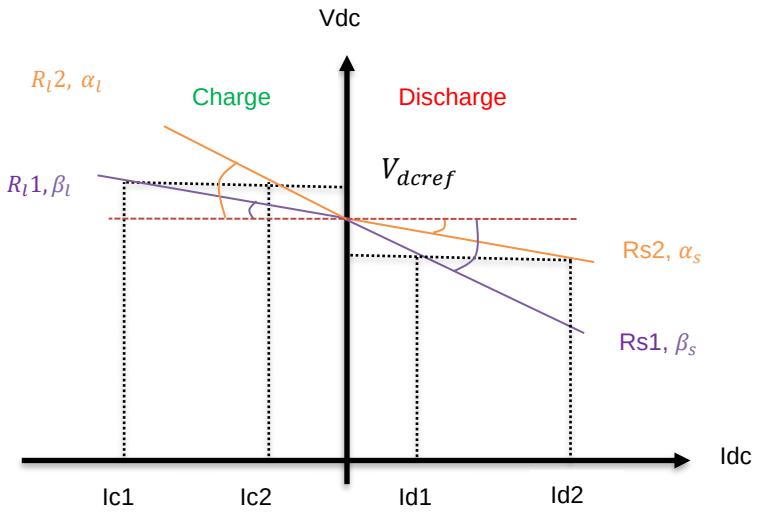

Figure 3-22 SOC Dependant Droop Control

where

R_l1 = Charging Droop Resistance of Battery 1
R_l2 = Charging Droop Resistance of Battery 2
R_s1 = Discharging Droop Resistance of Battery 1
R_s2 = Discharging Droop Resistance of Battery 2
β_l = Charging Droop Slope of Battery 1
β_s = Discharging Droop Slope of Battery 1
α_l = Charging Droop Slope of Battery 2
α_s = Discharging Droop Slope of Battery 2
SOC_1 = Battery 1 State of Charge level
SOC_2 = Battery 2 State of Charge Level

On the discharging side, it can be seen that battery 2 has smaller droop slope rather than battery 1. Hence, battery 2 will generate more power than battery 1 due to its higher SOC level. On the other hand, battery 1 has smaller droop slope than battery 2 under charging mode. This results in more power absorbed on battery 1 than on battery 2 due to its lower SOC level. The method proposed for shifting the charging droop value is by multiplying the initial droop value with multiplication factor assigned by:

$$R_l(SOC) = R_l * ((1 - mf) + (mf * SOC)) \quad (18)$$

While the relation for discharging droop is:

$$R_s(SOC) = R_s * (1 - (mf * SOC)) \quad (19)$$

Where, mf is the constant droop multiplier value when the battery is full (SOC =1) under discharging mode and when the battery is empty (SOC = 0) under charging mode. Example of shifted droop calculation with the proposed method is shown in Table 3-3 below with initial *Rpl* and *Rps* value of 1. Moreover, the illustration of linear droop multiplication for charging and discharging mode are presented in Figure 3-23 and Figure 3-24.

Table 3-3 Droop Shifting Value

SOC	Rs	Rl	mf	Rs(SOC)	Rl(SOC)
1	1	1	0.6	0.4	1
0.9	1	1	0.6	0.46	0.94
0.8	1	1	0.6	0.52	0.88
0.7	1	1	0.6	0.58	0.82
0.6	1	1	0.6	0.64	0.76
0.5	1	1	0.6	0.7	0.7
0.4	1	1	0.6	0.76	0.64
0.3	1	1	0.6	0.82	0.58
0.2	1	1	0.6	0.88	0.52
0.1	1	1	0.6	0.94	0.46
0	1	1	0.6	1	0.4

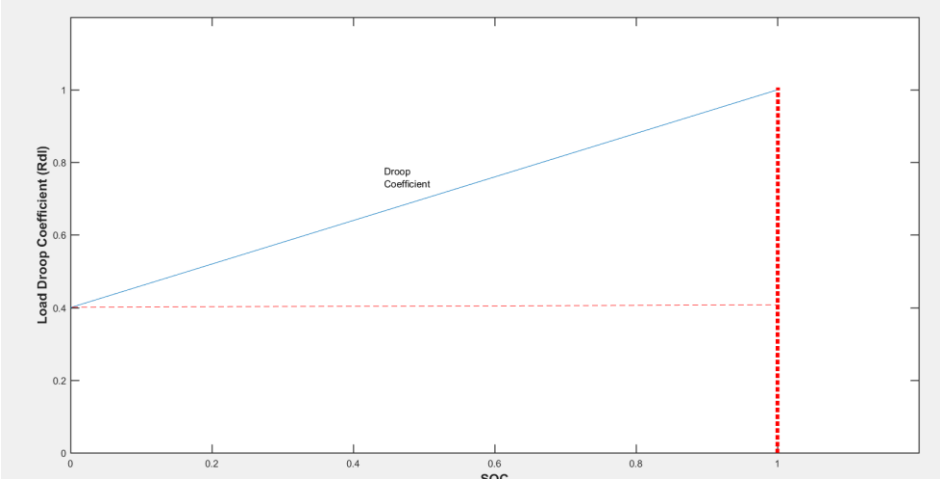

Figure 3-23 Linear Charging Droop Multiplication Factor

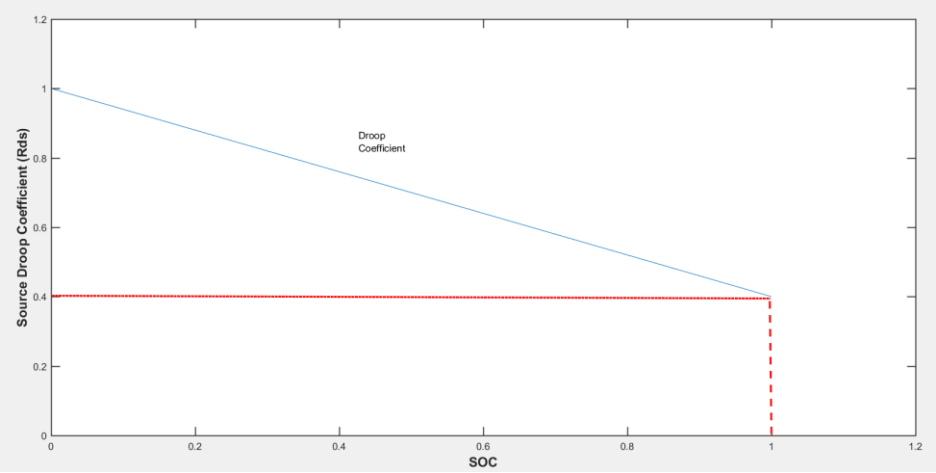

Figure 3-24 Linear Discharging Droop Multiplication Factor

As a result of applying the additional droop controller to the block converter with different level of SOC as projected in Table 3-3, the battery converter operation modes illustrated in Figure 3-16 has been varied as shown in Figure 3-25.

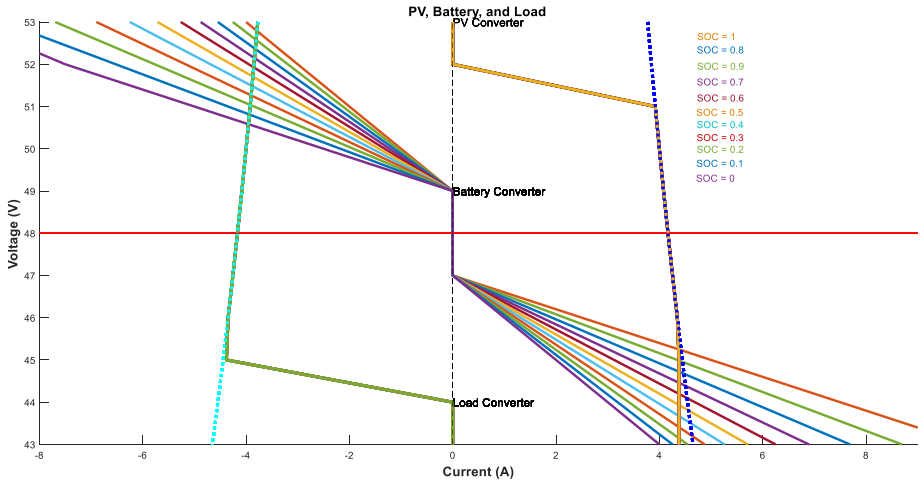

Figure 3-25 Battery Droop Variation

3.4. Solar Home System Operation

The initial step of analyzing the power transfer mechanism between interconnected SHS is performing the simulation of individual SHS. By doing this, the proposed controller method can be tested whether it is doing its function in a single house system. Mainly, the primary decentralized controller which act as local controller should be able to regulate the power flow between PV panels, Battery, and loads. Additional component applied in this model is the impedance of the wiring which simplified as a single resistance (R) circuit between elements and a DC-link capacitor for higher power density [37]. The simulation is executed by defining parameters above in the MATLAB file that will refer to the Simulink block presented in Figure 3-26 below. The performance of the SHS is monitored for one full day with sampling data every 15 minutes for faster computation time.

Table 3-4 SHS Parameters

Parameters	Nominal
Battery	
Power Capacity	72Ah
Voltage	48
Initial SOC	85%
Droop Resistance	0.01
PV Panel	
Voltage	48
Power Capacity	400 Wp
Droop Resistance	0.01
Loads	
Nominal Voltage	48
Total Consumption	1242 Wh
Load Peak	125 W
Droop Resistance	0.01
Line Resistance	0.07 Ω
Line Inductance	0.5 µH
DC Link Capacitor	5 µF

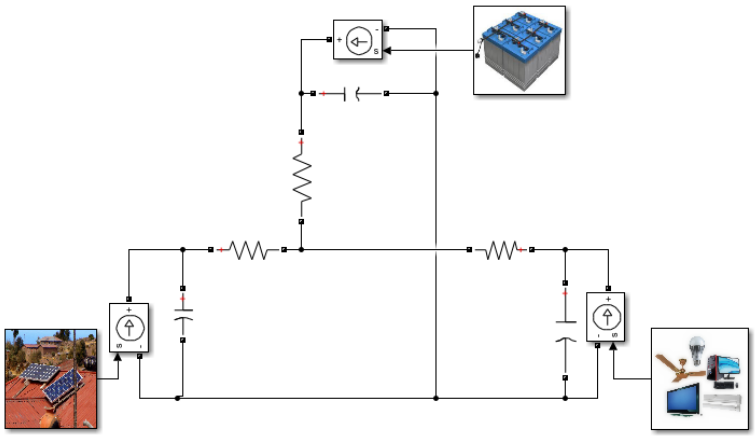

Figure 3-26 SHS Operation Model

Nominal voltage for rural SHS is selected to be 48 V according to [33] with the allowed ± 10% of voltage deviation [27]. As a result, the operating voltage of the SHS should be between 45.6 V and 50.4 V. Hence, every converter coupled with power components in the network should be given current limiter for maintaining their operation under allowed voltage range. The specified current limit for each converter is provided in Table 3-5 below. To avoid misunderstanding, positive (+) sign is determined by the current going out from the converter to the network. On the contrary, the negative (-) sign shows that the current going into the converter from the network.

Table 3-5 Current Limit

Converter	Current Limit (A)
PV	9.259
Battery	± 9.259
Load	-9.259

According to system parameters in Table 3-4 and Table 3-5, the voltage set points can be calculated based on equation (7) – (13). Hence, this voltage set points will determine the converter current output as presented in Table 3-6. Due to various aspects that need to be monitored, simulation results are illustrated separately. Figure 3-27 represents the converter operation mode, Figure 3-28 shows the voltage level at the terminal output converter, Figure 3-29 Illustrates the controlled output current of the converter and Figure 3-30 reflects the SOC level of the battery.

Table 3-6 Voltage Set Points

Voltage Set points	Mode	Converter Mode	PV	Battery	Load
V0	0	Max Current	≤ 43.2	≤43.2	-
V1	1	Constant Power Source	43.2	43.2	-
V2	2	Source Droop	52.7	46	-
V3	3	Zero Current	53	47	≤43.2
V4	4	Load Droop	-	49	43.2
V5	5	Minimum Current	-	50	44
V6	6	Constant Power Load	-	>50	≥44

By comparing the voltage set points in Table 3-6 with the converter operation mode and voltage level presented in Figure 3-27 and Figure 3-28, it can be checked whether the converter model works aligned with the calculated values. The most explicit signal is the PV converter operation, which can be seen in tune with the PV potential power illustrated in Figure 3-11. It stays in zero current mode until around 6 AM due to the unavailability of solar power before the sun rises. After that, it switches into constant power mode until around 11 AM because the voltage is higher than 43.2 V, yet below the 52.7 V of source droop set point. There is a multiple switching occurred from 11 AM until 5 PM which might be happened due to the sufficient amount of power in load and fully charged battery. Further explanation will be discovered after the current and SOC signal is analyzed from Figure 3-29 and Figure 3-30. Then, it goes back into zero current modes from 5 PM until the rest of the day because the sun has set and there is no more generated power by the PV panel.

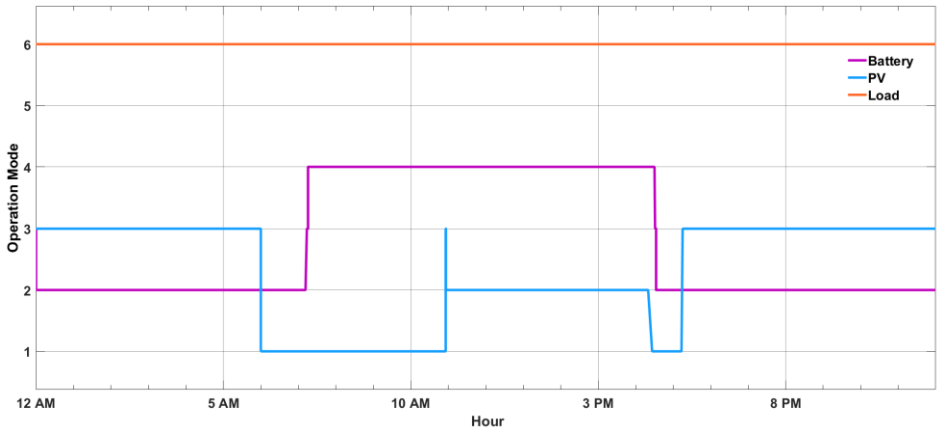

Figure 3-27 Converter Operation Mode

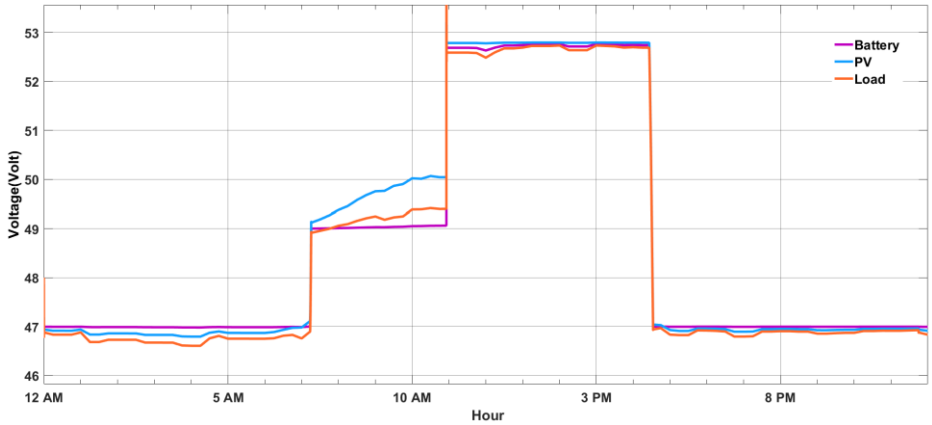

Figure 3-28 Converter Output Voltage

After the simulation result of converter operation mode has been checked, the current behavior in Figure 3-29 of each component also needs to be observed so that the system responsible for maintaining its power flow can be proven. As we can see from 12 AM until around 6 AM, all the load demand is taken care only by battery due to the absence of solar power. It can be seen that from 6 AM until 7 AM, the battery is still supplying about 75% of load demand even the PV has generated some power due to the small PV power production in the morning. This battery behavior is also reflected in the SOC curve from Figure 3-30, It is depleted from 85 % of its capacity until around 25% at 7 AM. The turning point happens after 7 AM when PV currently is sufficient enough to supply all the load demand. At that moment, the battery stop discharges its power and start to be charged instead. While the PV power production keeps increases, the current output flows both into the load and the battery. Because the load demand is much lower than the PV production, the battery is continuously being charged until its full capacity at 11 AM. When the battery is fully charged, it stops to absorb power, and the PV current only goes for the load. Hence, PV power is curtailed from 11 AM until around 4.30 PM because the current needed in the system is much smaller than the

production at that time. The comparison between controlled power and demanded power of each component can be observed in appendix A.

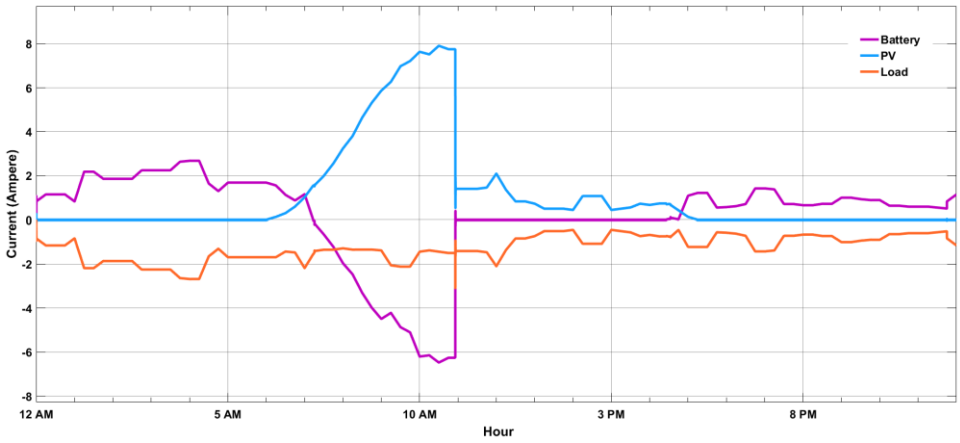

Figure 3-29 Converter Output Current

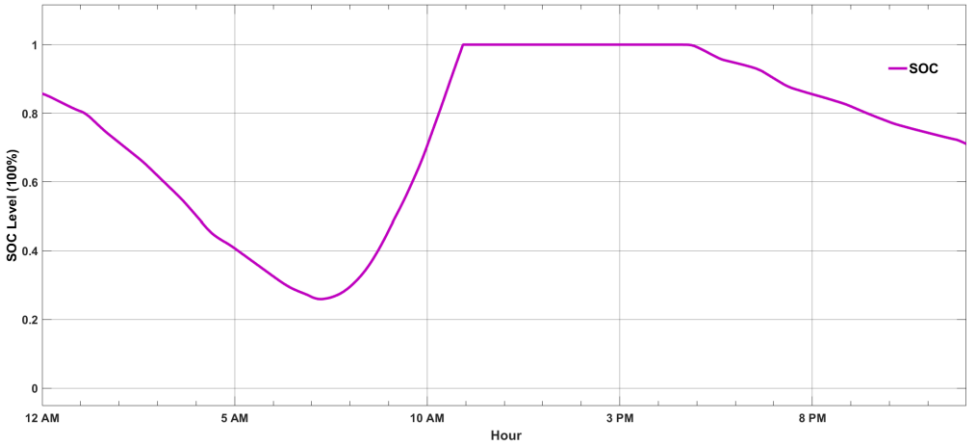

Figure 3-30 Battery SOC Level

3.5. Balancing Multiple Batteries

In some cases, several storage systems might be installed for a particular purpose under one SHS owner. This can be used for different load according to the different priority that desired by them, such as for a private farming house or private water pump. Those loads might not be the primary needs in the rural area, yet some people consider it as a good support for their activities. The example of multiple batteries model is depicted in Figure 3-31 below, as the house has two storage system that connected to home power network separately. Even though the desired usage of each battery is different, there is no centralized controller for managing the power contribution for each of them. As a result, both batteries will generate the amount of total energy demand in the house according to the voltage level at their converter terminal. Therefore, a decentralized coordinated control according to the adaptive droop control based on SOC will play an Important part here. The modified droop coefficients algorithm will equalize the injected or absorbed power amount of each battery according to their SOC level.

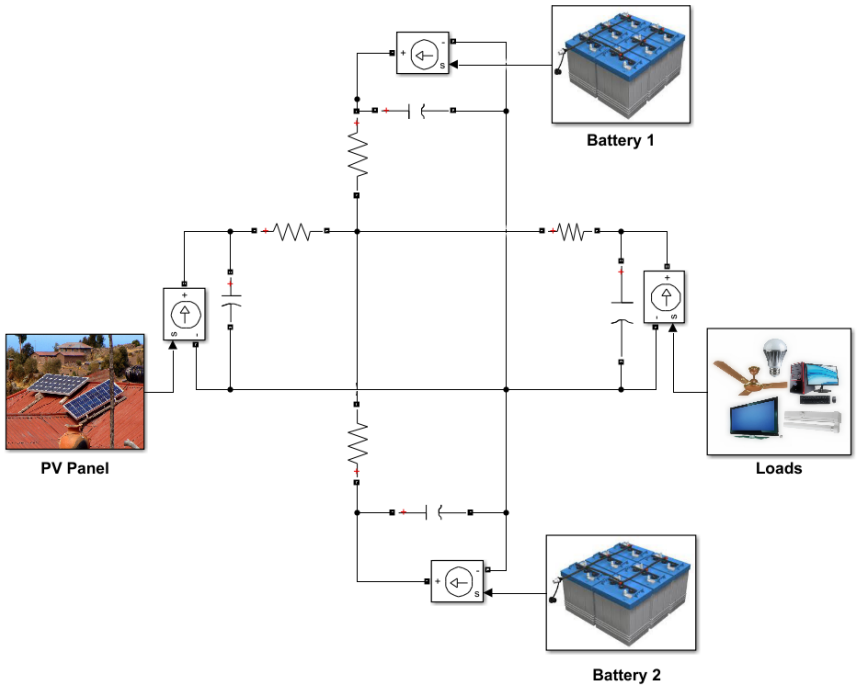

Figure 3-31 Multiple Batteries Model

The parameter of modeled system is similar to the previous model which is presented in Table 3-4, yet the difference is in the second battery initial SOC. Battery 1 starts with SOC level of 90%, while battery 2 starts at 10% of its capacity. It is likely designed to show how the battery will adapt their output or input according to their SOC level.

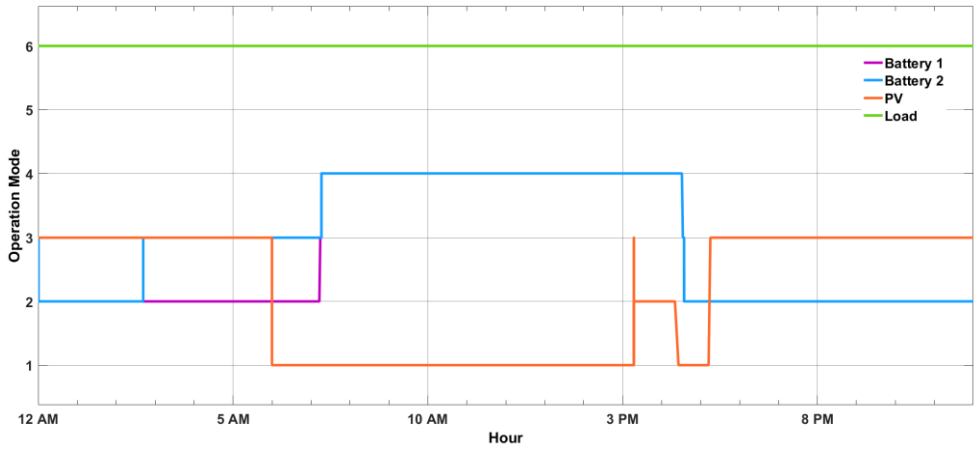

Figure 3-32 Multiple Batteries Operating Mode

First of all, the operation mode of each converter is observed according to Figure 3-32 before goes into the current flow observation. PV operation is quietly the same as single SHS operation, with the multiple switching occurred from around 3 PM until 5.30 PM. The expected operation is that the excess power from PV needs to be divided into 2 batteries. Therefore the rate of charge for both battery will not be as rapid as the previous model and resulted in longer charging time. Another notable point takes place at around 2.30 AM, where battery 2 has moved into zero current operation mode while battery 1 still operates in droop mode. The current behavior should be inspected at that moment because it is where the adaptive droop controller should give its function.

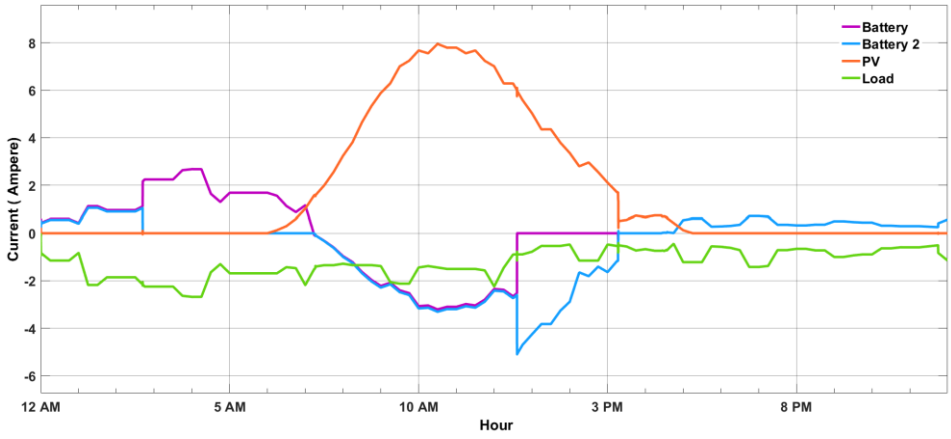

Figure 3-33 Current Characteristic of Multiple Batteries

Since the initial SOC of both batteries as depicted in Figure 3-34 are different; it can be seen that the adaptive droop controller works well for managing the amount of current output for each battery. As illustrated in Figure 3-33, battery 2 with lower SOC level gives less power than battery 1 and is keep being discharged until it is empty. At the moment battery, 2 has already depleted, the adaptive droop

controller once again shifts the output current of battery 1, so it can increase its production capability.

On the contrary, the battery is 2 controlled to consume more power than battery 1 when they are being charged under droop mode. It occurred because, at the initial time when the battery goes into load droop mode, battery 2 has lower SOC value than battery 1. More detailed measurement values of controlled power for each component can review in Appendix B.

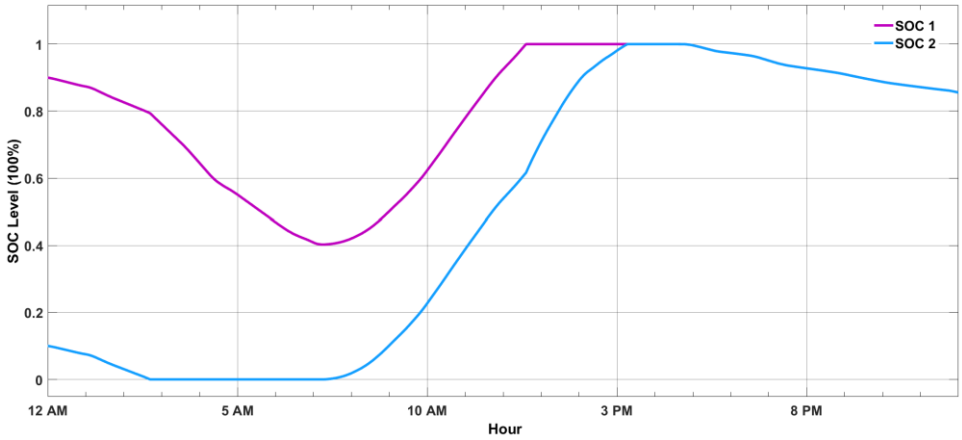

Figure 3-34 SOC Level of Batteries

4

Interconnection of Solar Home System

Rural areas commonly exist far from the distribution network as mentioned in Chapter 1 of this thesis, which leads to the lack access to electricity. Consequently, it is practical to install SHS as an off-grid stand-alone for supplying their load demands. As a result, electrification ratio of rural area increases gradually and also leads to more decent life. To ensure the decent operation of SHS, the commercial components of SHS are tested and designed to be able to fulfill the highest load demand at the area. By doing this, it is assumed that the designed SHS is applicable for any load demand. However, the diversity of load consumption will lead to not optimal usage of SHS capability. There will be a wasted amount of energy for the low load profile consumers, as the potential power from the PV is not stored anywhere after the battery is already fully charged.

The assumption above is observed by doing the Loss of Load Probability (LLP) analysis of existing SHS performance as already described in Chapter I. Based on the amount power from designed PV capacity, the annual mean PV output power generated is around 2200 Wh/day. Afterward, the amount of PV output power is compared with the load demand which has been classified as low, medium and high consumption. Each comparison of SHS performance is illustrated in Figure 4-1 (a), (b), and (c) consecutively.

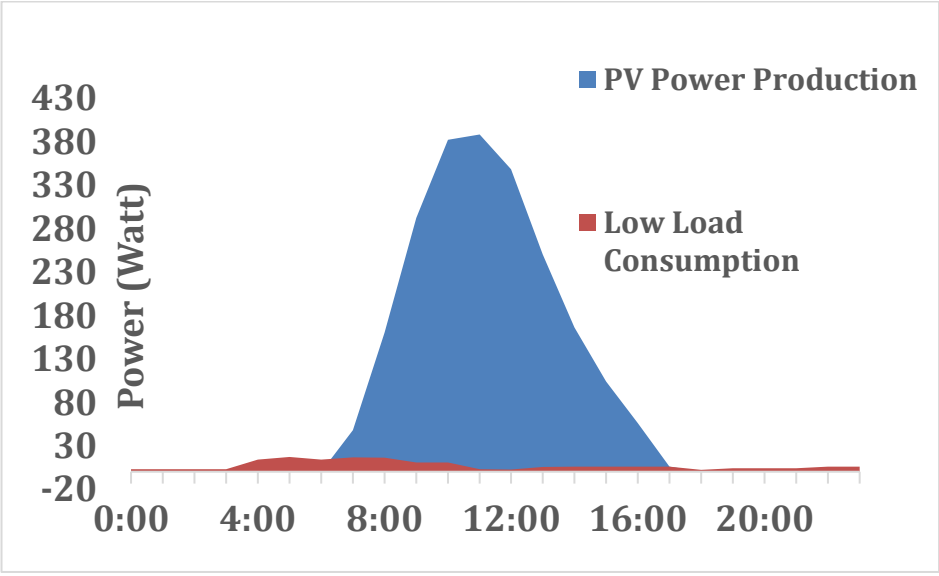

(a)

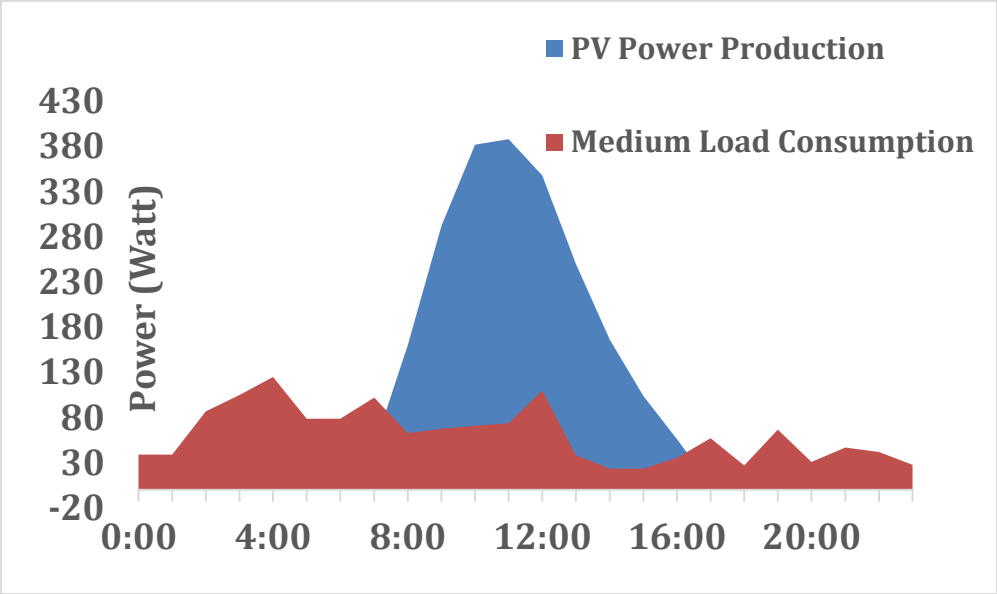

(b)

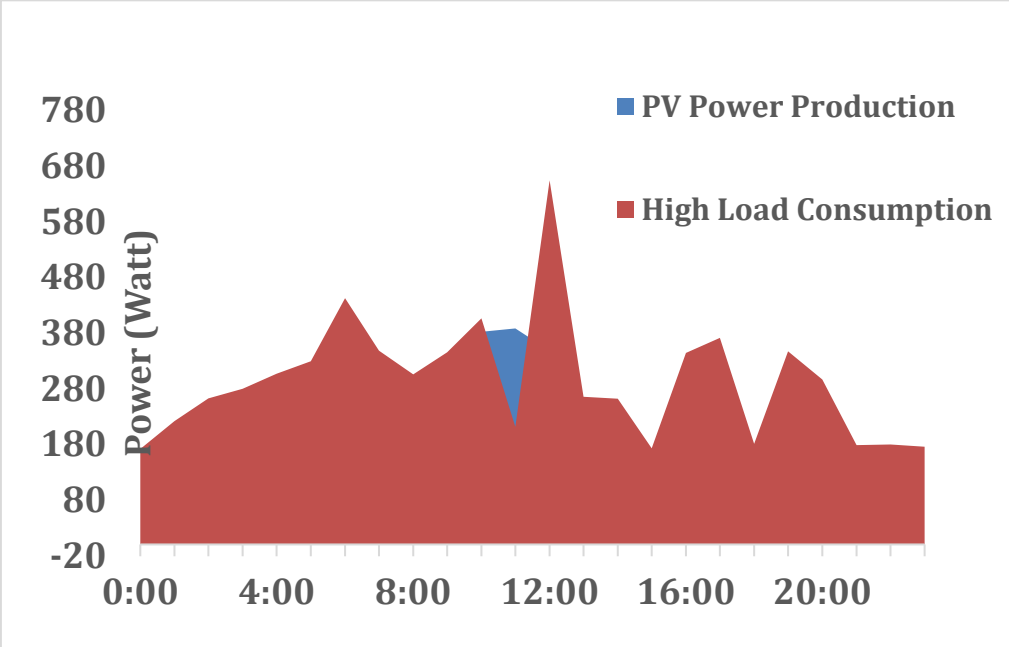

(c)

Figure 4-1 (a) Low (b) Medium (c) High Power DIfference with PV Production

As we can see from the three graphs above, PV power output is optimum around midday while the peak load demand is happening at night when the PV stop to produce power anymore. Therefore, it is the duty of battery system for providing sufficient power for the rest of the day. As a result, the battery sizing should be calculated appropriately to prevent unserved load due to a shortage of battery capacity or extravagance cost due to the excess capacity. From the measured load

profile, the minimum size of battery system based on the different capacity of PV panel with regard to 0 LLP can be generated as summarized in Table 4-1 [38].

Table 4-1 Battery System Sizing According to PV Panel Capacity

	Wp_50 (Wh)	Wp_100 (Wh)	Wp_200 (	Wp_300 (Wh)	Wp_400 (Wh)
2017_low		445	445	444	444
2017_medium					2800
2017_high					32948

The gray blocked area is an indication that regardless the battery capacity installed, the value of LLP will not reach zero value, and there will be the amount of load that will be unserved. Therefore, even for recent load profile, there will be some consumer whose load demand is not fulfilled with the existing SHS if they insist on using PV panel rating less than 400 Wp. The customers who are classified as a high-consuming power need to adapt their electricity consumption based on the limitation of their storage system. Only the customer with low load profile that still able to use the minimum PV rating of 100 Wp. The amount of battery capacity is calculated with concern to minimize zero value of LLP. According to Table 4-1, the amount of battery capacity required for high-level consumer is too much to be installed for single SHS and categorized as economically infeasible [7].

Therefore, the interconnection of SHS is proposed in this part of the thesis. The proposed interconnection topology is divided into two models, which are directly in the 48V level or 350V level. The following sub-section will describe the advantages and drawbacks of each model.

4.1. Interconnection Topology in 48 V Grid

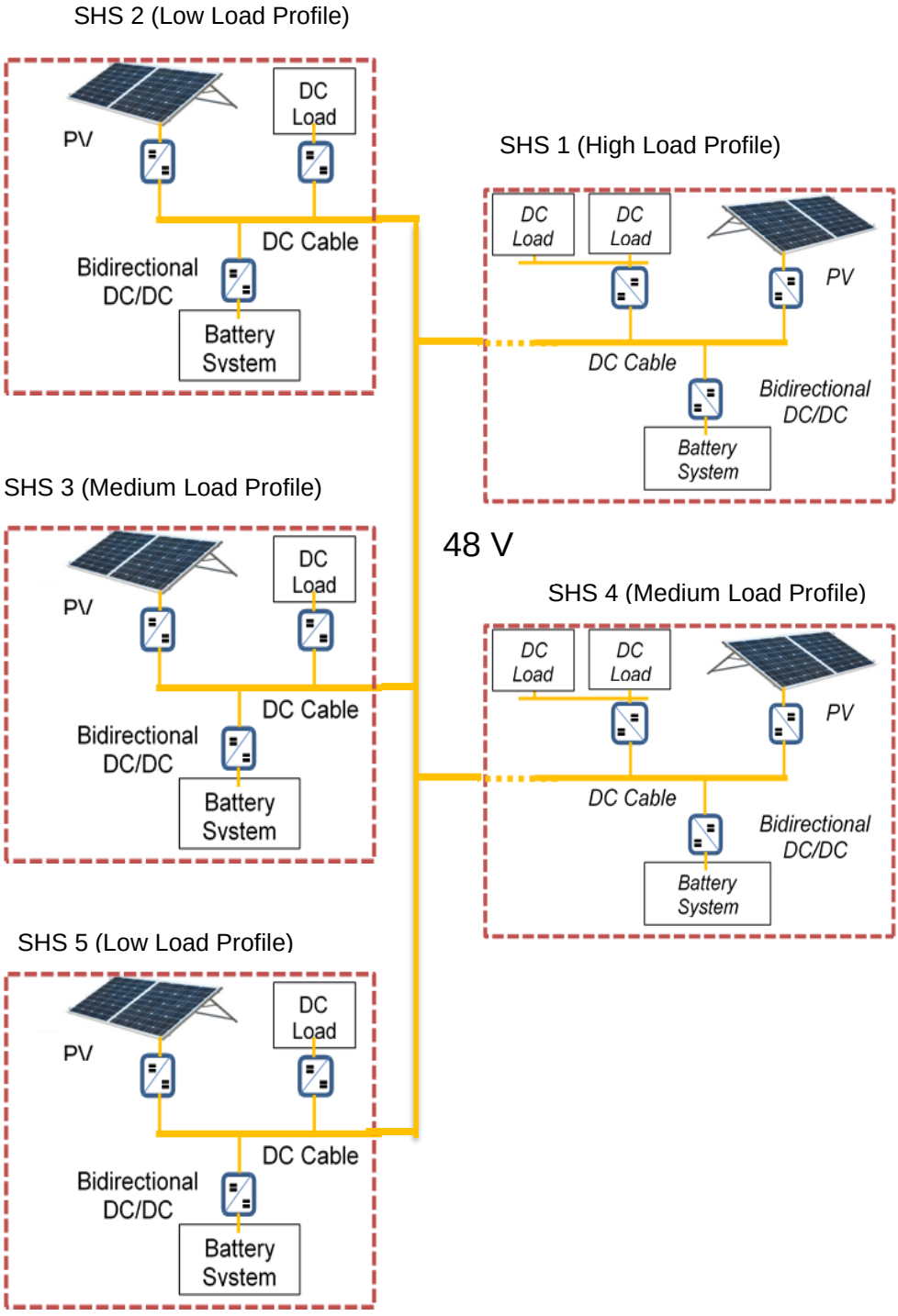

Figure 4-2 Interconnection Topology in 48V

As the individual SHS operation has been modeled in the previous Chapter, the interconnection of the system in 48 V can be modeled as a bigger SHS with several power sources, loads and batteries with the extended DC cable line within a particular area. The complexity of interconnection system is different from the single SHS operation due to the effect of each SHS voltage deviation. In any case, there is a voltage deviation in one of the connected house, it could affect the voltage grid interconnection and results to shift the others power flow operation. The amount interconnected houses in this simulation is limited to be 5 in order to show sufficient amount of system complexity without sacrificing too much time for model simulation. The illustration of interconnected 48V SHS is presented in Figure 4-2 and overall system parameters are shown in Table 4-2.

Additional load profile for low and medium consumers are generated here, so there is no identical load characteristic for the same load consumption level. To avoid misconception between the primary load profile and the additional ones, the later one will be stated as “low#2” and “medium#2” which is presented in Figure 4-3 and Figure 4-4

Table 4-2 48 V Interconnection System Characteristic

	House 1	**House 2**	**House 3**	**House 4**	**House 5**
Load Profile	High	Low	Medium	Medium #2	Low #2
Max Converter Load Power	800 W	400 W	400 W	400 W	400 W
Max Converter Load Current	18.5 A	4.63 A	4.63 A	4.63 A	4.63 A
Battery SOC	80 %	97%	85%	85%	94%
Droop Coefficient	0.01	0.01	0.01	0.01	0.01
Line Resistance	0.07Ω	0.07Ω	0.07Ω	0.07Ω	0.07Ω
Line Inductance	0.5 µH	0.5 µH	0.5 µH	0.5 µH	0.5 µH

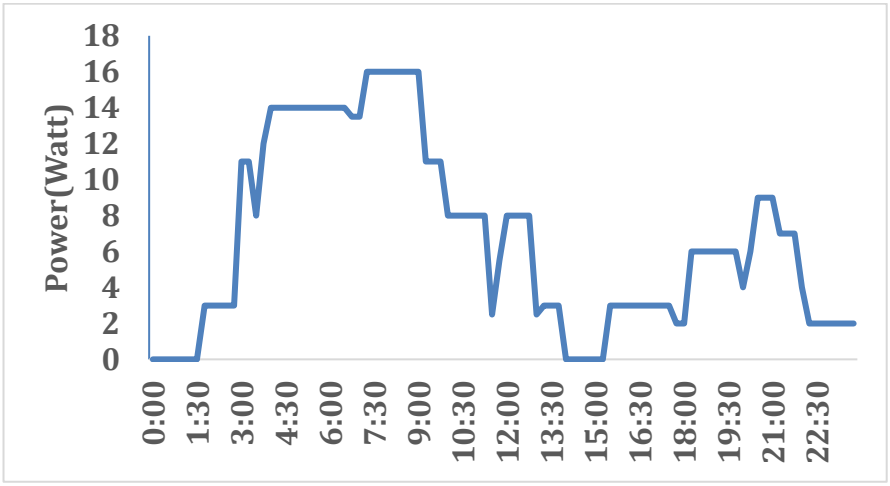

Figure 4-3 Additional Low Load Profile

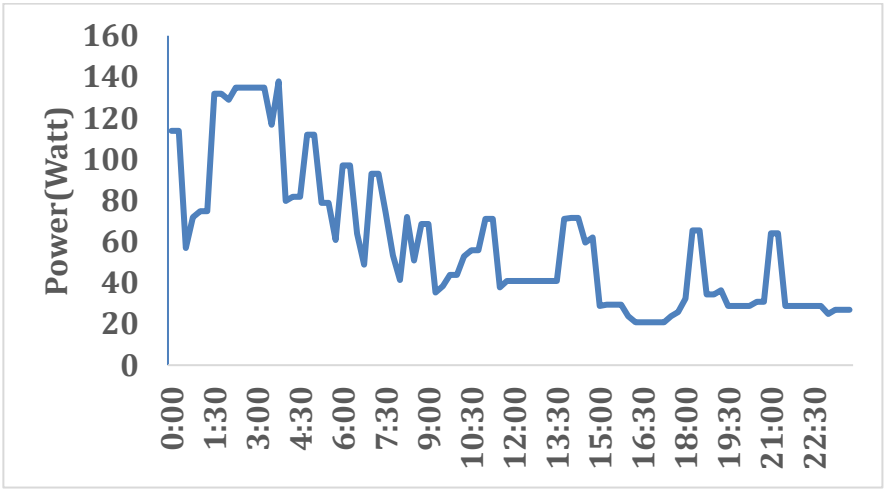

Figure 4-4 Additional Medium Load Profile

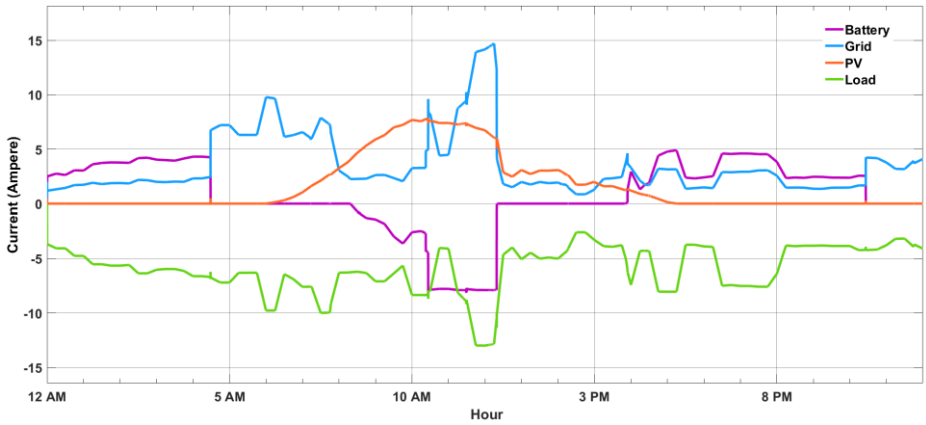

Figure 4-5 House 1 Current Characteristic

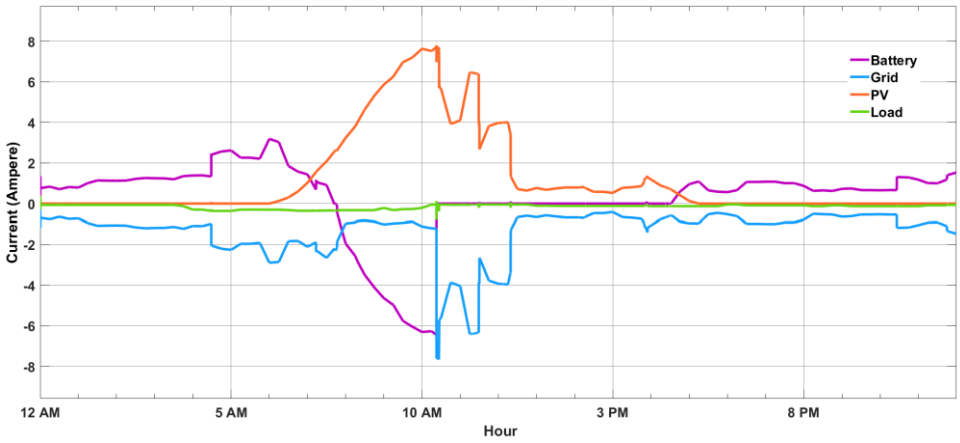

Figure 4-6 House 2 Current Characteristic

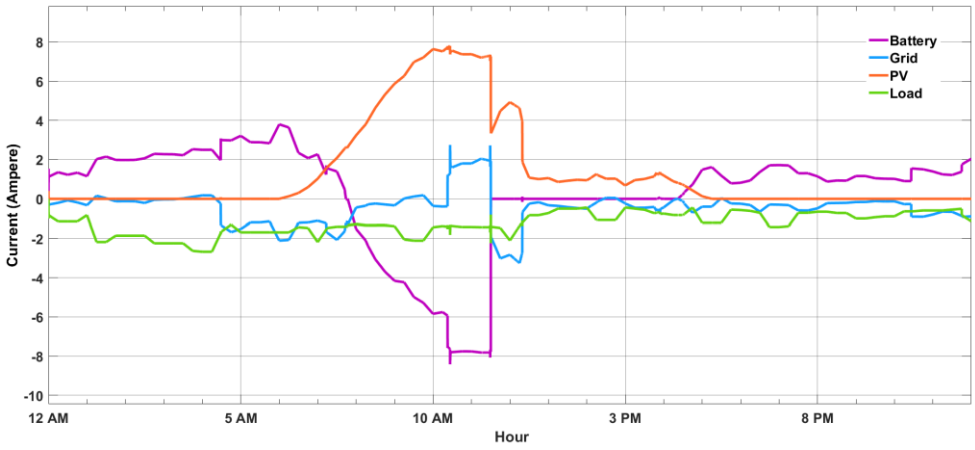

Figure 4-7 House 3 Current Characteristic

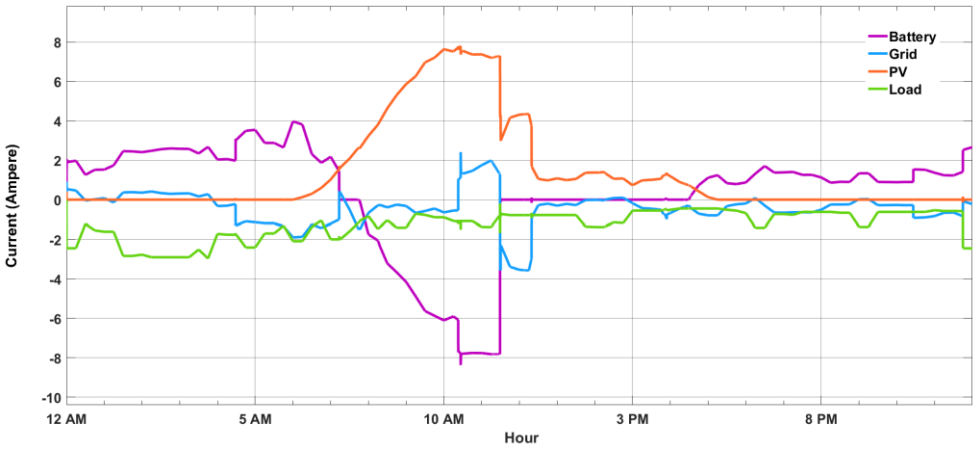

Figure 4-8 House 4 Current Characteristic

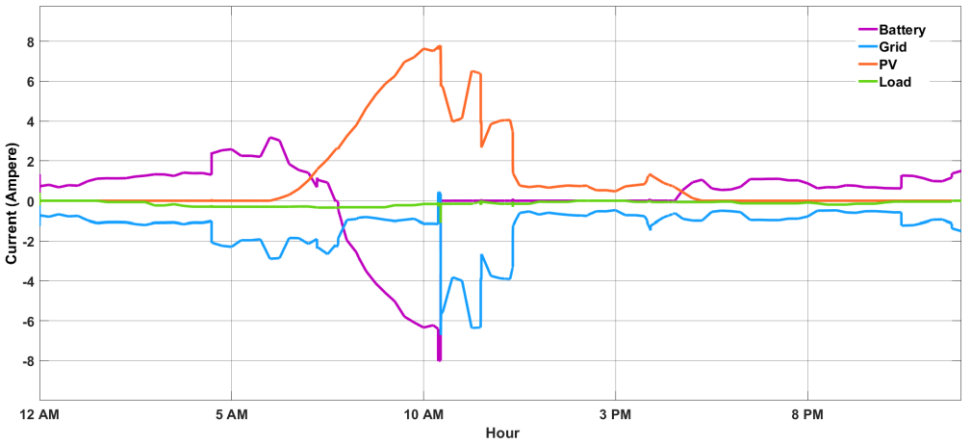

Figure 4-9 House 5 Current Characteristic

As multiple houses are taken into account in this modeling, the current measurement for each house will be presented separately for the sake of better observation. Figure 4-5 is for house number 1 current behavior, Figure 4-6 is for house number 2, Figure 4-7 is for house number 3, Figure 4-8 is for house number 4, and Figure 4-9 is for house number 5. By interconnecting these 5 houses, it is expected for decentralized power-sharing mechanism between them to be happened. Each of battery system SOC level is also monitored and presented in Figure 4-10.

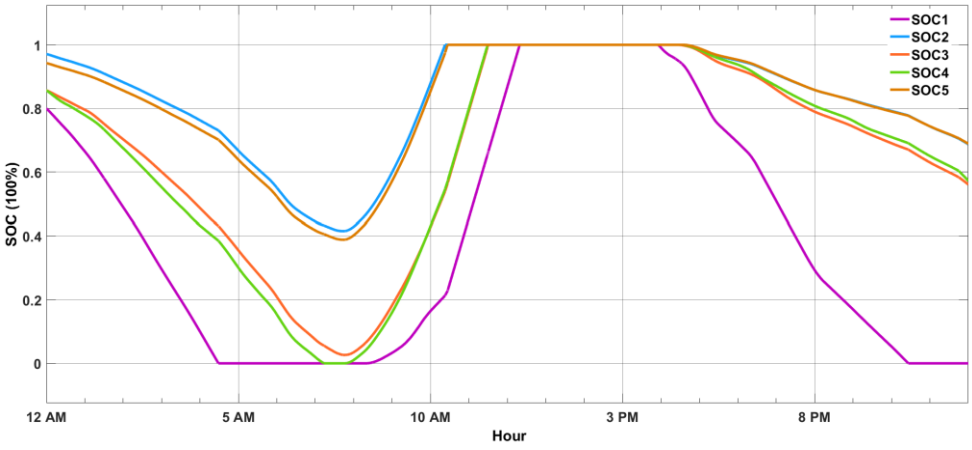

Figure 4-10 SOC of Batteries in the Interconnected Houses

Since the beginning of the operation, a local controller installed on each house gives respond to other local houses without any communication links. They can only adapt their output based on the measured voltage on their converter terminal for maintaining the sustainability of power supply in the system. To avoid any misunderstanding for grid's current observation, positive (+) value is defined as the moment when current goes into the house. On the contrary, the minus (-) sign shows when the current goes from house to the interconnection line.

The first prominent event ensues at the beginning of operation time at 12 AM when load demand in house 1 increase while its battery SOC level is the lowest amongst them. Instead of consuming more power from its battery, house 2 and house 5 share their battery power through the interconnection line. As both of the houses have the highest SOC level at that time, they discharge their battery the most for power-sharing. House 2 slightly transfers more power than house 5 because it has higher SOC level, even though it is just around 3%. Furthermore, it can also be seen that even house 3 and house 4 are also acquired power from them between 1 AM until 4 AM.

Secondly, at around 4.30 AM when the battery at house 1 is already empty, the rest 4 houses transfer their battery power through interconnection line with concern of their SOC condition at the corresponded time. Thus, house 2 and house 5 still contribute more power than house 3 and house 4 because of their SOC still higher than the other two.

When the battery of house 2 and 5 are already fully recharged at around 10.30 AM, the local controller does not directly curtail the amount of PV power output into zero. It allows for the PV power to be shared for battery of house 1, 3, and 5. That is also explaining an increase in battery charging speed from the steeper gradient in SOC measurement. Moreover, it can be said that the load demand is very low for house 2 and house 5 at this time, yet they let the PV power to be used for the neighbors. After all the 5 batteries are already full at around 12 PM, the PV power is curtailed again and operate only for satisfying local load demand

Lastly, house 1 with high load profile has been proved unable to operate as a stand-alone system. The evidence is that it needs power from grid for the whole operation day even its battery and PV work normally. It can also be seen from Table 4-2 that the load power rating is much bigger than the allowed power rating for the local power sources [33]. More detailed power flow measurement of this model is documented in Appendix C

4.2. Interconnection Topology in 350 V Grid

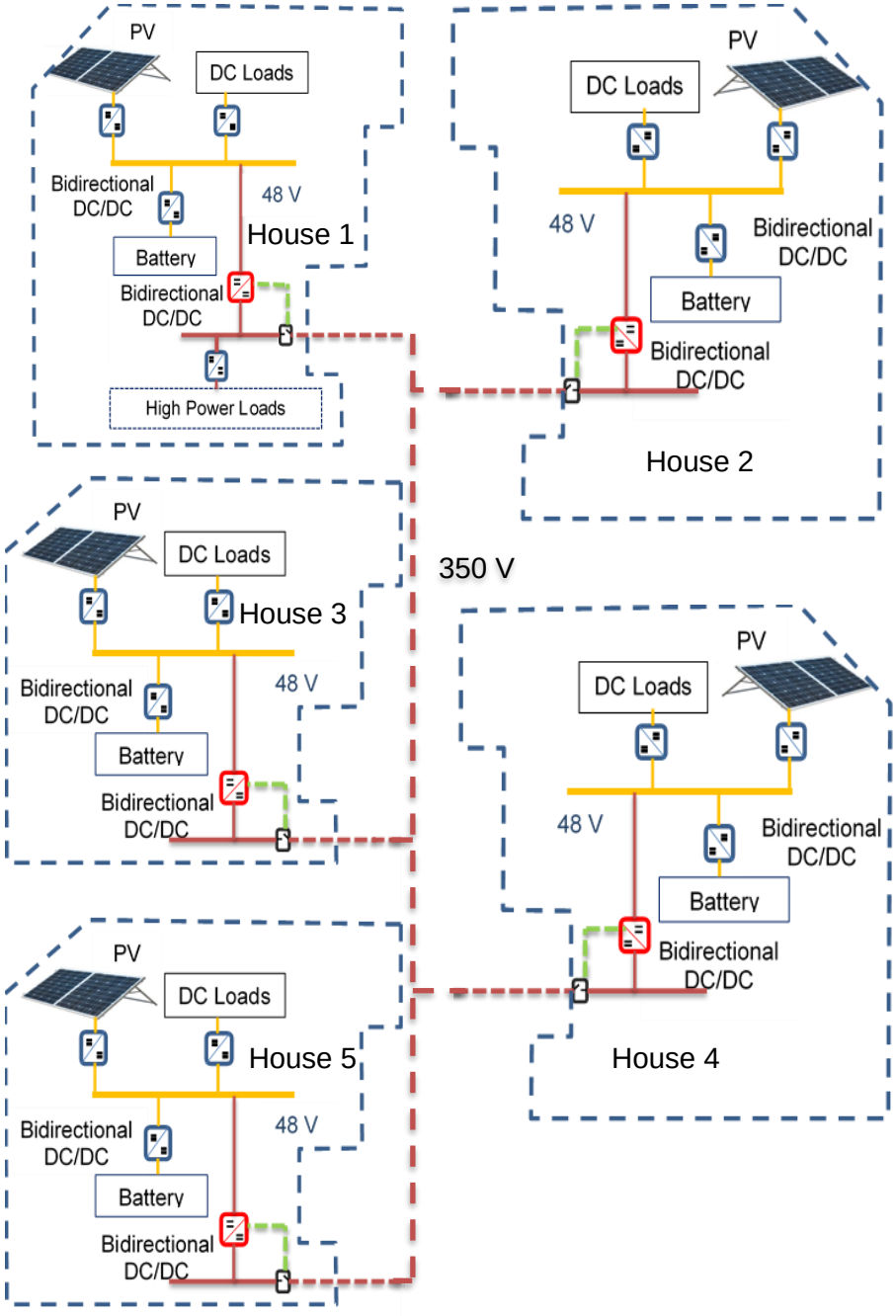

Figure 4-11 Interconnection Topology in 350V

Electrical industries have been tremendously increasing in numbers as the power electronic components show promising future of producing electrical houseware with a lower price. As a result, it is expected that the future load consumption of SHS user will grow simultaneously. Electrical loads such as iron, water kettle, rice cooker or even refrigerator that were too pricey can be purchased now. Hence, this occurrence shifts consumer's behavior of electrical usage to be more consumptive and increases their load profiles higher. Those devices take more power which absorbs more current in the existing power lines. Therefore, the designed current capability rating in 48V line conductor might be insufficient for higher current operation. Even they are capable, maximum usage of current conduction in the cable for a long time will lead them to the breakdown.

One of the solutions for anticipating high power consuming loads is by connecting them to higher level voltage so that the conducted current is lower. The recommended voltage level for residential usage is ± 350V, which is also commonly used for DC links with AC power sources [33], [39]. It is allowing the possibility of elevating the voltage level into ± 700 V for a larger load and ± 1400 V for larger PV power plant, which is still under the limit of 1500 V imposed by IEC60038 [39]. To allow the interconnection occurred, additional 48 V to 350 V bi-directional converter is needed for each of the SHS. It might be seen as an extra cost for system installation. However, the price is considered to be worth it compared with the given potential. It can be used for common loads such as water irrigation, street lighting, or even common antenna receiver. The illustration of two level voltage usage and interconnection in 350 V between 5 houses are presented in Figure 4-11. The primary load consumption for each house is modeled to be similar with the 48V interconnection. There are additional high power loads installed in house 1 which will be assembled in the 350V line cables. These loads are typically absorbing high amount of current; even the operating time is short. The load profile for this load is depicted in Figure 4-12.

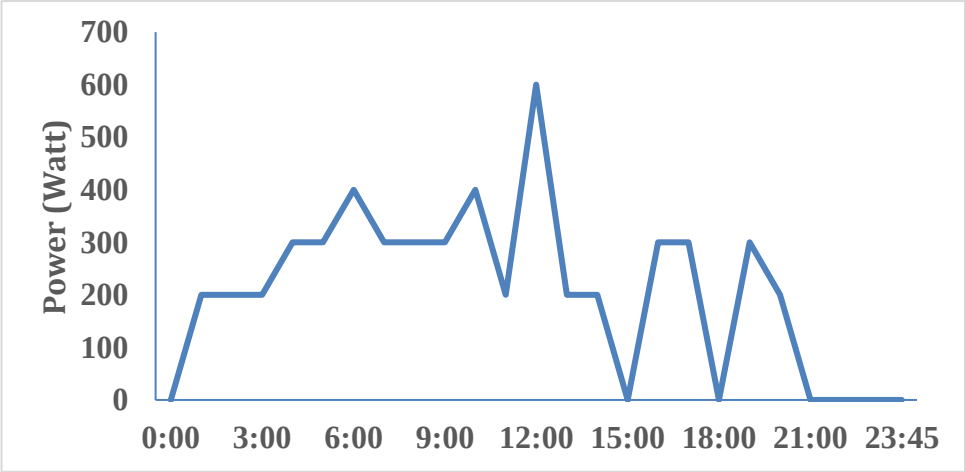

Figure 4-12 Load Power Consumption in 350V Grid

Even though that additional converter is needed for allowing the system interconnection, the proposed primary and additional adaptive controller is not needed at this interconnection level. They are substituted by multilevel controller proposed in this research. The multilevel controller works according to the conventional transformers concept of power preservation on both sides of the converter as:

$$V_{48} * I_{48} = V_{350} * I_{350} \quad (20)$$

Where

V_{48} = Voltage at 48V converter terminal

I_{48} = Current at 48V converter terminal

V_{350} = Voltage at 350V converter terminal

I_{350} = Current at 350V converter terminal

The amount of current flow through the 350V line is decided by integrating a similar method of droop slope between voltage and current. However, the slope here is generated between normalized voltage ratio of V_{350} and V_{48} with I_{350}. Proposed multilevel controller slope is illustrated in Figure 4-13.

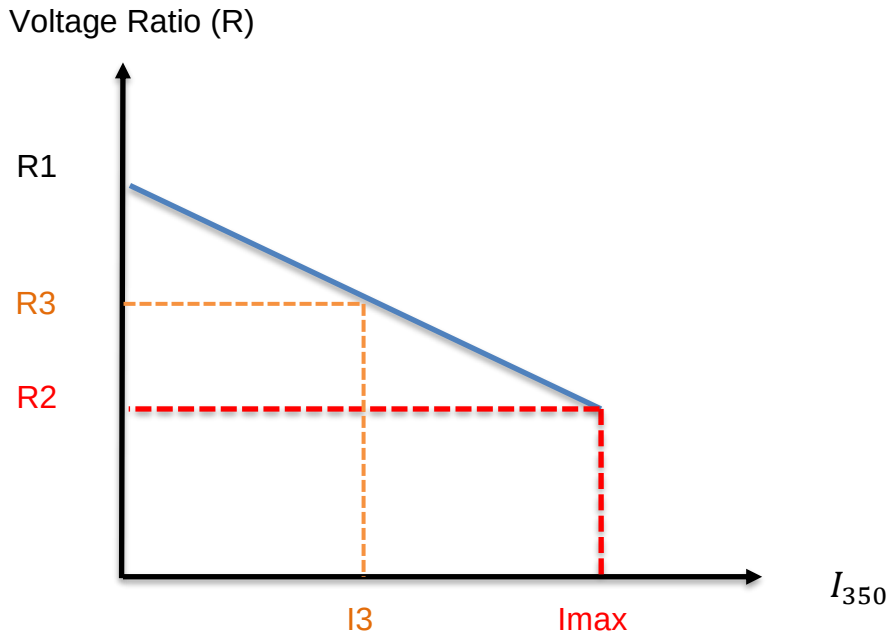

Figure 4-13 Current Multilevel Controller

R1 shows that the voltage stays at its nominal value when it is being normalized. The normalization process occurred by comparing the measured voltage over the nominal set voltage according to:

$$R = \frac{Vmeas_{350}}{Vmeas_{48}} * \frac{Vnom_{48}}{Vnom_{350}} \quad (21)$$

Where
$Vmeas_{350}$ = Measured voltage at 350V converter side
$Vmeas_{48}$ = Measured voltage at 48V converter side
$Vnom_{350}$ = nominal voltage of 350V
$Vnom_{48}$ = nominal voltage of 48V

From Figure 4-13 above, it can be seen that the slope of multilevel controller reaches maximum current at the time when minimum allowed voltage deviation took place. Here, the minimum voltage deviation ratio is represented by *R2*. Thus, two equations can be generated from information provided as:

$$\Delta R_{max} = R1 - R2 \quad (22)$$

$$\Delta R_{max} = slope * Imax \quad (23)$$

Then, by substituting equation (22) into (23):

$$slope = \frac{R1 - R2}{Imax} \quad (24)$$

It is important to notice that $Imax$ in the equation above is not the same as the maximum current output set at the grid converter for 350 V side (I_{350max}). The value of $Imax$ is defined according to the amount of maximum current allowed in the 350V power cable. The slope is a fixed value because it follows the voltage deviation within the allowed voltage range. As a result, the determination value of I_{350} for any voltage ratio can be executed by modifying equation (24) with the measured voltage ratio (R3) into:

$$I_{350} = \frac{R1 - R3}{slope} \quad (25)$$

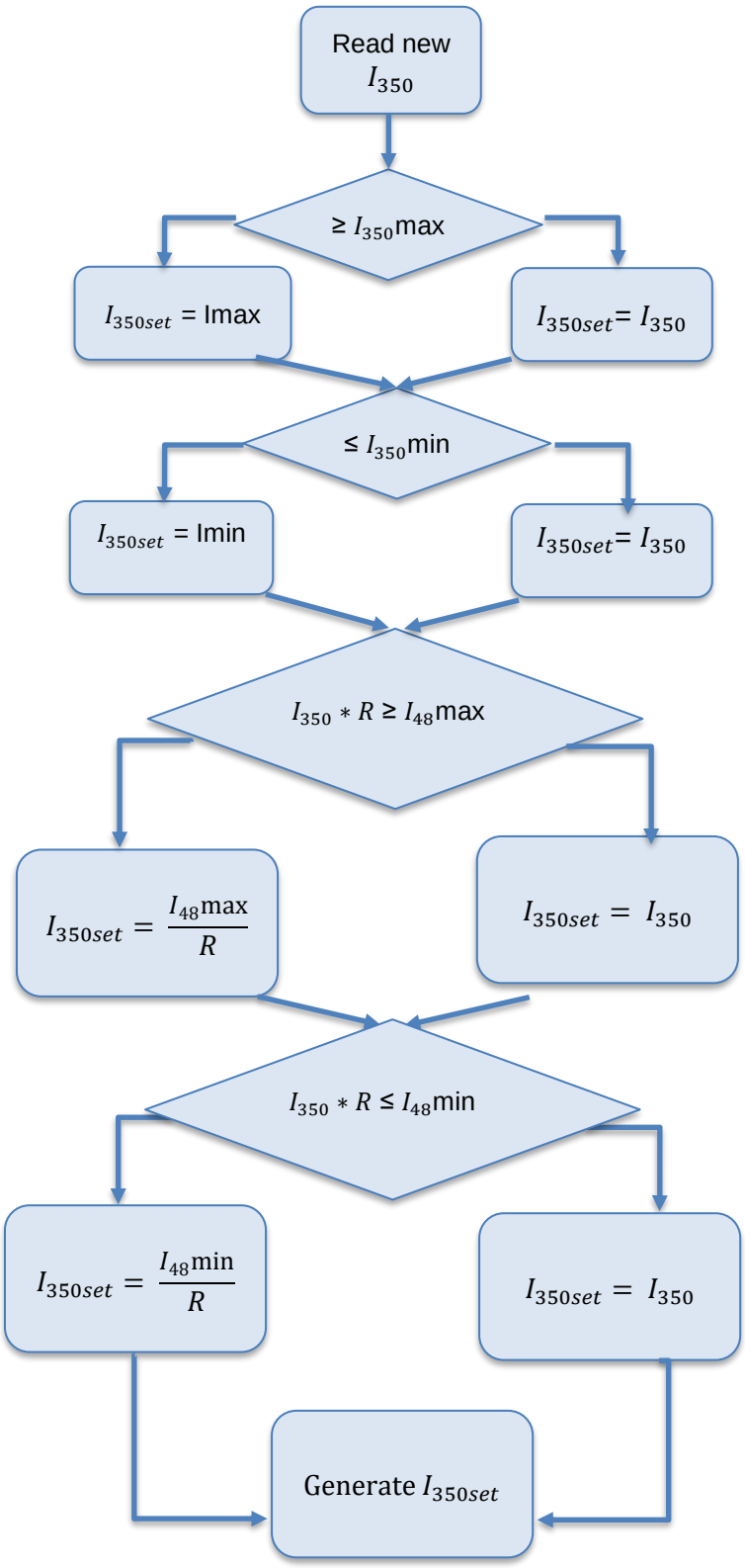

Figure 4-14 Current output limit check

Due to the characteristic of power line cables, the current can only flow in one direction at a time to prevent line congestion. Also, the amount of current output should satisfy the current limit on both sides of the converter which is different. As a result, I_{350} from equation (25) should be checked for preventing overcurrent in the cables. the process of checking current limit is depicted in Figure 4-14.

Finally, the generated output current after the limit check is the one that can be transferred through the 350V power cable. On the other hand, the current at the 48 V converter terminal receiver is calculated by dividing generated output current from Figure 4-14 with the ratio (R) as mentioned in:

$$I_{48set} = I_{350set} * R \tag{26}$$

The system modeled in this interconnection consists of five houses with different load consumption, to see the interaction between them. Each house represents high, medium, and low consumption of electricity separately. Also, the house with high load profile has some load that is installed in the 350V grid due to its massive power amount. The load that consumes ≥ 200 W power are categorized as high consuming power loads which are needed to be installed in the higher grid voltage level. By doing this, the stress in 48V power cable can be reduced because the current load is conducted with the lower current level in 350 V cables. Battery initial level is also varied in this model because it is assumed that different power usage on each load profile will lead to different SOC level at the end of the day. It is expected that primary, additional adaptive, and multilevel controller described previously, work synchronously in this interconnection mode. Table 4-3 below presents the condition of each connected SHS in the system

Table 4-3 350 V Interconnection System Parameter

	House 1	House 2	House 3	House 4	House 5
48 V Grid					
Load Type (48V)	High	Low	Medium	Medium#2	Low#2
Battery SOC (%)	80%	97%	85%	85%	91%
Max Load Power	400 W	400 W	400 W	400 W	400 W
Max Load Current	9.259 A	9.259 A	9.259 A	9.259 A	9.259 A
Droop Coefficient	0.01	0.01	0.01	0.01	0.01
350 V Grid					
Load in 350 V network	Yes	No	No	No	No
Maximum Load Power	800 W	800 W	800 W	800 W	800 W
Maximum Load Current	2.53 A	2.53 A	2.53 A	2.53 A	2.53 A
Droop Coefficient	0.05	0.05	0.05	0.05 A	0.05 A
Maximum load in Power Cable	13 A	13 A	13 A	13 A	13 A

As the system parameters have been described in Table 4-3, slope coefficient of 0.05 is selected by integrating equation (21) and (24) into Figure 4-13. The value of *R2* which represents the minimum voltage ratio deviation, located when the voltage at 350 V side of the converter is minimum and voltage at 48 V side of the converter is maximum. So, by using equation (21), we could get:

$$R2 = \frac{Vmeas_{350}}{Vmeas_{48}} * \frac{Vnom_{48}}{Vnom_{350}} = \frac{315}{52.8} * \frac{48}{350} = 0.8$$

Then, the slope coefficient is calculated by adding R2 value into equation (24):

$$slope = \frac{R1-R2}{Imax} = \frac{1-0.8}{13} = 0.015$$

To see the current flow on components level of each house, the current measurements are presented separately within the location of where they are installed. Current flow for components in house 1 is presented in Figure 4-15, house 2 is in Figure 4-16, house 3 in Figure 4-17, house 4 in Figure 4-18, and house 5 in Figure 4-19. All of the SOC levels for the batteries are presented together in Figure 4-20. Besides of the current measurement in local 48 V houses, the current measurement is also done in the 350 V grid interconnection as depicted in Figure 4-21. When the current is transferred from 48 V to 350 V, the 48 V converter side will detect the current direction is going into them. On the other hand, 350V converter side will recognize that the current goes out from them.

The first major difference of system compared to 48 V interconnection takes place around 04.30 AM. Previously, battery in house 1 is already depleted at this moment because all the load demand is taken care by its own battery. In 350 V interconnection, the high power-consuming loads have been separated and would not burden only local battery. As a result, the load demand from house 1 is already shared with other interconnected batteries in the system. The amount of transferred power is also reflecting the SOC droop control from local battery controller. Battery 2 and Battery 5 transfer more power compared to the rest because they have the highest initial SOC level. The system directly ask power from local battery in 48V houses because there is an absence of power source in 350 V grid

Hence, it can be said that the location of installed load is not the problem for power supply. As long as the voltage level of the grid is sufficient for each component to produce more power, it can be transferred through the interconnection line.

The other interesting point occurs at the time battery in house 2 and 5 are fully charged at around 10.30 AM. It can be seen that even the load demand is low, the PV power is not immediately curtailed. It is transferred to other houses so that they charge their battery sooner. Lastly, at around 03.30 PM when the load demand in house 1 is higher than its local PV production, the power is backed up by the PV from other houses. This can happen because the load demand on the other house are relatively lower than their PV production. As a result, the battery power is not absorbed earlier and can be used later when the sun has gone. The rest of measurement result can be accessed through Appendix D.

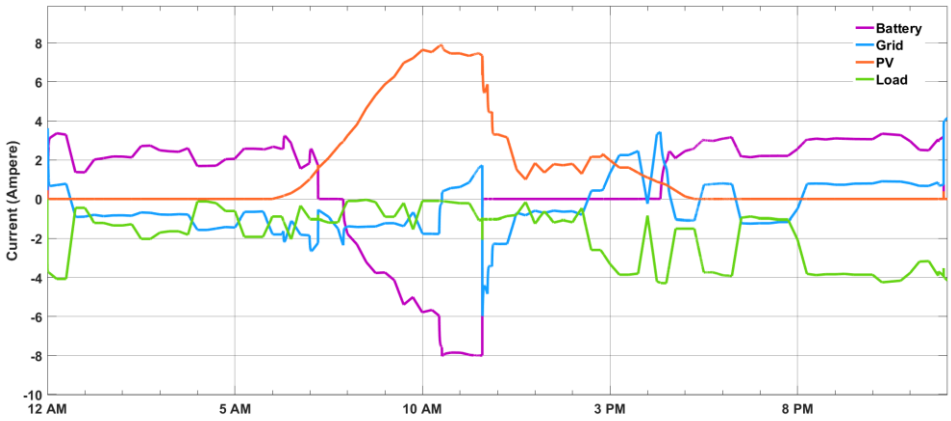

Figure 4-15 Current Flow in House 1

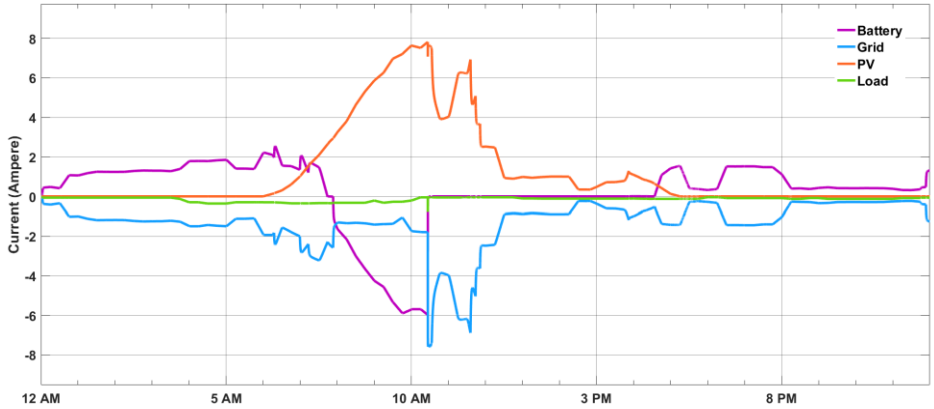

Figure 4-16 Current Flow in House 2

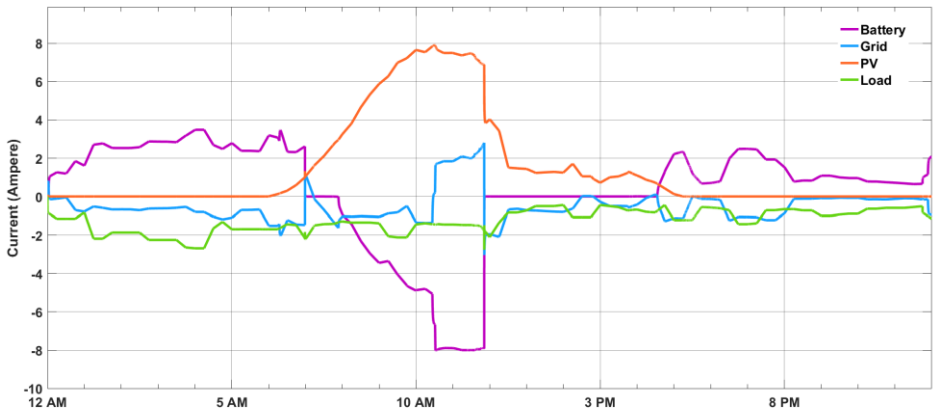

Figure 4-17 Current Flow in House 3

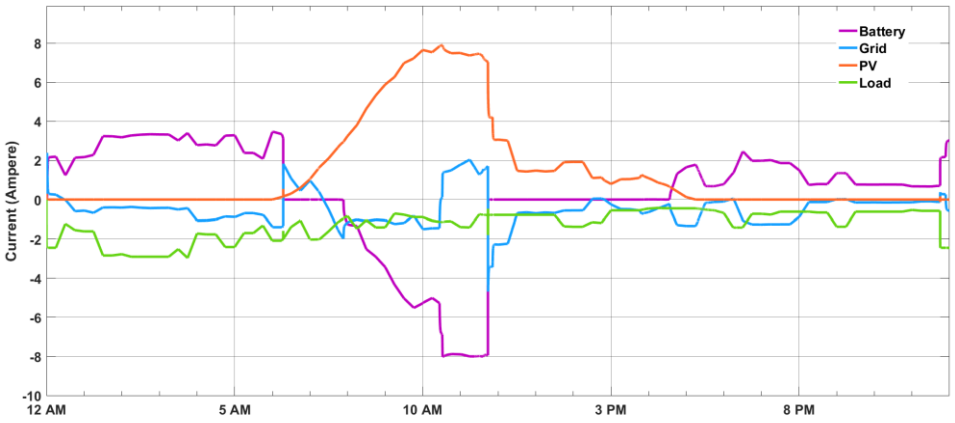

Figure 4-18 Current Flow in House 4

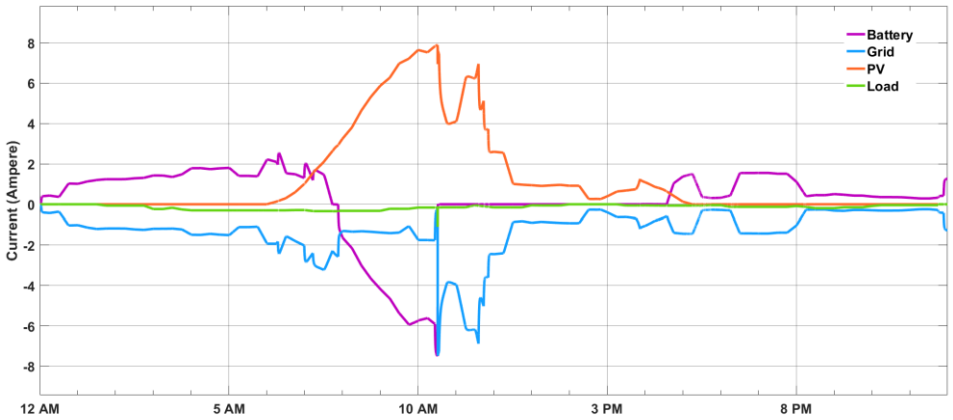

Figure 4-19 Current Flow in House 5

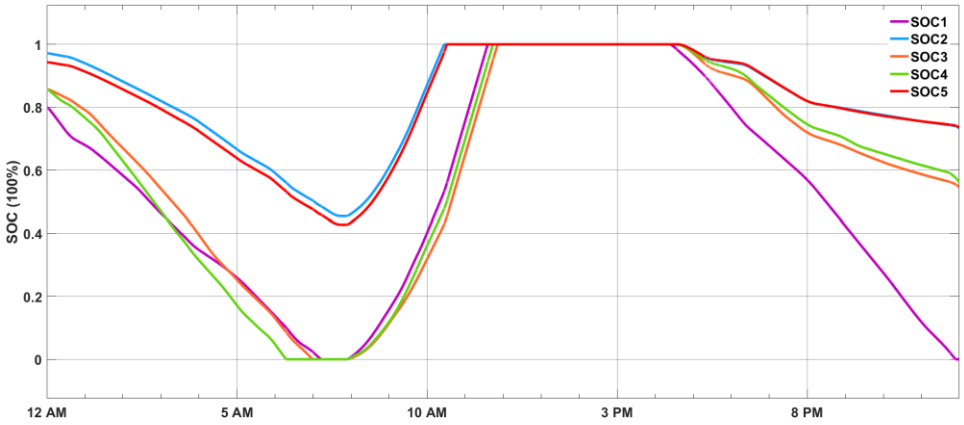

Figure 4-20 SOC level of Interconnected Batteries

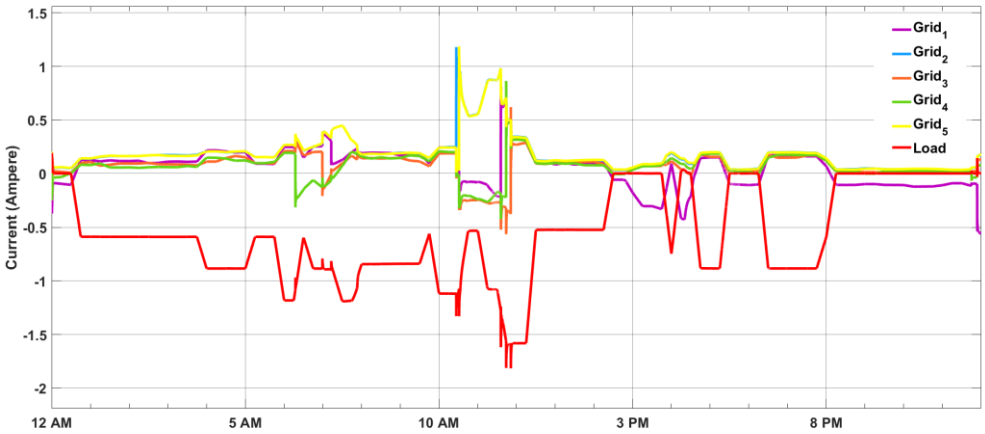

Figure 4-21 Current Flow in 350 V line

5

Conclusions and Recommendations

5.1. Conclusions

This thesis was carried out to study an attempt for increasing electrification ratio of rural areas through off grid electrification. The study has observed several possibilities of using Solar Home System as a bottom-up approach for LVDC grid forming. The manifestation of the concept is for enabling power-sharing between independent SHS within a limited area.

- ***What control method can we use to maintain power balance in Solar Home System without communication link?***

Decentralized control for the different purpose have been proposed in Chapter 3 of this thesis. On the local SHS level, a primary controller which works based on the fuzzy method of local voltage has been introduced. It classifies the operation mode of the converter into 7 modes. The modeled controller block decides the amount of generated current according to this operation mode.

- ***How to preserve SOC balance between batteries in the Solar Home System?***

The other studied controller is the adaptive droop based on SOC, which is responsible for maintaining SOC balance of interconnected batteries in the system. By applying this, the amount of power from and into the battery will be controlled differently based on their SOC level. Battery with lower SOC will receive more power in charging mode rather than the higher one. On the other hand, battery with higher SOC will inject more power than the lower one under discharging mode.

- ***How can Solar Home Systems be connected into off-grid LVDC network?***

The realization of interconnecting SHS has been analyzed in Chapter 4 of this thesis. There are three layers structure that has been defined in this work. The first layer determines control of power flow within a unit of SHS. It has been underlined that for simplicity and low maintainability of the control system, the decentralized control method is the most suitable one for rural areas. After independent SHS power flow has been controlled, the second layer is the physical

interconnection between each unit need that to be defined. DC simple cable is modeled in this thesis by applying line resistance between houses. As the group of SHS has been linked, the last layer is for applying power flow interaction between local SHS without any communication link installed between them. Therefore, the second level of control method has been proposed in this unit for balancing power operation in the system.

There are two presented methods of interconnecting SHS here, which are interconnection in 48 V or 350 V. The advantage of using direct interconnection on the same voltage level as in 48 V is that there is no extra cost for additional grid converter. However, it can suffer from the shifted load behavior of the consumers in the future. The consumers desire DC high-power loads such as iron, rice cooker, or water kettle for their daily usage. Therefore, the current consumption will be high and could heavily burden the line and storage system. On the other hand, interconnection in 350 V gives more flexibility of using high-power loads due to the smaller current conduction needed for those loads operation. However, it introduces additional grid converter which can increase the initial cost for system installation. Both of the interconnection mode has successfully conducted transfer power between components apart from their installed location.

- ***How to control the interconnected Solar Home Systems with the two voltage levels DC-DC converter?***

Lastly, a bi-directional controller for two voltage levels converter is studied in the last part of the simulation in this thesis. The concept of voltage ratio deviation is applied to form a look alike droop slope for shifting the output current. The slope is set to be fixed for maintaining the operation of the system within the allowed voltage range.

5.2. Recommendations

As the work of this thesis is considered as an initial step for bigger work of realizing DC smart system, there are several suggestions that can be used for next research studies:

- **The Model**

Firstly the converter modeled in this thesis is not the physical model, the switching effect of the converter is not taken into account, and therefore its effect is neglected. Secondly, the efficiency factor of each component is assumed to be ideal. The effect of efficiency can play interesting parts in deviating the amount of controlled current, which can also affect the controller accuration.

- **The Scenarios**

The picked scenarios of this thesis are selected such a way so that it can show the expected behavior of it in the simulation. For future research, it is advised to use more extreme scenarios that might happen. More houses and more complex load profiles could be used to simulate a more mature system that might already exist in real life.

- **The controller**

The proposed idea of the controller in this thesis is still a general design which has not been translated into physical components. Therefore, it will be nice if the controller can be physically designed, so the unseen events from the simulation or the simplification effect can also be observed as a reminder for the new controller design

Bibliography

[1] International Energy Agency, “WEO - Energy access database,” 2016. [Online]. Available: http://www.worldenergyoutlook.org/resources/energydevelopment/energyaccessdatabase/. [Accessed: 01-Aug-2017].

[2] International Energy Agency, “How to make modern energy access universal?,” 2010.

[3] D. Palit and K. R. Bandyopadhyay, “Rural electricity access in South Asia: Is grid extension the remedy? A critical review,” *Renew. Sustain. Energy Rev.*, vol. 60, pp. 1505–1515, 2016.

[4] T. Den Heeten *et al.*, “Understanding the present and the future electricity needs: Consequences for design of future Solar Home Systems for off-grid rural electrification,” in *2017 International Conference on the Domestic Use of Energy (DUE)*, 2017, pp. 8–15.

[5] Y. Nagarjun, “Effectiveness of On-grid and Off-grid rural electrification approaches in India,” in *Proceeding - 2015 International Conference on Sustainable Energy Engineering and Application: Sustainable Energy for Greater Development, ICSEEA 2015*, 2016, pp. 65–70.

[6] G. Zubi, R. Dufo-López, G. Pasaoglu, and N. Pardo, “Techno-economic assessment of an off-grid PV system for developing regions to provide electricity for basic domestic needs: A 2020–2040 scenario,” *Appl. Energy*, vol. 176, pp. 309–319, 2016.

[7] V. Bolgov and M. Laanetu, “Economical feasibility of off-grid hybrid power supply for estonian remote areas—part 1: Hybrid components sizing,” in *2016 Electric Power Quality and Supply Reliability (PQ)*, 2016, pp. 179–186.

[8] S. M. Harish, G. M. Morgan, and E. Subrahmanian, “When does unreliable grid supply become unacceptable policy? Costs of power supply and outages in rural India,” *Energy Policy*, vol. 68, pp. 158–169, 2014.

[9] J. H. Lucio, R. Valdis, and L. R. Rodriguez, “Loss-of-load probability model for stand-alone photovoltaic systems in Europe,” *Sol. Energy*, vol. 86, no. 9, pp. 2515–2535, Sep. 2012.

[10] A. N. Celik, “Effect of different load profiles on the loss-of-load probability of stand-alone photovoltaic systems,” *Renew. Energy*, vol. 32, no. 12, pp. 2096–2115, Oct. 2007.

[11] SOLARGIS, “Global solar resource maps,” 2016. [Online]. Available: http://solargis.com/products/maps-and-gis-data/free/download/world. [Accessed: 01-Aug-2017].

[12] S. Nykamp, V. Bakker, A. Molderink, J. L. Hurink, and G. J. M. Smit, “Break-even analysis for the storage of PV in power distribution grids,” *Int. J. Energy Res.*, vol. 38, no. 9, pp. 1112–1128, Jul. 2014.

[13] P. Sandwell *et al.*, “Off-grid solar photovoltaic systems for rural electrification and emissions mitigation in India,” *Sol. Energy Mater. Sol. Cells*, vol. 156, pp. 147–156, 2016.

[14] UNFCCC, *Report of the Conference of the Parties on its sixteenth session, held in Cancun from 29 November to 10 December 2010*, no. March. United Nations, 2011, pp. 1–31.

[15] K. Unger and M. Kazerani, “Organically grown microgrids: Development of a solar neighborhood microgrid concept for off-grid communities,” in *IECON 2012 - 38th Annual Conference on IEEE Industrial Electronics Society*, 2012, pp. 5663–5668.

[16] M. R. Khan and E. D. Brown, “DC nanogrids: A low cost PV based solution for livelihood enhancement for rural Bangladesh,” in *2014 3rd International Conference on the Developments in Renewable Energy Technology (ICDRET)*, 2014, pp. 1–5.

[17] D. J. Becker and B. J. Sonnenberg, “DC microgrids in buildings and data centers,” in *2011 IEEE 33rd International Telecommunications Energy Conference (INTELEC)*, 2011, pp. 1–7.

[18] D. Antoniou, A. Tzimas, and S. M. Rowland, “Transition from alternating current to direct current low voltage distribution networks,” *IET Gener. Transm. Distrib.*, vol. 9, no. 12, pp. 1391–1401, Sep. 2015.

[19] T. Hakala, T. Lahdeaho, and P. Jarventausta, “Low-Voltage DC Distribution-Utilization Potential in a Large Distribution Network Company,” *IEEE Trans. Power Deliv.*, vol. 30, no. 4, pp. 1694–1701, Aug. 2015.

[20] L. Mackay, T. Hailu, L. Ramirez-Elizondo, and P. Bauer, “Towards a DC distribution system - opportunities and challenges,” in *2015 IEEE First International Conference on DC Microgrids (ICDCM)*, 2015, pp. 215–220.

[21] J. Han *et al.*, “Modeling and Analysis of a Low-Voltage DC Distribution System,” *Resources*, vol. 4, no. 3, pp. 713–735, Sep. 2015.

[22] A. Werth, N. Kitamura, and K. Tanaka, “Conceptual Study for Open Energy Systems: Distributed Energy Network Using Interconnected DC Nanogrids,” *IEEE Trans. Smart Grid*, vol. 6, no. 4, pp. 1621–1630, Jul. 2015.

[23] T. Dragicevic, X. Lu, J. Vasquez, and J. Guerrero, “DC Microgrids Part I: A Review of Control Strategies and Stabilization Techniques,” *IEEE Trans. Power Electron.*, pp. 1–1, 2015.

[24] L. Meng *et al.*, “Review on Control of DC Microgrids,” *IEEE J. Emerg. Sel. Top. Power Electron.*, pp. 1–1, 2017.

[25] X. Lu, K. Sun, J. M. Guerrero, J. C. Vasquez, L. Huang, and R. Teodorescu, “SoC-based droop method for distributed energy storage in DC microgrid applications,” in *2012 IEEE International Symposium on Industrial Electronics*, 2012, pp. 1640–1645.

[26] S. Anand, B. G. Fernandes, and J. Guerrero, “Distributed Control to Ensure Proportional Load Sharing and Improve Voltage Regulation in Low-Voltage DC Microgrids,” *IEEE Trans. Power Electron.*, vol. 28, no. 4, pp. 1900–1913, Apr. 2013.

[27] T. Morstyn, B. Hredzak, V. G. Agelidis, and G. Demetriades, “Cooperative control of DC microgrid storage for energy balancing and equal power sharing,” in *2014 Australasian Universities Power Engineering Conference (AUPEC)*, 2014, pp. 1–6.

[28] N. Yang, D. Paire, F. Gao, A. Miraoui, and W. Liu, “Compensation of droop control using common load condition in DC microgrids to improve voltage regulation and load sharing,” *Int. J. Electr. Power Energy Syst.*, vol. 64, pp. 752–760, Jan. 2015.

[29] N. S. Narayan, “Solar Charging Station for Light Electric Vehicles: A Design and Feasibility Study.” 2013.

[30] A. H. M. Smets, K. Jäger, O. Isabella, R. A. van Swaaij, and M. Zeman, *Solar energy : the physics and engineering of photovoltaic conversion, technologies and systems*. .

[31] J. Chiasson and B. Vairamohan, “Estimating the state of charge of a battery,” *IEEE Trans. Control Syst. Technol.*, vol. 13, no. 3, pp. 465–470, May 2005.

[32] T. Dragicevic, J. M. Guerrero, J. C. Vasquez, and D. Skrlec, “Supervisory Control of an Adaptive-Droop Regulated DC Microgrid With Battery Management Capability,” *IEEE Trans. Power Electron.*, vol. 29, no. 2, pp. 695–706, Feb. 2014.

[33] E. Rodriguez-Diaz, F. Chen, J. C. Vasquez, J. M. Guerrero, R. Burgos, and D. Boroyevich, “Voltage-Level Selection of Future Two-Level LVdc Distribution Grids: A Compromise between Grid Compatibiliy, Safety, and Efficiency,” *IEEE Electrif. Mag.*, 2016.

[34] S. Gaurav, C. Birla, A. Lamba, S. Umashankar, and S. Ganesan, “ScienceDirect Energy Management of PV -Battery based Microgrid System,” *Procedia Technol.*, vol. 21, pp. 103–111, 2015.

[35] S. Chaudhuri, L. Mackay, T. G. Hailu, L. Ramirez-elizondo, and P. Bauer, “Hybrid Power Balance Controller for DC Microgrids,” 2016.
[36] D. Linden and T. B. Reddy, *Handbook of batteries*. McGraw-Hill, 2002.
[37] D. Boroyevich, I. Cvetkovic, R. Burgos, and Dong Dong, “Intergrid: A Future Electronic Energy Network?,” *IEEE J. Emerg. Sel. Top. Power Electron.*, vol. 1, no. 3, pp. 127–138, Sep. 2013.
[38] N. Narayan, J. Popovic, J.-C. Diehl, S. Silvester, P. Bauer, and M. Zeman, “Developing for developing nations: Exploring an affordable solar home system design,” in *2016 IEEE Global Humanitarian Technology Conference (GHTC)*, 2016, pp. 474–480.
[39] L. Mackay, N. H. van der Blij, L. Ramirez-Elizondo, and P. Bauer, “Toward the Universal DC Distribution System,” *Electr. Power Components Syst.*, vol. 45, no. 10, pp. 1032–1042, Jun. 2017.

A

SHS Simulation

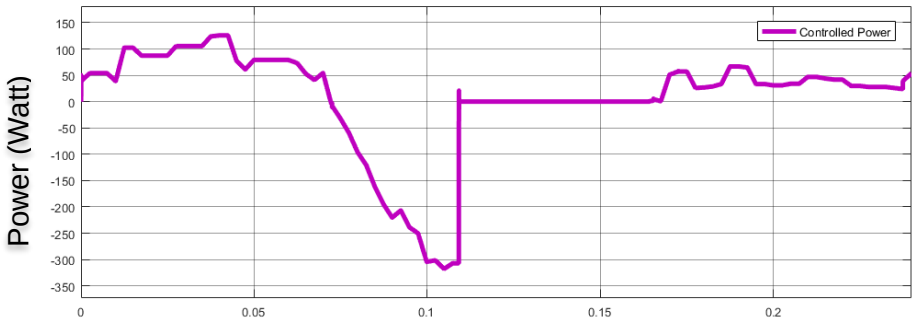

Fig. 1. Battery Power

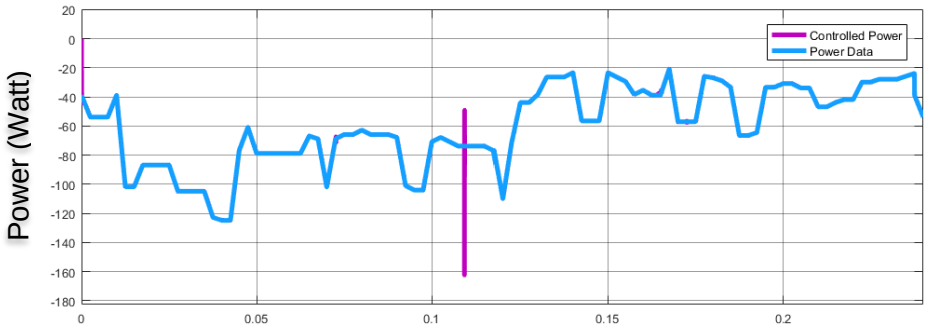

Fig. 2. Load Power

B

Multiple Batteries Simulation

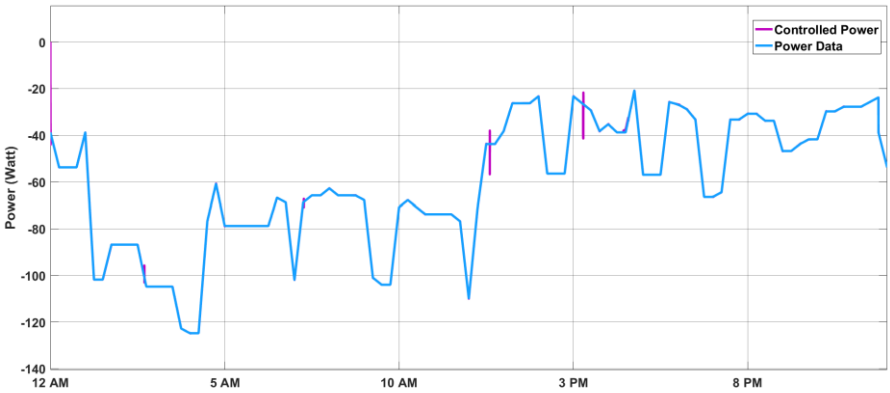

Fig. 3. Load Power

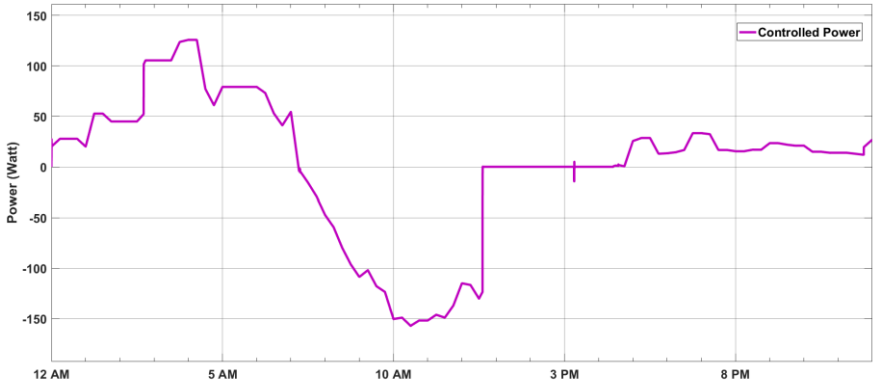

Fig. 4. Battery 1 Power

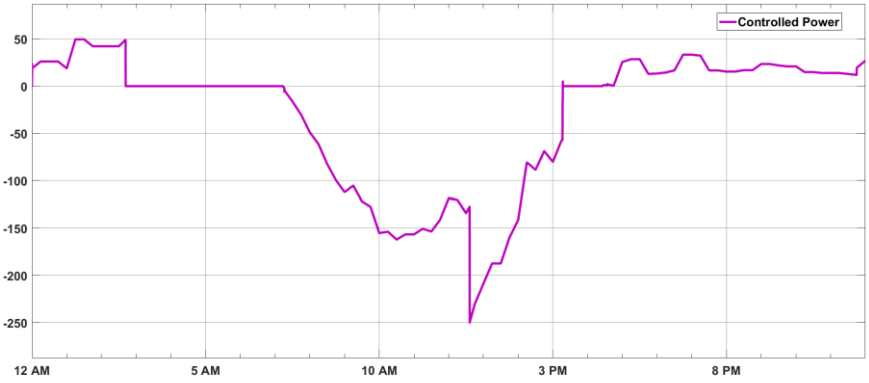

Fig. 5. Battery 2 Power

C

48 V Interconnection Simulation

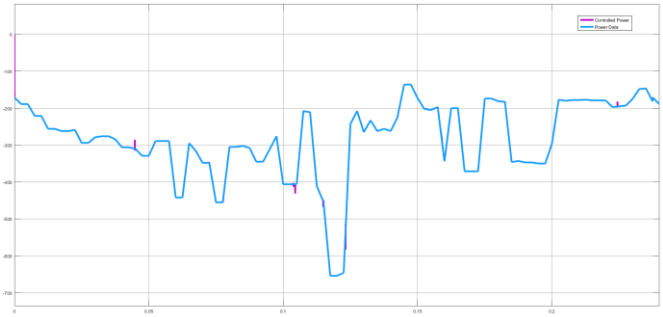

Fig. 6. Load Power of House 1

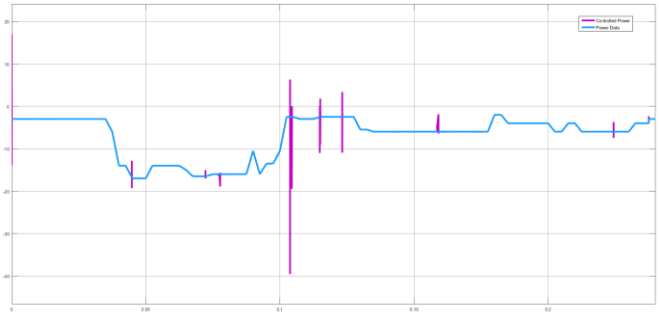

Fig. 7. Load Power of House 2

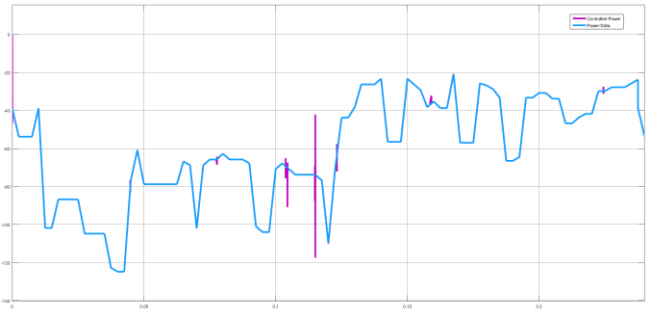

Fig. 8. Load Power of House 3

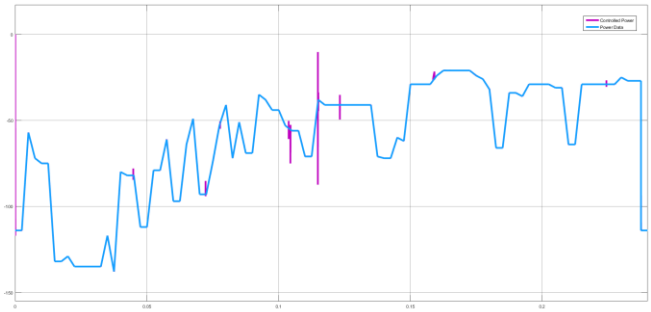

Fig. 9. Load Power of House 4

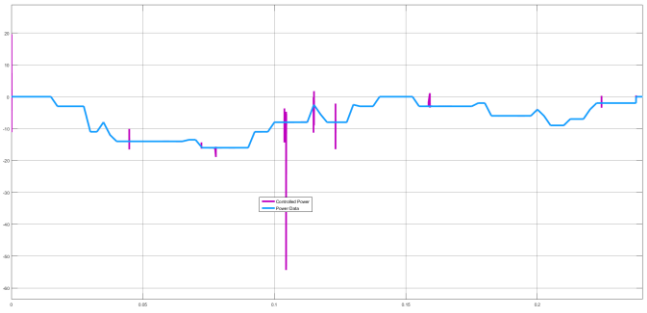

Fig. 10. Load Power of House 5

D

350 V Interconnection Simulation

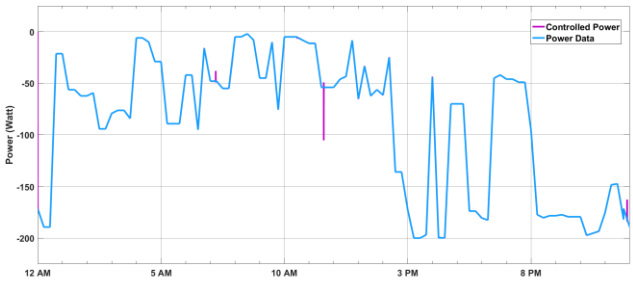

Fig. 11. Load Power of House 1

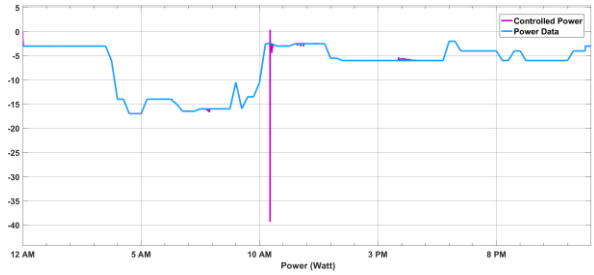

Fig. 12. Load Power of House 2

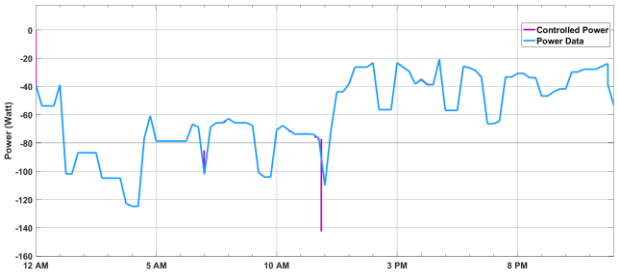

Fig. 13. Load Power of House 3

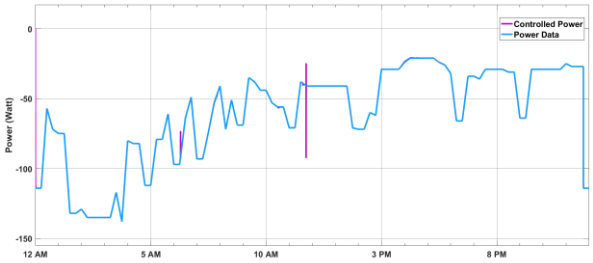

Fig. 14. load Power of House 4

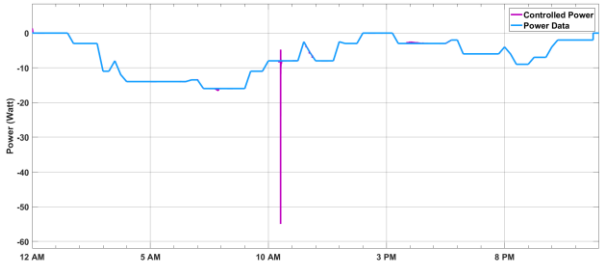

Fig. 15. Load Power of House 5

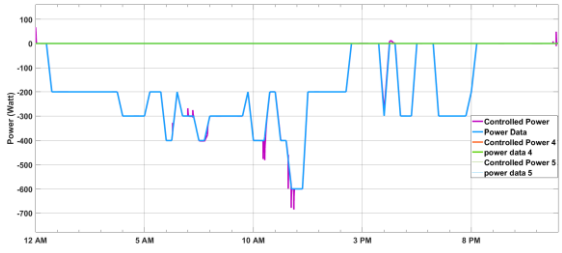

Fig. 16. Load Power in 350 V